Role of RAF kinases in Dendritic Cells

Dissertation

Zur Erlangung des Grades

Doktor der Naturwissenschaften

Am Fachbereich Biologie

Der Johannes Gutenberg-Universität Mainz

Kristina Riegel

geb. am 19.05.1989 in Ochsenfurt

Mainz

2019

Table of Contents

Abbreviations

AC	Adenylyl cyclases
ANF	Atrial natriuretic factor
APC	Antigen processing cells
APS	Ammonium persulfate
ASK1	Apoptosis signal-regulating kinase-1
ATP	Adenosine triphosphate
BM	Bone marrow
BMDC	BM-derived dendritic cells
BSA	Bovine serum albumin
°C	degree Celsius
Cat. No.	Catalogue number
CCR	C-C chemokine receptor
CD	Cluster of differentiation
cDC	Conventional dendritic cells
cDNA	copy DNA
CDP	Common dendritic cell progenitor
CO_2	Carbon dioxide
CR	Conserved regions
CRD	Cysteine-rich domain
DAMP	Danger-associated signals
DC	Dendritic cells
dH_2O	Distilled water
DMEM	Dulbecco's modified Eagle's medium
DMSO	Dimethylsulfoxide
DNA	Deoxyribonucleic acid
dNTP	Deoxyribonucleoside triphosphate
DTME	Dithio-bismaleimidoethane
DTT	Dithiothreitol
E.coli	Escherichia coli
ECL	Enhanced chemiluminescence
EDTA	Ethylenediamine tetra-acetic acid
EGF	Epidermal growth factor
ELISA	Enzyme-linked immunosorbent assay
ERK	Extracellular signal-regulated kinase
FCS	Fetal calf serum
FDA	Food and Drug Administration
Fig.	Figure
FSC	Forward scatter
fw	Forward
GM-CSF	Granulocyte-macrophage colony-stimulating factor
h	hour
HRP	Horseradish peroxidase

iDC	Immature dendritic cell
IFN	Interferon
IgG	Immunoglobulin G
IH-segment	Isoform-specific hinge segment
IKK-β	Inhibitor of nuclear factor kappa-B kinase subunit beta
IL	Interleukin
infDC	Inflammatory DC
IP	Immunoprecipitation
IRAK	Interleukin-1 receptor-associated kinase
JNK	c-Jun N-terminal kinase
kb	Kilobase pairs
kDa	Kilodalton
LB	Luria-Bertani medium
LC-MS	Liquid chromatography-mass spectrometry
LPS	Lipopolysaccharide
LY	LY3009120
MAL	MyD88-adaptor-like
MAP2K	MAPK kinase
MAP3K	MAPK kinase kinase
MAPK	Mitogen-activated protein kinase
MAPKAPK	MAP kinase activated protein kinases
MD	Mascot delta
MEK1/2	MAPK/ERK kinase 1/2
mg/µg	milligram/ microgram
MHC	Major histocompatibility complex
min	minutes
MKK	MAP kinase kinase
MKP	MAPK phosphatases
ml/µl	milliliter/ microliter
MLR	Mixed lymphocyte reaction
mmol/µmol	millimol/ micromol
moDC	Monocyte-derived DC
MS	Mass spectrometry
MTT	3-(4,5-dimethylthiazol-2-yl)-2,5-diphenyltetrazolium
MW	Molecular weight
Myd88	Myeloid differentiation primary response 88
MYPT	Myosin phosphatase
N-region	Negative-charge regulatory region
NFκB	Nuclear factor kappa-light-chain-enhancer of activated B cells
NLK	Nemo-like kinase
NP-40	Nonidet P40
NSCLC	Non-small cell lung cancer
PAK	p21-activated protein kinase
PAMPs	Pathogen-associated molecular patterns(s)
PBMC	Peripheral Blood Mononuclear Cells
PBS	Phosphate buffered saline

PCR	Polymerase chain reaction
pDC	Plasmacytoid DC
PGE_2	Prostaglandin E_2
PP	Protein Ser/Thr phosphatases
PRD	Proline rich domain
PRR	Pattern-recognition receptors
PSP	Protein Ser/Thr phosphatases
RAF	Rapidly accelerated fibrosarcoma
Ras	Rat sarcoma
Rb	Retinoblastoma tumor suppressor protein
RBD	Ras Binding Domain
rev	reverse
RIPA	radioimmunoprecipitation assay
RKIP	RAF kinase inhibitor protein
RNA	Ribonucleic acid
RPMI	Roswell Park Memorial Institute medium
RSK	Ribosomal S6 kinase
Ser or S	Serine
SDS	Sodium dodecyl sulphate
SDS-PAGE	Sodium dodecyl sulfate polyacrylamide gel electrophoresis
SEA	schistosome egg Ags
siRNA	small interfering RNA
SSC	Sideward scatter
TAK	TGFβ activated kinase
TEMED	N,N,N,N- Tetramethylethylendiamine
Th	T helper cell
Thr or T	Threonine
TIRAP	TIR-associated protein
TLR	Toll-like receptors
TNFα	Tumor necrosis factor alpha
Tpl-2	Tumor progression locus 2
TRAF	TNFR-associated factor
Tram	Trametinib
Treg	Regulatory T cell
TRIF	TIR-domain-containing adaptor protein-inducing IFNβ
Tris	Tris-hydroxymethyl-aminomethane
Tyr or Y	Tyrosine
v-raf	Virus induced rapidly accelerated fibrosarcoma
WT	wild type

Summary

Mitogen-activated protein kinases (MAPKs) are a family of serine/threonine protein kinases that regulate fundamental cellular processes like cell division, migration, differentiation and cell survival. There are 14 mammalian MAPKs described which define 7 distinct MAPK pathways. The classical MAPK signaling pathway consisting of RAF-MEK1/2-ERK1/2 gained enormous interest as the pathway is deregulated in many human cancers. Since RAS, which activates the RAF-MEK1/2-ERK1/2 cascade, as well as BRAF are among the most frequently activated oncogenes, lot of efforts were made to develop therapeutics to target the pathway. Drugs like vemurafenib or dabrafenib targeting the activated form of BRAF have shown enormous clinical success, but they unexpectedly induced MAPK activation in a BRAF-mutation free context by triggering RAF dimerization leading to paradoxical MAPK activation. Apart from targeted therapy, an efficient anti-cancer immune response is required for effective killing of cancer. But tumors can exploit several strategies, like secreting immune suppressive cytokines or inhibiting the presentation of tumor antigens to dampen immune responses. Thus, synergistic treatment regimes combining both targeted and immune therapy have been shown to benefit tumor patients. Since the role of the classical RAF-MAPK pathway in tumorigenesis has already been well described, we wanted to go further and investigate how MAPK signaling regulates innate and adaptive immune responses. Therefore, we initially evaluated the role of the classical RAF-MEK1/2-ERK1/2 pathway and especially of RAF kinases in dendritic cells (DCs). By employing a well-established *in vitro* culture, in which human monocytes are differentiated to moDCs, we investigated how RAF kinases contribute to the differentiation and maturation of moDCs. We observed that RAF kinases were stabilized at the protein level during moDC differentiation and detected RAF heterodimers between all three RAFs in moDCs. To validate the functional role of RAF kinases in moDCs we employed pan-RAF as well as MEK inhibitors to block MAPK signaling. Inhibition of RAF kinases but not MEK1/2 impaired the activation and migration of DCs. Furthermore, DCs treated with RAF inhibitors showed a reduced ability to activate allogeneic $CD4^+$ T cells. Additionally, we showed that RAF and MEK1/2 inhibition directly inhibited proliferation of $CD4^+$ T cells. Thus, our results point to a role of RAF kinases in moDCs in a MEK1/2-independent manner and that RAF kinases are required for DC activation and function.

Zusammenfassung

Die mitogenaktivierten Proteinkinasen (MAPK) sind eine Familie von Serin/Threonin-Kinasen, die fundamentale zelluläre Prozesse wie Zellteilung, Migration, Differenizierung und das Überleben der Zelle regulieren. In Säugetieren sind 14 MAPK beschrieben, die 7 verschiedene Signalwege definieren. Der klassische MAPK Signalweg, der aus der Kaskade RAF-MEK1/2-ERK1/2 besteht und durch Ras aktiviert wird, hat besonders großes Interesse erweckt, da der Signalweg in vielen menschlichen Krebszellen mutiert ist. Sowohl RAS als auch BRAF gehören zu den am häufigsten aktivierten Onkogenen. Aufgrund dessen sind erhebliche Anstrengungen unternommen wurden um Therapeutika zu entwickeln, die diesen Signalweg hemmen. Vemurafenib und Dabrafenib sind Inhibitoren der abnormen Form des BRAF Proteins und konnten enorme klinische Erfolge vorweisen. Überraschenderweise verursachten die Inhibitoren in Abwesenheit von BRAF Mutationen eine paradoxe Aktivierung des MAPK Signalweges, die auf eine induzierte RAF-Dimerisierung zurückzuführen ist. Abgesehen von einer zielgerichteten Therapie ist eine effiziente Immunantwort gegen die Krebszellen erforderlich um diese zu eliminieren. Jedoch wenden Tumorzellen verschiedene Strategien an, wie die Sekretion von immunsuppressiven Zytokinen oder die Herunterregulierung der Antigenpräsentation, um die körpereigene Immunabwehr zu schwächen. Im Einklang dazu hat es sich gezeigt, das die Kombination aus zielgerichteter Therapie und Immuntherapie förderlich für die Behandlung von Krebspatienten ist. Da die Rolle des RAF-MAPK Signalweges in der Tumorgenese gut beschrieben ist, wollten wir einen Schritt weitergehen und untersuchen wie der MAPK Signalweg die angeborene und erworbene Immunantwort beeinflusst. Zunächst haben wir die Rolle des klassischen RAF-MEK1/2-ERK1/2 Signalweges und besonders von RAF Kinasen in Dendritischen Zellen (DC) untersucht. Unter Verwendung einer gut etablierten *in vitro* Kultur, bei der humane Monozyten zu moDCs differenziert werden, haben wir untersucht wie RAF Kinasen an der Differenzierung und Reifung von moDCs beteiligt sind. Hierbei haben wir beobachtet, dass die RAF Kinasen während der moDC Differenzierung auf Proteinebene stabilisiert wurden. Des Weiteren haben alle drei RAF Proteine Heterodimere in moDCs ausgebildet. Die funktionelle Rolle der RAF Kinasen in moDCs wurde durch die Anwendung von pan-RAF sowie MEK Inhibitoren validiert. Die Inhibition von RAF Kinasen aber nicht von MEK1/2 hat die Aktivierung und Migration

von moDCs beeinträchtigt. Des Weitern zeigten moDCs nach der Behandlung mit dem RAF Inhibitor eine reduzierte Fähigkeit allogene $CD4^+$ T Zellen zu aktivieren. Außerdem haben wir nachgewiesen, dass die Inhibierung von RAF als auch MEK1/2 einen direkten hemmenden Einfluss auf die Proliferation von $CD4^+$ T Zellen hat. Daher deuten unsere Ergebnisse darauf hin, dass RAF Kinasen eine MEK1/2-unabhängige Funktion in moDCs haben, die für die Aktivierung und Funktion von DCs benötigt wird.

1 Introduction

1.1 The classical MAPK cascade

Mitogen-activated protein kinases (MAPK) are usually activated in a three tier-signaling cascade, which translates extracellular signals including growth factors, hormones, cytokines and stress into adaptive intracellular responses [1]. The MAPK cascade is conserved in eukaryotes and consists of a MAPK kinase kinase (MAP3K) phosphorylating and activating a MAPK kinase (MAP2K), which subsequently activates the terminal MAPK by dual phosphorylation on threonine (Thr or T) and tyrosine (Tyr or Y) residues [2, 3]. Once activated, MAPK regulate various physiological processes like proliferation, migration, differentiation, metabolism rate and apoptosis typically by targeting proteins throughout the cell, but mainly substrates coordinating changes in gene expression [1, 2]. By phosphorylating, MAPK can influence multiple aspects in their substrates including cellular localization, DNA binding, protein interaction and in some cases protein stability [4]. The specificity and efficiency of signal transmission by MAPK cascades is ensured by specific docking sites of interacting proteins and by scaffolding proteins, which have an influence on the kinetics of activation, signal duration, signal intensity and the cross talk with other pathways by bringing components of single pathways together [3, 5]. Beside this, protein phosphatases play a major role in restricting MAPK signaling by de-phosphorylating and inactivating the protein kinases [2, 6].

In mammals, 14 MAPKs have been identified and they are defining 7 distinct MAPK pathways (Fig. 1.1) [1]. Additionally, they can be classified into conventional MAPKs like the extracellular signal-regulated kinases 1/2 (ERK1/2), c-Jun N-terminal kinases (JNKs), p38 isoforms and ERK5 [7] and the atypical MAPKs including ERK3, ERK4, Nemo-like kinase (NLK) and ERK7/8 [1]. While conventional MAPKs are regulated via their Thr-Xaa-Tyr motif in the activation loop, the regulatory mechanisms and physiological functions of atypical MAPK are not well-known [1].

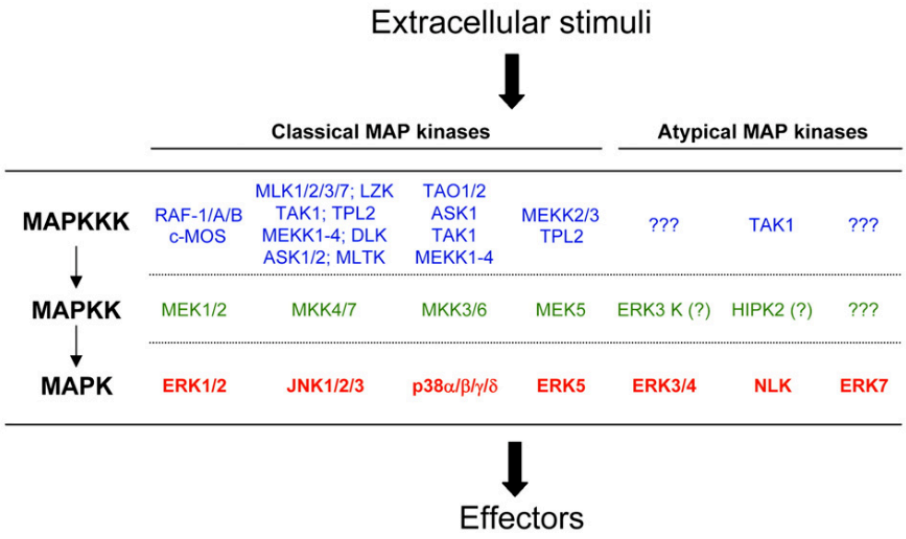

Figure 1.1 Human MAPK define 7 distinct signaling pathways. Adapted from Ref [1]

With ERK1/2 being the first identified MAPK, the RAF-MEK1/2-ERK1/2 pathway is the best-studied MAPK pathway and is the main focus of this work [3].

1.2 Activation of the RAF-MEK1/2-ERK1/2 pathway

Upon the stimulation of growth factor receptors, activation of the small GTPase rat sarcoma (RAS) is induced [3, 8], which subsequently recruits the MAP3K RAF to the plasma membrane [7]. RAF proteins bind to RAS with high affinity through their Ras Binding Domain (RBD) in their N terminus, which leads to the activation of the kinase in a multistep process [7]. RAF kinases catalyze the phosphorylation and activation of the dual-specificity MAP2Ks MEK1/MEK2, which in turn phosphorylate the Thr and Tyr residues within the activation loop motif Thr–Glu–Tyr of the MAP kinases ERK1 and ERK2 [1, 3].

There are three different **RAF** isoforms (A-, B- and CRAF) and all of them are able to activate MEK1 and MEK2 by phosphorylating on the serine (S) residues 218/222 and S222/S226, respectively. But as shown by Papin *et al.* with a yeast two-hybrid system BRAF binds more efficiently to MEK1/2 [9] and exerts a more robust and rapid ERK1/2 activation than ARAF and CRAF [10]. Additionally, a short conserved sequence in front of the kinase domain, called N-region, renders BRAF with a high basal kinase activity [11]. In contrast to ARAF and CRAF, the N-region of BRAF carries a constant negative charge as it contains aspartates (D448/D449) at positions where in ARAF and CRAF Tyr

residues are located (Y301/Y302 in ARAF, Y340/Y341 in CRAF). Further, the highly conserved serine within this region is constitutively phosphorylated in BRAF (S446) [12]. Hence, BRAF is perceived as the main MEK1/2 kinase in cells, while ARAF and CRAF contribute to the fine-tuning of ERK1/2 activation [11].

The kinases **MEK1 and MEK2** are highly homologous with an 80% overall similarity: While the kinase domains share even 90% identity, the catalytic domain flanking, short amino-terminal and carboxy-terminal regions as well as the proline rich domain (PRD) differ in their sequence (58-69% homology) [13]. Within the PRD, MEK1 has the unique phosphorylation site T292. This site is a target of an ERK1/2 mediated negative feedback loop, which blocks the PAK-dependent phosphorylation of S298 [14]. Phosphorylated S298 induces autophosphorylation and MEK1 activity towards ERK1/2 [15]. Furthermore, as shown by Catalanotti *et al.* the MEK1-specific negative regulatory residue contributes to the modulation of MEK2 phosphorylation, which requires MEK1–MEK2 heterodimer formation [16]. In the perspective of functional redundancy, both common and unique biological properties are described. For instance, MEK1 and MEK2 act redundant in the epidermis as only combined MEK1/2 deletion in mice led to hypoproliferation, apoptosis, skin barrier defects and death [17]. But distinct functions of MEK1 and MEK2 became clearer by comparing the corresponding knockout mice. While *mek2*$^{-/-}$ knockout mice are viable, and fertile with no apparent abnormalities [16, 18], *mek1*$^{-/-}$ knockout mice are, because of placental defects, embryonic lethal [16, 19]. Consequently, MEK2 cannot compensate the loss of MEK1 in this organ [16].

While MEK1 and MEK2 have narrow substrate specificity, with ERK1 and ERK2 being the only known physiological substrates, **ERK1 and ERK2** itself can phosphorylate hundreds of targets. Known targets of ERK1 and ERK2 include the transcription factors Elk1 [20] and c-Myc [21], the apoptotic proteins Bad [22] and Caspase 9 [23] and other kinases like the MAP kinase activated protein kinases (MAPKAPK), including RSK, MNK and MSK [24]. The ERK1/2 cascade transmits different and even opposing signals in the same cell. Hence, accurate regulation is required, which is mediated by several mechanisms including duration and strength of the signal, interaction with scaffold proteins, subcellular localization and cross-talk with other signaling pathways [25]. With an 84% identical sequence, ERK1 and ERK2 are highly homologous [26] and are usually seen as functionally interchangeable, although several recent studies suggest that ERK1 and ERK2 have distinct functions [27]. *Erk1*$^{-/-}$ knockout mice are viable and

fertile with minor defects including impaired thymocyte maturation [28]. In contrast, *erk2*$^{-/-}$ knockout mice are embryonic lethal due to a malfunction in mesoderm differentiation [29]. Hence, ERK1 cannot compensate for ERK2 in this case. In addition to non-redundant roles of ERK1 and ERK2, a study by Lefloch *et al*. claims that the ERK expression levels could be a critical factor in mouse survival [30]. Only animals with either two *erk2* alleles or with one *erk1* and one *erk2* survived. As ERK2 expression is usually higher than ERK1 expression, it is possible, that the severe effects in *erk2*$^{-/-}$ knockout mice occur because the total ERK content has decreased to a greater extent [26, 30].

As ERK1/2 are only active when both the Tyr and Thr residues are phosphorylated, inactivation of the kinases is mediated by the removal of phosphate from either the Tyr, the Thr or from both residues together. The dual-specificity MAPK phosphatases (MKP), a subgroup of the dual-specificity phosphatases (DUSPs), are the best-studied group of phosphatases, which shape the duration, magnitude and spatiotemporal prolife of MAPK activities [31, 32]. The conversion of the kinases to the inactive status can be further induced by protein Ser/Thr phosphatases (PSP), like PP2A [33] or by protein Tyr phosphatases, like PTP-SL [34]. Inhibition of the ERK1/2 signaling is additionally regulated by negative feedback phosphorylation [32]. Nearly all components of the ERK1/2 cascade including, BRAF [35], CRAF [36] and MEK1 [14], are targets of inhibitory feedback phosphorylation [32].

1.3 Structure and regulation of RAF kinases

RAF proteins are serine/threonine-specific protein kinases and are key modulators of the classical MAPK cascade. The first described RAF isoform is CRAF, which was discovered in 1983 as a transforming gene from the murine retrovirus 3611-MSV, designated as virus induced rapidly accelerated fibrosarcoma (*v-raf)* [37]. Pretty much around the same time, a new oncogene called *v-mil* from the avian retrovirus Mill-Hill No.2 was described [38], which was later identified as the avian CRAF homologue [39]. Around ten years later it was reported, that the MAPK kinase of ERK1 and 2 is an immediate downstream target of CRAF, thus identifying CRAF as a component of the ERK1/2 pathway [40]. The other two RAF isoforms ARAF and BRAF were discovered shortly after CRAF (ARAF: 1986 [41], BRAF: 1988 [42]) [11].

1.3.1 Structure and activation of RAF proteins

As shown in Fig. 1.2, the RAF kinases share three conserved regions (CR) with distinct functions. CR1 carries a RBD domain as well as a cysteine-rich domain (CRD), which are both required for membrane recruitment and RAS binding [11, 43, 44]. CR2 contains an inhibitory phosphorylation site [45], which serves as one of the binding sites of the regulatory protein 14-3-3 and is involved in the negative regulation of RAS binding and RAF activation [11, 43, 46]. The C-terminal CR3 encodes the kinase domain together with the activation segment [11, 43]. Overall, RAF proteins can be split into a regulatory N-terminal region and a catalytic C-terminal region.

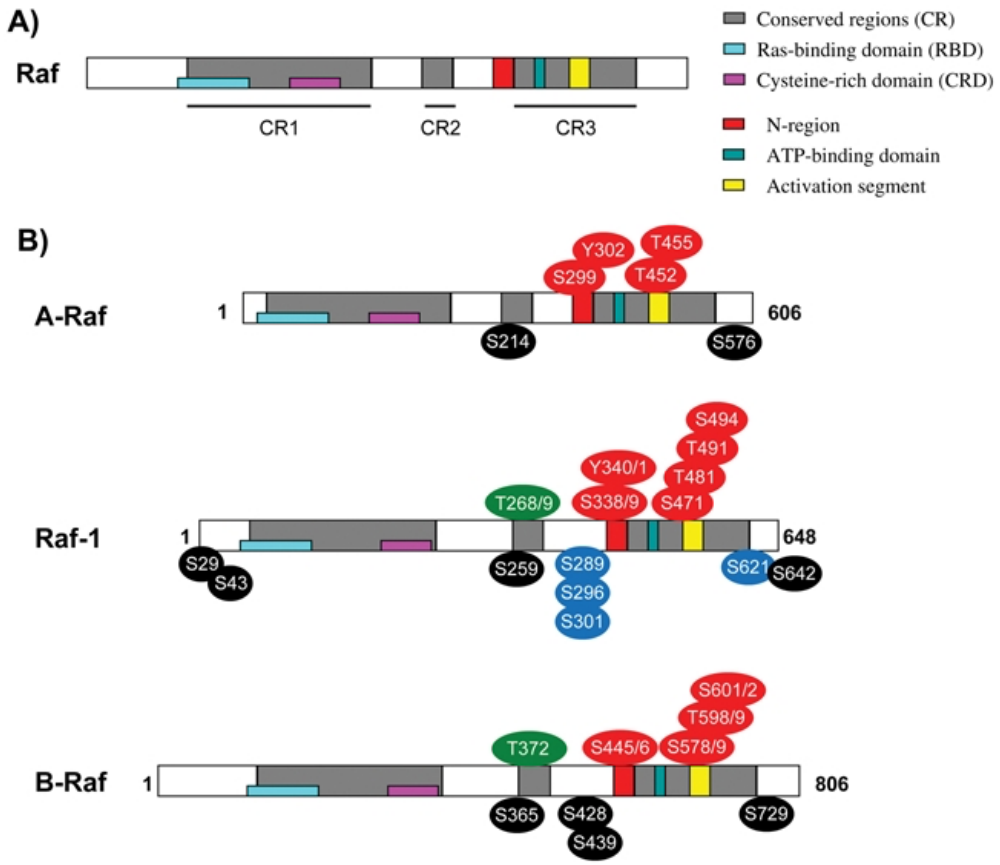

Figure 1.2 RAF structure (A) RAF proteins are characterized by three conserved regions (CR1, CR2, CR3) and (B) have common and distinct regulatory phosphorylation sites (red: activating, black: inhibitory, blue: described as activating and inhibitory, green: major *in vitro* autophosphorylation sites). Adapted from Ref [43]

Under basal conditions, RAF proteins are predominantly localized in the cytosol in a closed conformation, wherein the N-terminal region covers the catalytic region. The inactive state is stabilized by 14-3-3 [47, 48], which binds to the phosphorylation site within CR2 and to another one near the C-terminus [45]. The initial event of RAF activation is the dephosphorylation of a site in the CR2 region (ARAF: S214, BRAF: S365,

CRAF: S259) mediated by PP2A [43, 49], causing the displacement of 14-3-3 [46] and the exposure of the RBD and CRD domains. Subsequently, RAS-GTP directly binds to the N-terminal RBD domain and forms secondary interactions with the CRD domain, leading to the recruitment of RAF to the plasma membrane [11, 43]. However, RAF regulation is a highly complex process involving not just the N-terminus, but a number of activating phosphorylations in the C-terminus, too [11].

1.3.2 Regulation of RAF by phosphorylation

Phosphorylation plays an important role in RAF regulation. Thereby, RAF kinases have both common and distinct phosphorylation mechanisms to regulate kinase activity.

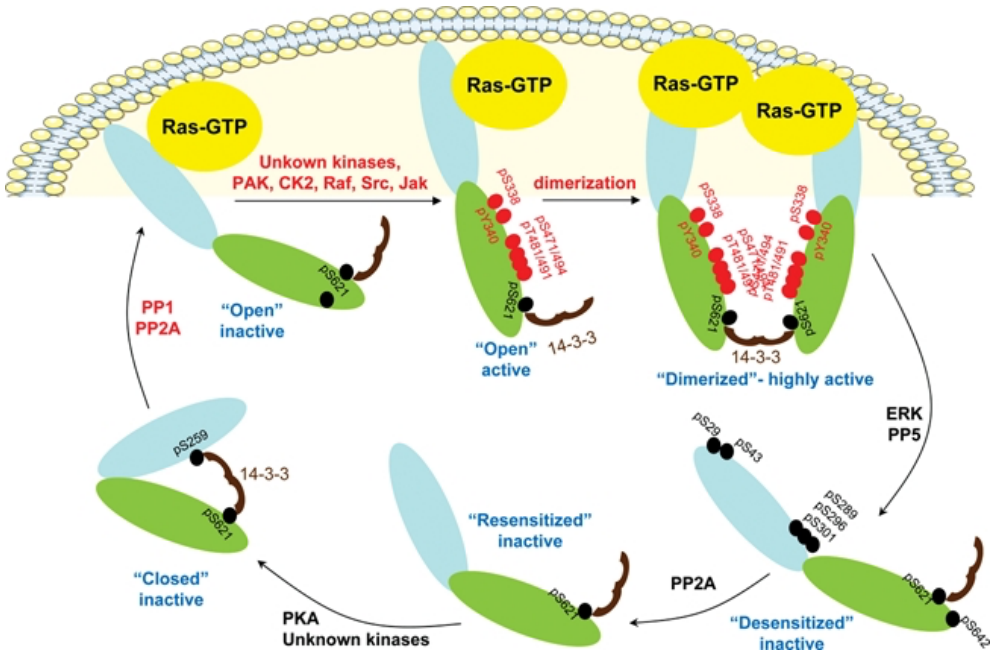

Figure 1.3 Activation and deactivation of CRAF. Multiple activating (red) and deactivating (black) steps are influencing the activation status of CRAF. Adapted from Ref [43]

In case of CRAF activation (see Fig. 1.3), phosphorylation of the sites within the activation segment (T491, S494) [50] and the N-region are required (S338, Y341) [50, 51]. The N-region defines a negative charge regulatory region upstream of CR3. ARAF is thought to be regulated in a comparable way to CRAF, since the phosphorylation sites required for CRAF activity are conserved in ARAF [11]. While the importance of T452/T455 within the activation segment of ARAF remains to be proven, it was shown that the conserved phosphorylation site S299 within the N-regions positively regulates ARAF activity [52]. Phosphorylation of T599/S602 within the activation segment of

BRAF is essential for its activation, as mutation of these residues abolished BRAF activation without altering the association of BRAF with other signaling proteins [53]. As already discussed above, the N-region of BRAF carries a constant negative charge making it dispensable for further regulatory modifications. Hence, the major regulation mechanism for BRAF activation are RAS and 14-3-3 binding [43].

1.3.3 RAF dimerization regulating RAF activity

Another important regulation mechanism is the RAF homo- and heterodimerization, which seems to induce and stabilize the activated conformation. In a side-to-side conformation the main contacts are made between the N-terminal lobes [54]. The CRAF-BRAF heterodimers have a higher kinase activity compared with homodimers and are stabilized by 14-3-3 [55]. As 14-3-3 proteins are displaced from the phosphorylation site within the CR2 region (CRAF: S256, BRAF: S365), one arm is left free, which can subsequently crosslink CRAF and BRAF by binding to the C-terminal sites on each kinase [43]. BRAF is the only RAF kinase, which can act as an allosteric activator because of its negatively charged N-terminal acidic motif. Heterodimerization with BRAF induces cis-autophosphorylation in the activation loop of the receiver kinase [56]. Additionally, BRAF may present MEK to CRAF being then approachable for CRAF to phosphorylate [54, 56]. Subsequently, MEK phosphorylates CRAF at the N-terminal acidic motif and because of that CRAF gets converted to an allosteric activator [56].

1.3.4 Deactivation of RAF proteins

RAF activation is shut off by different mechanisms. PP5, a serine/threonine phosphatase, is known to dephosphorylate pS338 thus initiating the deactivation of CRAF [43, 57]. Additionally, RAF kinase inhibitor protein (RKIP) binds to the phosphorylated N-region [43, 58, 59] and dissociates RAF and MEK [43, 60]. Feedback phosphorylation by ERK on 6 sites limits CRAF activation as well [43, 61] and serves as an additional tool to dynamically regulate the signaling. It is also reported, that ERK feedback phosphorylation of a subset of these sites can positively influence CRAF activity. In this regard, Balan *et al.* described three sites S289/S296/S301, which are targeted by ERK and if phosphorylated enhance the kinase activity of CRAF [36].

1.3.5 Alternative RAF substrates

Because of the presence of three mammalian RAF isoforms it is hypothesized, that there are other RAF substrates possible besides MEK1/2. Phylogenetic studies identified BRAF as the original RAF precursor and therefore it is seen as the archetypal MEK1/2 kinase. In case of ARAF and CRAF, MEK1/2-independent functions are considered. CRAF was reported to activate adenylyl cyclases (AC) by direct phosphorylation [62, 63]. As a result of this, cAMP is generated and subsequently PKA is activated, which is another important negative regulator of CRAF. Thus, the activation of AC by CRAF could serve as a further negative feedback event [43]. Other possible targets of CRAF could be the retinoblastoma tumor suppressor protein (Rb), whose CRAF-dependent inactivation would lead to cell cycle progression [64], and the myosin phosphatase (MYPT), whose inhibition by CRAF-induced phosphorylation results in enhanced cell motility [65]. Luciferase reporter gene experiments in primary cardiac myocytes showed, that an estradiol-inducible form of CRAF activated ANF expression, while increased MEK activity inhibited the CRAF-induced expression [66]. Atrial natriuretic factor (ANF) is a hypertrophic marker which is regulated by several different signaling pathways including the MAPK pathway [67]. Further, separate DNA elements in the ANF promoter were identified, through which the RAF-dependent activation and MEK1/2-dependent inhibition was achieved [66]. In this study they postulated, that RAF activates at least two signaling pathways that compete against each other to regulate the ANF promoter [66]. Another study to suggest a MEK1/2 independent function for CRAF was performed by Pearson *et al*., who investigated the effect of a kinase active, but MEK1/2 binding deficient CRAF mutant on different cellular responses. The CRAF mutant can efficiently stimulate morphological changes in PC12 cells indicative of differentiation events, NF-κB-dependent gene expression, and activation of p90 ribosomal S6 kinase (RSK), despite severely impaired ERK1/2 activation [68]. In terms of finding new RAF substrates there is also the possibility of RAF signaling to other effectors in a kinase-independent manner. An example for this is the apoptosis signal-regulating kinase-1 (ASK1). Binding of CRAF to ASK1 suppresses its pro-apoptotic activity and only the release from CRAF leads to the induction of apoptosis [69]. Additionally, Ehrenreiter *et al*. showed, that CRAF controls the migration of keratinocytes and fibroblasts in a kinase-independent manner. Physical interaction of CRAF with the Rho effector Rok-α is required to regulate the localization and activation of Rok-α. Consequently, the loss of CRAF results in a

hyperactivity and incorrect localization of Rok-α to the plasma membrane and thus to defects in adhesion and motility [70].

1.4 MAPK signaling in cell survival and oncogenesis

The ERK1/2 pathway is deregulated in many human cancers, with aberrations occurring throughout the whole pathway ranging from abnormal receptors, mutated RAS and RAF proteins to amplified nuclear targets [3]. The three mammalian RAS proteins (N-RAS, K-RAS, H-RAS) are proto-oncogenes, which promote oncogenesis when activated through mutation at the codons 12, 13 or 61 [71]. Mutation of one of these sites prevents GTP hydrolysis resulting in constitutively active RAS, which hyper-activates the downstream signaling pathways like the MAPK cascade. *Ras* mutation occurs in around 20% of all human tumors making it to the most frequent oncogene [72]. The frequency of mutation in the individual *ras* genes differs depending on the cancer type. Compared to the other *ras* genes, *K-ras* mutation predominantly occurs in pancreatic carcinoma and lung adenocarcinoma [73] with a total mutation frequency of 66% and 19%, respectively. With a mutation frequency of 17% in malignant melanoma and of 13% in acute myeloid leukemia (Catalogue of Somatic Mutations in Cancer (COSMIC) database [74]), *N-ras* is among the *ras* genes the dominating oncogene in these cancers [73]. *H-ras* is the isoform with the least overall mutations in human cancers, but has a mutation frequency of 13 % in urinary tract cancers and 12 % in salivary gland carcinoma, hence accounting for a higher mutation rate compared to *N-ras* and *K-ras* in these cancer types (COSMIC database [74]).

Besides the *ras* genes, BRAF is frequently mutated in various human cancers and is among the most commonly mutated kinases. BRAF mutations are very common particularly in malignant melanoma [75] with an average mutation rate of 43%. Other cancer types, which frequently bear BRAF mutations, are thyroid cancers (43%) and colorectal cancers (17%) (COSMIC database [74, 75]). Mutations in BRAF occur in mainly two regions of the BRAF kinase domain: within the activation segment and in the glycine-rich loop. Mutations in the activation segment of BRAF are the most common and acidic substitutions of certain residues usually lead to enhanced kinase activity as the introduced negative charge disrupts its interaction with the P-loop [75]. Among others, mutation of the BRAF V600 residue to glutamic acid (E) is the most prevalent BRAF mutation and it allows BRAF to be active without dimerization [76]. Other

mutations that resulted in impaired kinase activity were also identified. But these mutants cause increased CRAF activity [77, 78] as they signal as constitutive dimers [79]. In contrast, mutations of ARAF [80] and CRAF [81] are rare in human cancer. But as shown in the studies of Karreth *et al*. and Blasco *et al.*, tumor initiation by oncogenic KRAS in a lung cancer mouse model is primarily dependent on CRAF [82, 83]. Thus, without being directly mutated, CRAF plays a pivotal role in KRAS dependent cancers such as non-small cell lung cancers (NSCLCs). Lung cancers are the major cause of cancer-associated lethality and KRAS is mutated in around 17% of lung cancer patients. Depending on the cancer histology, the mutation frequency of KRAS account for up to 24% in large cell carcinoma, 19% in adenocarcinoma and 19% in non-small cell carcinoma (COSMIC database [74]).

1.5 Targeting the MAPK pathway in human cancer with a focus on RAF kinases

Kinases constitute the major part of the "druggable genome" and targeting the "oncogenic" kinases with ATP competitive and non-competitive inhibitors in genetically defined human cancers has beeb successful in the clinics. However, patients often develop resistance and there is a need to further understand and explore the biology of kinases to adroitly administer rational, new generation of kinase therapeutics.

To date, the Food and Drug Adminstration (FDA) has approved 28 kinase inhibitors for targeted therapeutics [84]. The first FDA approved inhibitors against RAF kinases were vemurafenib (PLX4032) and dabrafenib (GSK2118436), which were designed to specifically target BRAF V600E and showed a remarkable therapeutic effect in melanomas with mutant BRAF [85-88]. But despite the clinical success, concerns came up due to fast developing drug resistance and occurrence of secondary malignancies, predominantly squamous cell carcinomas and keratoacanthomas, which is a low-grade rapidly growing skin tumor [85, 88, 89]. The secondary skin lesions frequently carried RAS mutations and showed a paradoxical activation of MAPK signaling [90]. RAS activation typically results in RAF dimerization and in line with this, Poulikakos *et al.* and others demonstrated, that the observed paradoxical activation is probably caused through a drug-induced transactivation of these dimers [91]. Consequently, RAF inhibitors like PLX4032 effectively block the MAPK pathway driven by mutant BRAF

resulting in tumor cell death. But without BRAF-activating mutations, the ERK1/2 pathway is rather dependent on other mechanisms with RAF dimerization being a crucial step. In this case, the inhibitor-bound RAF subunit promotes the activation of the other drug-free RAF subunit, mostly CRAF, and could even lead to enhanced tumor growth [92, 93]. The paradoxical pathway activation and the increased BRAF/CRAF dimer formation [94] can be explained by structural mechanisms. First of all, binding of ATP competitive RAF-inhibitor destabilizes the autoinhibitory interaction between the regulatory domain and kinase domains of the RAF proteins, which promotes the interaction with RAS [76, 95]. Additionally, a static dimer interface is induced probably because of a higher immobility of the kinase domain itself [96]. In more detail, the N-terminal lobe αC-helix of the RAF kinase domain carries on the one hand a leucine residue (L505 in BRAF), which is involved in the formation of a regulatory spine to adopt the active "IN" conformation [76]. On the other hand, the adjacent arginine residue (R506 in BRAF) is critical for dimer formation [97] and for this reason RAF dimerization and activation is allosterically linked. Inhibitors can bind RAF proteins in the active or inactive conformation. Binding to the active conformation induces more RAF dimer formation, as it is the case, when inhibitors target the inactive conformation, thus stabilizing the αC-helix in the inactive conformation as well [76, 98]. An example for an inhibitor targeting the inactive conformation is PLX4032, which promotes just marginal RAF dimerization compared to other inhibitors [98]. But for this kind of inhibitor RAF dimerization itself limits the drug effectiveness. Through negative cooperativity the affinity of the inhibitors are significantly reduced to the second protomer of a RAF dimer after binding to the first protomer [76, 98].

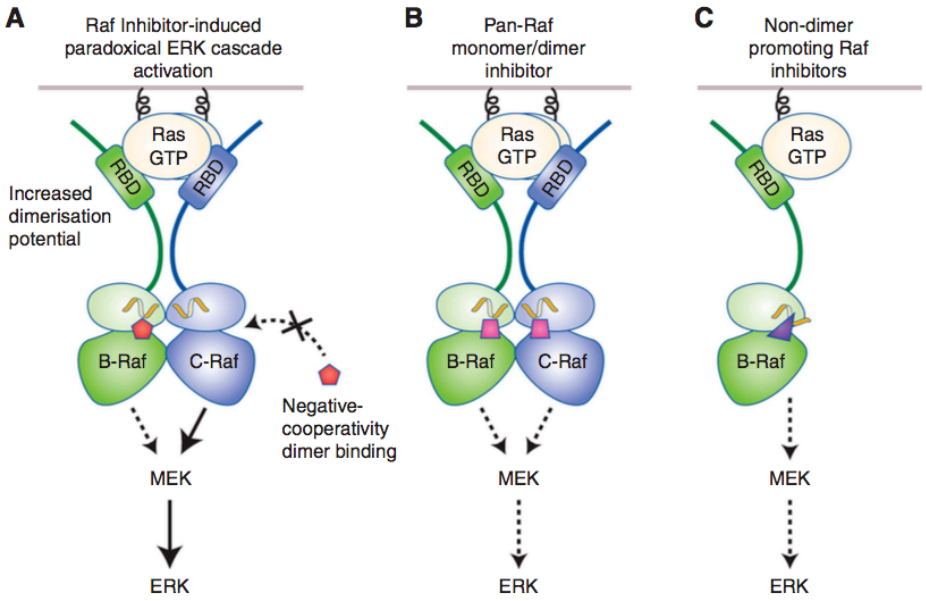

Figure 1.4 Strategies to target RAF kinases. (A) First-generation RAF inibitors increase RAS-dependent RAF dimerization leading to paradoxical ERK pathway activation. Furthermore, negative cooperativity impedes the binding of the inhibitor to the second protomer of a dimer. Alternative approaches to combat the observed difficulties with RAF inhibitors could be the development of (B) pan-RAF inhibtors and (C) inhibitors preventing RAF dimerization. Adapted from Ref [76]

To prevent the paradoxical ERK1/2 activation, new strategies of how to target the MAPK pathway are necessary (see Fig. 1.4). One approach is to develop next generation RAF inhibitors. Therefore drugs are developed, which inhibit the monomeric and dimeric RAF proteins with equal efficiency. These so-called pan-RAF inhibitors include LY3009120 [99], MLN2480/TAK-580 and BGB659. Anti-proliferative effects of LY3009120 were proven in various cancer cell lines [100, 101], including $BRAF^{mut}$ and $KRAS^{mut}$ cell lines. Further anti-tumor activity was demonstrated using an *in vivo* $BRAF^{mut}$ and $KRAS^{mut}$ colorectal cancer xenograft model [102]. Another type of next generation inhibitors are compounds, which block RAF dimerization directly [76].

In addition to RAF inhibitors, several MEK inhibitors are available. But due to higher toxicity their clinical use is limited. The first FDA approved MEK inhibitor is the allosteric inhibitor trametinib, which has been accepted as a single agent for the treatment of advanced BRAF V600 mutant melanoma [103]. To circumvent drug resistance, combination therapy with RAF and MEK inhibitors is another therapeutic strategy. The combinatorial treatment with the RAF inhibitor dabrafenib and the MEK inhibitor is an FDA-approved therapy for BRAF mutated non-small cell lung cancer and metastasized melanoma [104, 105].

The development of targeted therapeutics to interfere with the deregulated oncogenic signaling in tumor cells resulted in profound tumor responses in genetically defined patient populations [106]. As the response is often not durable, improved and prolonged induction of progression-free survival new cancer treatment regimens should now also include a concurrent induction of anti-tumor immunity [106]. To successfully combine targeted and immune therapeutics, it is crucial to understand the biological function of the drugged targets in the immune cells and to evaluate potential effects of the drugs on the regulation of the immune system.

1.6 Dendritic cells – link between innate and adaptive immune system

Dendritic cells (DCs) were first described in 1973 by Steinman and Cohn, who discovered a small cell population in mouse peripheral lymphoid organs with a characteristic stellate morphology [107]. In the following years, Steinman and his colleagues identified DCs as antigen processing cells (APCs), which could stimulate T cells in primary mixed lymphocyte reactions (MLR) *in vitro* [108] and initiate antigen-specific cellular immune responses *in vivo* [109].

1.6.1 Activation of dendritic cells

DCs are seen as the bridge between the innate and adaptive immune system. Due to their ability to recognize pathogen- and danger-associated signals (PAMPs/DAMPs), they belong to the innate immune cells. However, DCs form the interface between the innate and adaptive immune system, since they are also capable of presenting processed antigens in the context of major histocompatibility complex (MHC) molecules and transporting them to draining lymph nodes to prime naïve T cells. For this a number of fundamental properties are necessary, which is achieved through functional maturation.
In steady state, the so-called immature DCs (iDCs) excessively capture antigens by phagocytosis, macropinocytosis or receptor-mediated endocytosis, which they further process and display as peptides loaded on MHC molecules [110]. They are further characterized by a low surface expression of MHC and co-stimulatory molecules like cluster of differentiation 80 (CD80), CD86 and CD40. In the absence of inflammation they contribute to the maintenance of peripheral tolerance through their constant migration to local lymph nodes [111].

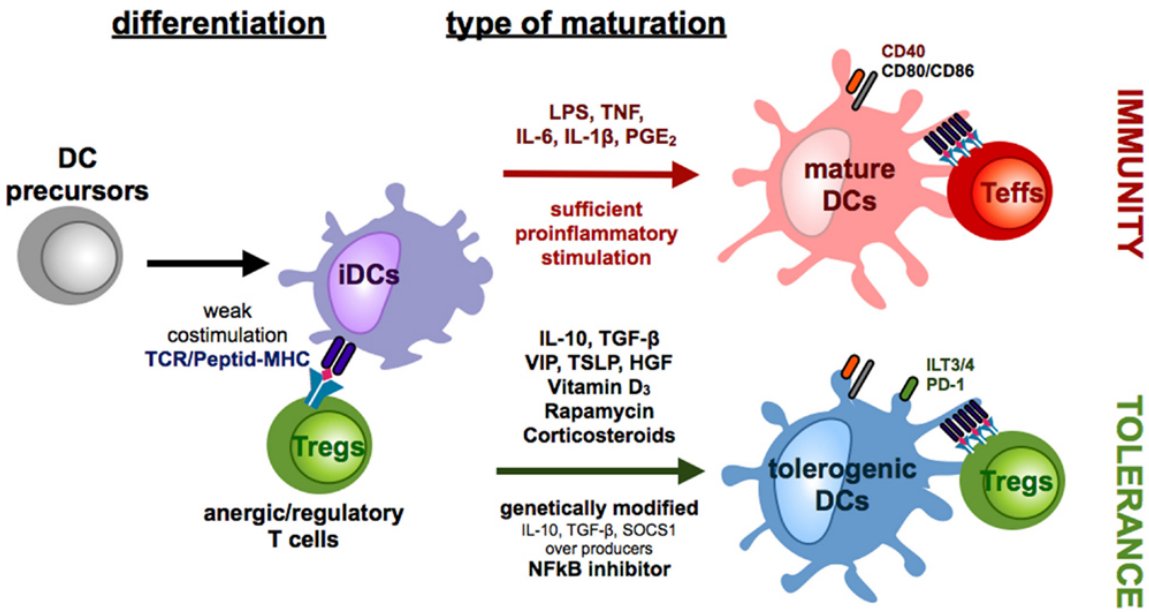

Figure 1.5 Activation of dendritic cells. DC precursor from peripheral blood differentiate to immature DCs (iDCs), which reside in the periphery and capture exogenous antigens. Stimulation of T cells with iDCs induce regulatory T cells (Tregs). Sufficient maturation signals include bacterial components signaling through toll-like receptors and distinct combinations of proinflammatory cytokines. Maturation of DC results in a migratory/stimulatory phenotype. In contrast, several mediators or genetic modifications of DCs in the presence or absence of maturation factors can induce tolerogenic DCs. Adapted from Ref [112].

Under inflammatory conditions, DCs undergo an immunogenic maturation, which leads to the upregulation of MHC-II, co-stimulatory molecules and C-C chemokine receptor type 7 (CCR7) dependent migration to the lymph nodes, as well as to the induction of cytokine release. Mature DCs are then capable of inducing clonal expansion of antigen-specific naïve T cells. The cytokine profile of DCs is dependent on the stimuli they sense and is required to trigger the differentiation of T cells into different effector T cell types [113]. The ability to sense invading microorganisms or endogenous “danger” signals is given through pattern-recognition receptors (PRR) like the most widely studied toll-like receptors (TLR), which recognize PAMPs [113, 114].

1.6.2 Ontogeny and subtypes of dendritic cells

DCs are located throughout the body and different subsets of DCs exist in distinct locations [115]. Mammalian DCs can be categorized into the four major classes (see Fig. 1.6): plasmacytoid DC (pDC), the conventional DCs cDC1 and cDC2, and monocyte-derived DC (moDC). The different DC subpopulations are derived from hematopoietic stem cells, which have to go through a series of fate decisions following a hierarchy of

multipotent progenitors. While the DC subgroups pDC, cDC1 and cDC2 can be traced back to a phenotypically defined population, called common dendritic cell progenitor (CDP), monocyte-derived DCs are a distinct entity [116]. Recently, the view on the classical model changed in a way, that every cell of every progenitor population does not have equal potential for two mutually exclusive fates, but that the lineage is already primed in early progenitors. This means that a progenitor population has a common phenotype, but the cells have just a distinct developmental pathway [116].

The different DC subsets contribute to a sophisticated network necessary for a comprehensive interaction with different populations of lymphocytes. pDCs are primarily equipped to respond to viral infections. Thus, the major physiological function is a high production of type I interferons (IFN) after sensing viral antigens [117]. Human cDC1s are found in lymph nodes, bone marrow, tonsil and blood, and they are competent to cross-present viral antigens via MHC-I. They also express high levels of TLR3, IL-12p70 and IFNβ, which confers them the ability to activate $CD8^+$ T cells and to promote T helper type 1 (Th1) response [118]. The $CD141^+$ cDC1 are supposed to be the equivalents to the mouse $CD8^+$ DCs [119]. The human cDC2 cells are the major population of myeloid DCs in blood, tissues and lymphoid organs [116]. The frequency of the single cDC subsets and the ratio of cDC2/cDC1 are further dependent on the type of tissue. For instance, circulatory DCs have a low cDC1 frequency with a high cDC2/cDC1 ratio, while lymphoid tissues have a cDC2/cDC1 average ratio of 2:1 [120]. They are equipped with a wide range of toll-like receptors (TLRs: TLR2, 4, 5, 6 and 8), NOD-like receptors (NOD2, NLRP1, NLRP3 and NAIP) and RIG-I-like receptors [116, 121]. Accordingly, cDC2s are able to activate Th1, Th2, Th17 and $CD8^+$ T cells *in vitro,* implying their role in a wide range of immune responses *in vivo*, as well. Just recently, a human cDC2 subgroup was described. Human $CD1c^+$ cDC can be distinguished by their CD5 expression, with $CD5^{high}$ DCs showing a higher migration towards CCL21 and stronger induction of IL-10, IL-22 and IL-4 producing T cells. In contrast, $CD5^{low}$ DCs induce higher levels of IFN-γ producing T cells [122].

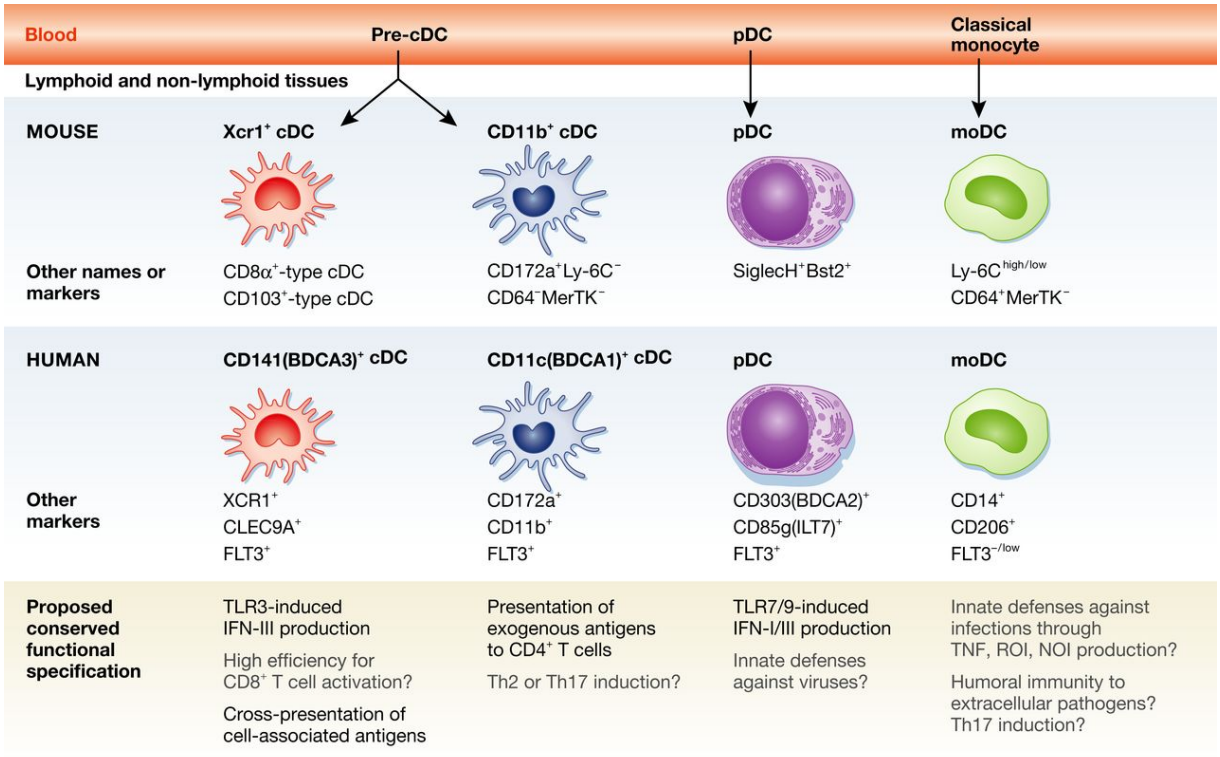

Figure 1.6 DC subsets in human and mice. The main DC subsets are the conventional DCs, which are further subdivided in cDC1 (mouse: Xcr1+, human: CD141+) and cDC2 (mouse: CD11b+, human: CD11c+), the plasmacytoid DCs and the monocyte-derived DCs. Adapted from Ref [113]

In mice it was demonstrated that under inflammatory conditions, monocytes can be recruited to the site of infection and can differentiate into moDCs [123, 124], which are also referred to as inflammatory DCs (infDC). Because of their rapid recruitment and the high cytokine expression they are thought to play an important role in the initiation of inflammation and to be a crucial reservoir of APC [125]. Although in humans, the evidence of monocytes differentiating to DCs is still lacking, human infDCs, which could be the counterparts to mouse infDC, were identified. In the synovial fluid of Rheumatoid Arthritis patients as well as in inflammatory tumor ascites from breast and ovarian cancer patients, a DC population was characterized, which shared gene signatures with moDCs [126, 127]. Furthermore, the study of Segura *et al.* showed, that the infDCs stimulated CD4+ T cells and induced a Th17 cell differentiation [127]. Additionally, in the context of gluten-induced inflammation in celiac disease patients, a DC subset was described in the gut mucosa, which could potentially be derived from newly recruited monocytes because of the CCR2 and CD14 expression [128]. Although it needs further investigations to clarify the origin of these infDCs, it is long known, that monocytes can be differentiated to moDCs *in vitro* in the presence of granulocyte-macrophage colony-

stimulating factor (GM-CSF) and interleukin-4 (IL-4) [129], so that *in vitro* generated DCs are the best-studied human DC subsets [125].

1.6.3 TLR signaling in dendritic cells

There are 10 known TLRs in human, which can be largely classified into two subfamilies based on their localization. TLR1, TLR2, TLR4, TLR5, TLR6 and TLR10 are localized on the cell surface, whereas TLR3, TLR7, TLR8 and TLR9 are intracellular receptors present in the endosome [130]. The TLR members recognize different PAMPs with surface TLRs mainly recognizing microbial membrane components and intracellular TLRs sensing viral and bacterial nucleic acids. Upon ligand binding, TLRs dimerize and translate the signal to different downstream signaling pathways by recruiting TIR-domain-containing adaptor molecules, such as myeloid differentiation primary response 88 (Myd88), TIR-associated protein (TIRAP)/MyD88-adaptor-like (MAL) and TIR-domain-containing adaptor protein-inducing IFNβ (TRIF)[114].

In general, TLR signaling can be divided into the MyD88-dependent and TRIF-dependent pathways. MyD88, which is utilized by all TLRs upon stimulation with the exception of TLR3, associates with the cytoplasmic portion of TLRs and complexes with IL1-R-associated kinase 4 (IRAK4) and IRAK1. IRAK4 activates IRAK1 via phosphorylation, which in turn associates with the E3 ubiquitin ligase TNFR-associated factor 6 (TRAF6). Together with an ubiquitin-conjugating enzyme complex consisting of UBC13 and UEV1A, TRAF6 promotes K63-linked polyubiquitination of TRAF6 itself and of the TAK1 protein kinase complex, which leads to the activation of TGFβ activated kinase 1 (TAK1). Subsequently, TAK1 phosphorylates and activates inhibitor of nuclear factor kappa-B kinase subunit beta (IKK-β) and MAP2K6, which results in the activation of MAPK and of the transcription factor nuclear factor kappa-light-chain-enhancer of activated B cells (NFκB), which in turn regulate the expression of cytokines, chemokines and type I IFN [114, 130].

The TRIF-dependent pathway occurs after TLR3 or TLR4 activation and leads to the activation of IRF3 and to the induction of type I IFN production [114]. In general, IFN-I production is restricted to TLR4 as well as to TLR3 and the other nucleic acid sensing TLRs, although these receptors mediate it via a MyD88-dependent activation of IRF7 [113, 131].

1.7 MAPK signaling in dendritic cells

As already mentioned, DCs express different TLRs, which enable them to respond to different stimuli and to induce different Th responses. For example, the TLR4 ligand *Escherichia coli* lipopolysaccharide (LPS) and TLR5 ligand flagellin, trigger a Th1 response, while schistosome egg Ags (SEA) [132], and certain forms of *Candida albicans* activate mainly Th2 responses [133]. In a study by Agrawal *et al.* a correlation between the distinct Th responses and the differential modulation of the MAPK p38, JNK and ERK1/2 was shown. First, they observed that different types of stimuli generated distinct cytokine profiles. Stimulation with *Escherichia coli* LPS and flagellin induced strong IL-12p70 and TNFα, while stimulation with the TLR2 ligand Pam3cys induced low IL-12p70 and reduced TNFα levels. Second, the duration of p38 and JNK phosphorylation was enhanced upon TLR4 and TLR5 activation, while TLR2 activation via Pam3Cys caused a higher and more sustained ERK1/2 phosphorylation. In correlation with this, blocking p38 or JNK with inhibitors largely abrogated IL-12p70 production, whereas chemical inhibition of ERK1/2 enhanced IL-12p70 production [132]. The review article by Nakahara *et al.* summarizes and compares the role of the three MAPK p38, JNK and ERK1/2 during human DC maturation revealed with help of kinase-specific inhibitors (Fig. 1.7). Various maturation stimuli activate the three MAPK p38, JNK and ERK1/2 signaling pathways during monocyte-derived DC maturation, but they seem to have different consequences. While p38 is apparently essential for the complete maturation into functional DCs, JNK inhibition negatively influences the surface antigen expression and cytokine secretion, but not the allostimulatory function of DCs. In contrast, ERK1/2 signaling negatively regulates phenotypic maturation, IL-12 production and allostimulatory capacity of monocyte-derived DCs to some degree, while it positively regulates inflammatory cytokine production.

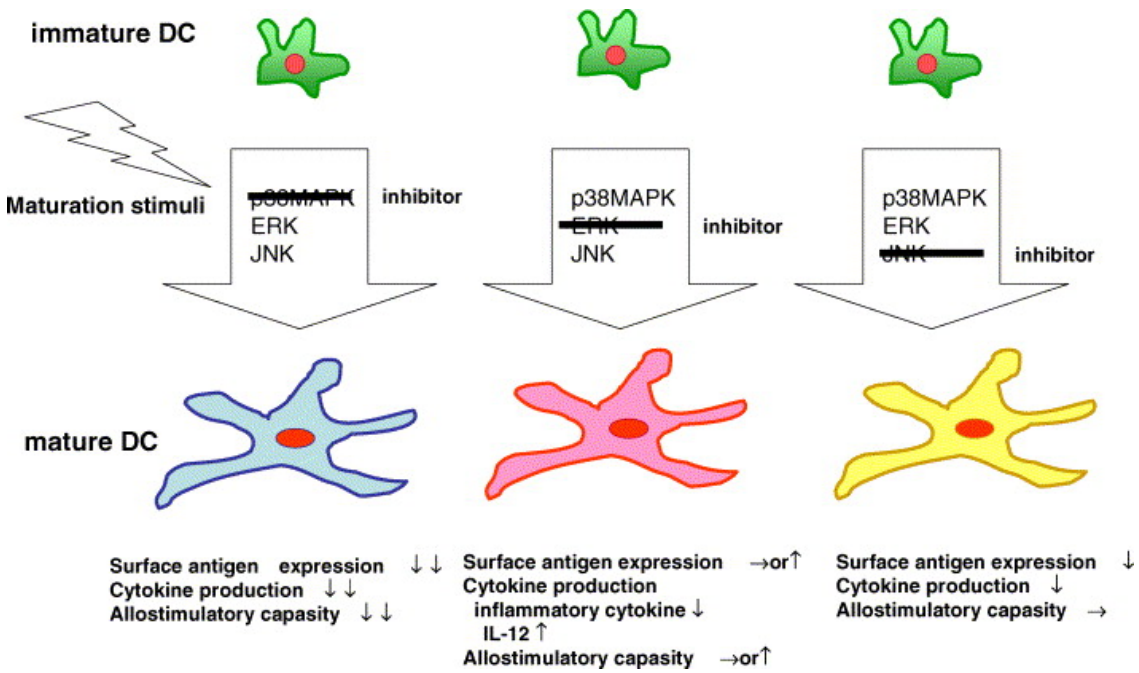

Figure 1.7 Blocking p38, JNK or ERK by using inhibitors have different effects on human DC maturation. Adapted from Ref [134]

Consequently, the balance of phosphorylation of the three MAPKs could be critical for a sufficient DC maturation and for the development of distinct DCs, which induce an optimal immune response [134]. The study of Puig-Kröger *et al.* further suggested, that the inhibitory effect of ERK1/2 on DC maturation could be the result of the negative regulation of NFκB-dependent gene expression by ERK1/2. NFκB-signaling is essential for DC maturation and ERK1/2 inhibition augmented the DNA-binding activity of NFκB as well as the IκBα level itself, which is known to increase during DC maturation [135]. In contrast to this, Resicgno *et al*. showed that ERK1/2 inhibition did not impede DC maturation or NFκB nuclear translocation, but negatively influenced DC survival [136].

1.8 Aim of the study

Kinases constitute the major part of the "druggable genome" and deregulation in the function of the kinome is either directly or indirectly related to nearly 400 human diseases [137, 138]. The interest in understanding the biology of the kinases was provoked because of the success of ATP competitive and non-competitive inhibitors against oncogenic kinases in genetically defined human cancers. While a lot of studies have focused on uncovering the role of the kinases in tumorigenesis, relatively less is known on the physiological role of the kinome in the regulation of the immune system.

Until 2016, the FDA has approved 28 kinase inhibitors for targeted therapeutics [84]. However; the function of the targeted kinases in immune regulation is not well understood.

MAPK pathways are usually activated in a three tier-signaling cascade where the effector MAPK typically activates the transcription of target genes by phosphorylating transcription factors [2, 3]. Among the 14 MAPKs, the classical MAPK signaling pathway consisting of RAF-MEK1/2-ERK1/2 gained enormous interest as it is often deregulated in human cancer controlling tumor cell proliferation, migration and metastasis [3]. RAS [72] and BRAF [75] are among the most frequent oncogenes and mutations lead to the hyperactivation of the ERK1/2 pathway. Drugs targeting the activated form of BRAF have shown enormous clinical success. However, in patients that carry RAS mutations, these drugs unexpectedly induce MAPK activation by triggering RAF dimerization and leading to paradoxical MAPK activation [90].

In my thesis I aim to evaluate the role of the classical RAF-MEK1/2-ERK1/2 pathway in the regulation of immune responses. MAPKs are fundamental kinases that regulate basic cellular processes like proliferation, migration, differentiation and cell death. Consequently, it is to be expected that inhibition of these kinases may, besides affecting tumor cells, exhibit unknown effects on cells of the immune system like on dendritic cells. Dendritic cells represent the bridge between the innate and adaptive immune system and are required for T cell mediated-cancer immunity. Since the immune system plays an important role in successfully combating cancer it is beneficial to know, how the administered inhibitors could alter the immune response. I initially focused on the role of RAF-MEK1/2-ERK1/2 pathway in dendritic cells and worked with a well-established *in vitro* culture, in which human monocytes purified from healthy donors were differentiated to moDCs in presence of GM-CSF and IL-4. Since there is not much known on RAF kinases and their role in moDCs, RAF activation and regulation was investigated. Further, a variety of RAF and MEK inhibitors were employed to examine the effect on the phenotypical maturation of moDCs. Functional consequences caused by the inhibitor treatment were stated through the investigation of moDC induced T cell activation. Additionally, direct effects of the inhibitors on the proliferation of $CD4^+$ T cells were studied. The obtained data on human moDCs were initially verified with murine BMDCs. After observing comparable effects on human moDCs and murine

BMDCs after RAF inhibition an *in vivo* study was performed to evaluate the physiological role of RAF inhibitors on the activation of DCs from spleen and LN *in vivo*.

2 Material and Methods

2.1 Molecular Biology Methods

2.1.1 Vector, constructs and primer

Vector:

pcDNA3 Dest 40	ThermoFisher Cat. No. 12274015
pDONR223 ARAF	Addgene Cat. No. 23725
pDONR223 CRAF	Addgene Cat. No. 23832

Constructs:

pcDNA3/V5-CRAF (WT)
pcDNA3/V5-CRAF (R401H)
pcDNA3/V5-CRAF (S296A)
pcDNA3/V5-CRAF (S296D)
pcDNA3/V5-CRAF (S301A)
pcDNA3/V5-CRAF (S301D)
pcDNA3/V5-CRAF (S296/301A)
pcDNA3/V5-CRAF (S296/301D)
pcDNA3/V5-ARAF (WT)
pcDNA3/V5-ARAF (Y301/302D)
pcDNA3/V5-ARAF (R362H)
pcDNA3/V5-ARAF (S257A)
pcDNA3/V5-ARAF (S257D)

Oligonucleotides/mutagenesis primers:

hCRAF S296A fw	5'-cagattgttgggggcactggacagggctgaagg-3'
hCRAF S296A rv	5'-ccttcagccctgtccagtgcccccaacaatctg-3'
hCRAF S296D fw	5'-ctcagattgttggggtcactggacagggctgaaggtg-3'
hCRAF S296D rv	5'-caccttcagccctgtccagtgaccccaacaatctgag-3'
hCRAF S301A fw	5'-gaccagcctgttggggccagattgttggggct-3'
hCRAF S301A rv	5'-agccccaacaatctggccccaacaggctggtc-3'
hCRAF S301D fw	5'-gtgaccagcctgttgggtccagattgttggggctac-3'
hCRAF S301D rv	5'-gtagccccaacaatctggacccaacaggctggtcac-3'
hARAF S257A fw	5’-gctggctgggctgggggccccccgggggggttccatc-3’

hARAF S257A rv	5’-gatggaacccccgggggcccccagcccagccagc-3’
hARAF S257D fw	5'-ctgggctggggtccccccgggggg-3'
hARAF S257D rv	5'-ccccccgggggacccagcccag-3'

Oligonucleotides/sequencing primers:

CRAF (738-) fw	5’-caccacaacacacaactttgctcgga-3’
ARAF S432D fw	5’-catcatccaccgagatctcaaggataacaacatcttcctacatgac-3’

Real time PCR primer:

18S	5'-agaaacggctaccacatcca-3’ / 3'-caccagacttgccctcca-5’
CRAF	5'-acagatattctacacctcacg-3’ / 3'-aattgcatcctcaatcatcc-5’
ARAF	5'-cccatcttgacaaaatctaagg-3’ / 3'-ccttgtctagagagtcgtag-5’
BRAF	5'-atatctggaggcctatgaag-3’ / 3'-ctgaaagagatgaaggtagc-5’
IL-12A	5'-atgagagttgcctaaattcc-3’ / 3'-cataaaagaggtctttctggag-5’
IL-12B	5'-agaaagatagagtcttcacgg-3’ / 3'-aagatgagctatagtagcgg-5’
TNFα	5'-aggcagtcagatcatcttc-3’ / 3'-ttatctctcagctccacg-5’
IL-6	5'-gcagaaaaaggcaaagaatc-3’ / 3'-ctacatttgccgaagagc-5’
CCR7	5'-ttgtcattttccaggtatgc-3’ / 3'-aatgatggagtacatgataggg-5’

2.1.2 Site directed Mutagenesis and plasmid generation

The point mutations in ARAF (S257A, S257D) and CRAF (S296A) were generated using the *Pfu* Polymerase (Cat. No. 600250, Agilent Technologies). In case of CRAF S296D the Q5® High-Fidelity DNA Polymerase (Cat. No. M0491S, New England Biolabs) was employed. The contents of the mutant strand synthesis PCR reaction was set up as listed in following table 2.1.

Tab.2.1 PCR reaction mix for site directed mutagenesis

Components	**Final concentration**
Buffer	1x
Forward primer (10 µM)	0.2 µM
Reverse primer (10 µM)	0.2 µM
dNTP (10 mM)	0.2 mM
Template DNA	40 ng
Pfu Polymerase 2,5 U/µl	0.05 U/µl
OR	
Q5® High-Fidelity DNA Polymerase	0.02 U/µl
ddH2O	Ad 50 µl

The pDONR223 ARAF (Cat. No. 23725, Addgene) and pDONR223 CRAF (Cat. No. 23832, Addgene) were used as template DNA. The timings for the PCR reaction are summarized in table 2.2.

Tab.2.2 Thermocycling conditions

	Temperature Pfu Polymerase	**Temperature Q5 Polymerase**	**Time**	**Repeats**
Initial denaturation	95°C	98°C	3 min	1x
Denaturation	95°C	98°C	30 s	
Annealing	58°C	58°C	1 min	25x
Extension	68°C	72°C	7 min	
Final extension	68°C	72°C	10 min	1x
Cool Down	4°C	4°C	unlimited	

The parental DNA template was digested by the endonuclease *Dpn-I*. The residual, mutation-containing, synthesized DNA was transformed into chemocompetent *E. coli* bacterial cells. Therefore, *E. coli* were incubated with the DNA for 30 min on ice, heat shocked at 42°C for 90 s and cooled for additional 5 min on ice. After adding 500 µl of antibiotic free LB-medium (Cat. No. 4425, Applichem), the bacterial cells were shaken at 37°C, 350 rpm for 1 h before they were plated on antibiotic containing LB agar plates. The used pDONR223 carries the bacterial selection marker spectinomycin (Sigma). Single colonies were expanded in antibiotic containing LB medium at 37°C for a minimum of 16 h. The GeneJET DNA purification Kit (Thermo Scientific) was subsequently used to purify the respective plasmids. After the confirmation of the inserted point mutation by DNA sequencing (GATC), a clonase reaction to transfer the gene of interest (wild type and mutated gene) into the destination vector pcDNA3 Dest 40 was performed using a Gateway® LR Clonase® II Enzyme mix (Cat. No. 11791-020, Thermo Fisher) according to manufacturer's instructions. The pcDNA3 vector carrying the insert was again heat shock transformed and propagated in *E. coli* bacterial cells in the presence of ampicillin (Cat. No. A0839, Applichem), as the expression vector carries it as bacterial selection marker. The purified plasmids were used for overexpression studies.

2.2 Cell Biology Methods

2.2.1 Cell lines

The following cell lines (Tab. 2.3) were used to establish the RAF inhibitor LY3009120 (Cat. No. S7842, Selleckchem).

Tab.2.3 List of cancer cell lines

Cell line	Origin	RAS status	Source
HeLa	human epithelial adenocarcinoma	Kras WT	DSMZ
Calu-1	human epidermoid lung carcinoma	Kras mutated	Sigma Aldrich
MDA-MB231	human epithelial breast adenocarcinoma	Kras mutated	DSMZ
HCT-116	human colorectal carcinoma	Kras mutated	Gift from Ulf Rapp
NCI-H226	human squamous cell carcinoma	Kras WT	ATCC

HeLa, Calu-1, MDA-MB231 and HCT116 cell lines are cultured in Dulbecco's Modified Eagle Medium (DMEM) (Cat. No. 11965092, Gibco) supplemented with 10% fetal calf serum (FCS) (Cat. No. 51437093, Life Technologies), while H226 cells were grown in Rosewell Park Memorial Institute (RPMI) medium (Cat. No. R8758, Gibco) containing 10% FCS. For routine passaging, cells were trypsinized and splitted at ratios ranging from 1:5 to 1:10. All cell lines were kept at 37°C and 5% CO_2.

To determine the optimal working concentration of the RAF inhibitor LY3009120, a concentration gradient (0 – 10 µM) was performed. HeLa cells were seeded in 6-well plates (2.5 x 10^5/well) and were allowed to adhere over night. After a washing step with PBS, HeLa cells were treated with different concentrations of the inhibitor in medium without FCS. Cells were lysed after 6 h of inhibitor treatment in RIPA lysis buffer.

The influence of the LY3009120 inhibitor on the MAPK signaling pathway was investigated in HeLa, Calu-1 and MDA-MB231 seeded in 6-well plates (2.5 x 10^5/well) and treated with the LY3009120 inhibitor (1 µM) or with DMSO for 6 h in starvation medium. Cells were lysed either immediately after the treatment or after stimulation with EGF for 5 min (Cat No. RP-10927, Thermo Fisher Scientific).

To investigate the effect of the MEK inhibitor trametinib and the RAF inhibitor LY3009120 on the proliferation of the listed cell lines, 8000 cells per well were seeded in 96-well plates and incubated over night. The next day medium was changed to

inhibitor containing medium. After 72 h metabolic activity was measured using the MTT assay. All cell lines were authenticated.

2.2.2 Transient transfection

For transient overexpression experiments 2×10^5 HEK293T cells/well (gift from Andreas Ernst) were seeded in a 6-well plate and were allowed to adhere for minimum of 16 h. Transfection with various plasmids was performed using polyethylenimine (PEI; Cat. No. 23966, Polysciences Inc.) as the transfection reagent. Therefore, 1 µg DNA was transfected with 5.4 µl of 10 mM PEI. Analyses were performed 48 h after transfection.

2.2.3 Generation of human monocyte-derived dendritic cells

In accordance with the Declaration of Helsinki and with approval by the local ethical committee (Landesaerztekammer Rheinland-Pfalz) buffy coats were received from healthy volunteers at the University Medical Center Mainz. PBMCs were obtained from buffy coats following standard procedures [139] and were kindly provided by Helmut Jonuleit's group (Department of Dermatology of the University Medical Center of the Johannes Gutenberg-University Mainz, 55131 Mainz, Germany). Monocytes were isolated based on their ability to adhere. 1.5×10^6 cells were seeded in pre-warmed RPMI medium containing 1% autologous plasma (gained from buffy coats) per well of a 6-well plate. The cells were allowed to adhere to the plastic surface of a plate for 20 min at 37°C. Non-adherent cells were removed and the remaining adherent cells were differentiated into moDCs in X-VIVO-15 medium (Cat. No. BE04-418Q, Lonza) supplemented with 1% autologous plasma, 400 IU/ml human GM-CSF (Leukine, Sanofi) and 200 IU/ml recombinant human IL-4 (Cat. No. 11340045, Immunotools). After two days, 1 ml medium was replaced by 1 ml fresh X-VIVO-15 medium supplemented with 1% autologous plasma, 800 IU/ml GM-CSF and 200 IU/ml IL-4. Immature DCs were harvested on day 5 of culture and $1\text{-}2 \times 10^6$ cells were seeded per well of a 6-well plate in medium supplemented with 1% plasma, 400 IU/ml GM-CSF and 200 IU/ml IL-4 for further treatment.

2.2.4 Generation of mouse dendritic cells derived from bone marrow

Bone marrow of C57BL/6J mice was isolated by cutting the ends of femur and tibia and flushing the bone cavities with Phosphate Buffer Saline (PBS, pH 7.4), supplemented with 1% FCS using a 23G cannula. The bone marrow was collected in a 50 mL tube and centrifuged at 1300 rpm for 10 min, followed by lysis of erythrocytes by a two-minute incubation in Greys lysis buffer. The reaction was stopped by adding PBS with 1% FCS. The cell suspension was filtered through a 40 µm cell strainer (Greiner Bio-one) and the obtained cells were resuspended in IMDM culture medium (Iscove's Modified Dulbecoo's Medium, 5% FCS, 2 mM L-glutamine, 1% sodium pyruvate). Cells were seeded in 6-well non-adherent plates (3-6 x 10^6/well) and culture medium was supplemented with 1% GM-CSF and 2.5 ng/ml recombinant murine IL-4 (Cat. No. 12340043, Immunotools). On day 3 and day 5, medium changes were performed to remove non-adherent cells and to supplement cultures with fresh medium containing GM-CSF and IL-4. Immature DCs were harvested on day 7 of culture. For further treatment 2 x 10^6 cells/well were seeded into non-adherent 6-well plates and cultured in medium containing GM-CSF (1%) and IL-4 (2.5 ng/ml).

2.2.5 Stimulation and treatment of dendritic cells

To investigate the role of MAPK signaling in DCs of human and murine origin, inhibitors blocking components of the MAPK signaling were added to the cultures. LY3009120 (1 µM, Cat. No. S7842, Selleckchem), GDC-0879 (1 µM, Cat. No. S1104, Selleckchem), Raf265 (0.5 µM, Cat. No. S2161, Selleckchem), Kobe 0065 (10 µM, Cat. No. S8303, Selleckchem) and PLX4720 (10 µM, Cat. No. S1152, Selleckchem) were employed to block RAF Kinases. Trametinib (1 µM, Cat. No. S2673 Selleckchem) was used to block MEK1/2. All inhibitors were dissolved in DMSO.

Unless otherwise stated, immature DCs were treated with the inhibitors in the presence or absence of LPS stimulation (100 ng/ml, Cat. No L6143, Sigma) for 48 h and used for further analyses. Alternatively, DCs were stimulated with Pam3CSK4 (1 µg/ml, Cat. No. tlrl-pms, InvivoGen), Poly(I:C) (50 µg/ml, Cat. No. 27-4732-01, GE Healthcare) or with a combination of LPS and PGE_2 (1 µg/ml, Cat. No. 14010, Cayman, solved in X-VIVO-15/10% ethanol).

In order to investigate the ubiquitiniation of proteins during the differentiation of human monocytes to moDCs, cells on day 3 or day 5 of culture were treated with the proteasome inhibitor MG132 (10 µM). Cells were lysed after 6 h treatment and employed for immunoprecipitation (chapter 2.3.4) and/or immunoblot analysis (chapter 2.3.3).

2.2.6 Transfection of siRNAs

Immature, human moDCs were harvested and 0.6 x 10^6 cells/well were seeded in a 12-well plate. ARAF, BRAF and CRAF expression was silenced by transfection of validated siRNAs. To silence two RAF proteins at once, siRNAs were combined with each other. The mixture of two siRNAs was transfected using SaintRed. Each siRNA was employed at a concentration of 60 nM. A scrambled control siRNA, which served as a negative control, was transfected at a final concentration of 120 nM. The medium was changed 24 h after transfection and moDCs were stimulated for 30 h with LPS (100 ng/ml).

The siRNAs were purchased from Qiagen:

siControl (sense): 5´-UUCUCCGAACGUGUCACGU-3´ (Cat. No. 1027310)
siARAF (sense): 5´-GACUCAAGGGACGAAA-3´ (Cat. No. SI00287686)
siBRAF (sense): 5´-GCUAGAUGCACUCCAACAATT-3´ (Cat. No. S102632945)
siCRAF (sense): 5´-GGAUGUUGAUGGUAGUACA-3´(custom-made)

2.2.7 DTME Crosslinking

In an initial experiment, the working concentration of the cross-linker Dithio-bismaleimidoethane (DTME) was determined by treating moDCs (after 24 h LPS stimulation) with DTME concentrations at 0.05 mM, 0.1 mM or 0.2 mM for 30 min at 37°C. Cells treated with DMSO served as control. After a 10 min incubation with 1 M Tris (pH = 7.5), cells were thoroughly washed with PBS and lysed in sample buffer without Dithiothreitol (DTT). In order to cleave the DTME crosslinker 100 mM DTT was added to one half of the lysate and heated for 15 min at 95 °C.

In subsequent experiments, DTME was employed at a 0.2 mM concentration. Instead of lysing cells directly in sample buffer, cells were lysed in IP-buffer to precipitate CRAF according to the protocol described in section 2.3.4.

2.3 Biochemical Methods

2.3.1 Liquid chromatography-mass spectrometry (LC-MS)

Phosphoproteomics:

Liquid chromatography-mass spectrometry was perforemd to compare the phosphoproteome of human monocytes with moDCs. Monocytes were isolated from buffy coats and cultured for 24 h in X-VIVO-15 medium supplemented with 1% plasma. MoDCs were harvested on day 5 as described earlier. Cells were washed with PBS, lysed in RIPA buffer for 30 min on ice, frozen at -80°C until further use. The subsequent sample preparation and mass-spectrometric analysis was performed in Bernd Thiede's lab (Biotechnology Centre of Oslo, University of Oslo, 0317 Oslo, Norway). The cell lysates were precipitated with six volumes of acetone overnight, centrifuged at 13000 rpm for 10 minutes and air dried. The protein pellet was dissolved in 200 µl of 6 M urea in 100 mM ammonium bicarbonate. To the dissolved protein was added 10 µl of 200 mM DTT in 0.1 M Tris-HCl, pH 8 and incubated at 30°C for 30 minutes. 30 µl of freshly prepared 200 mM iodoacetamide was added and the sample was incubated at room temperature in the dark for 1 hour. Subsequently, 40 µl of 200 mM DTT was added and incubated at 30°C in 30 minutes. The sample was then diluted with 960 µl of 50 mM ammonium bicarbonate before 10 µg of trypsin GOLD (Promega, Madison, WI, USA) was added and incubated at 37°C for 16 h. The digestion was finally quenched by adding 20 µl formic acid (50%) and peptides were cleaned by SPE using a Strata C18-E cartridge (55 µm, 70 Å, Phenomenex, Værlose, Denmark). Phosphopeptides were enriched using TiO_2 beads (Titansphere, TiO_2, GL Sciences Inc, Japan) as previously described [140]. The tryptic phosphopeptides were dissolved in 10 µl 0.1% formic acid/2% acetonitrile and 5 µl were analyzed using an Ultimate 3000 RSLCnano-UHPLC system connected to a Q Exactive mass spectrometer (Thermo Fisher Scientific, Bremen, Germany) equipped with a nano-electrospray ion source. For liquid chromatography separation, an Acclaim PepMap 100 column (C18, 2 µm beads, 100 Å, 75 µm inner diameter, 50 cm length) (Dionex, Sunnyvale CA, USA) was used. A flow rate of 300 nL/min was employed with a solvent gradient of 4-35% B in 180 min. Solvent A was 0.1% formic acid and solvent B was 0.1% formic acid/90% acetonitrile. The mass spectrometer was operated in the data-dependent mode to automatically switch between MS and MS/MS acquisition.

Survey full scan MS spectra (from m/z 400 to 2,000) were acquired with the resolution R = 70,000 at m/z 200, after accumulation to a target of 1e6. The maximum allowed ion accumulation times were 60 ms. The method used allowed sequential isolation of up to the ten most intense ions, depending on signal intensity (intensity threshold 1.7e4), for fragmentation using higher-energy collisional induced dissociation (HCD) at a target value of 1e5 charges, NCE 28, and a resolution R = 17,500. Target ions already selected for MS/MS were dynamically excluded for 30 sec. The isolation window was m/z = 2 without offset. For accurate mass measurements, the lock mass option was enabled in MS mode.

Data were acquired using Xcalibur v2.5.5 and raw files were processed to generate peak list in Mascot generic format (*.mgf) using ProteoWizard release version 3.0.331. Database searches were performed using Mascot in-house version 2.4.0 to search the SwissProt database (Human, 20,279 proteins) assuming the digestion enzyme trypsin, at maximum one missed cleavage site, fragment ion mass tolerance of 0.05 Da, parent ion tolerance of 10 ppm, carbamidomethylation of cysteines as fixed modification, and phosphorylation of serines, threonines, and tyrosine, oxidation of methionines, and acetylation of the protein N-terminus as variable modifications. Scaffold (version Scaffold_4.4.8, Proteome Software Inc., Portland, OR) was used to validate MS/MS based peptide and protein identifications. Peptide identifications were accepted if they could be established at greater than 99.0% probability by the Scaffold Local FDR algorithm. Protein identifications were accepted if they could be established at greater than 99.0% probability and contained at least one identified peptide.

The criteria of phoshphopeptides, which were exclusively detected in monocytes or moDCs, were the detection of the peptide in all three biological replicates. The corresponding proteins of the phospho-peptides, which were exclusively detected in moDCs, was done using the Panther Classification System with the settings “GO:Slim Molecular Function”.

Identification of new RAF substrates:

The precipitate of cross-linked CRAF from LPS-stimulated human moDCs (see section 2.2.7) was analyzed by liquid chromatography-mass spectrometry. Immunoprecipitates with a non-specific IgG antibody served as control. In collaboration with Stefan Tenzer’s lab (Institute for Immunology, University Medical Center of the Johannes Gutenberg

University, 55131 Mainz, Germany), two biological replicates were measured and of each three technical replicates were made. Once, immobilized proteins on protein A/G agarose beads were directly eluted from the agarose beads by incubating in 40 µl of 2% (w/v) SDS in 50 mM ammonium bicarbonate at 60°C for 15 min. Supernatants (ca. 30 µL) were collected in fresh tubes. Another 30 µL of SDS buffer were added and the beads were again incubated at 95°C for 15 min. Supernatants were collected in separate tubes. Both eluates were further denatured by incubating at 95°C for 5 min. The samples were processed by single-pot solid-phase-enhanced sample preparation (SP3) [141] according to a modified protocol [142]. The other biological sample was first loaded on a 7.5 % polyacrylamide gel, which was stained with Instant Blue (Cat. No. ISB1L, Expedeon) and the respective gel bands for cross-linked CRAF were excised, cut into cubes (ca. 1 cm^3) and transferred to 1.5 ml Protein LoBind tubes (Eppendorf). 200 µl of 100 mM ammonium bicarbonate/acetonitrile (1:1, v/v) was added to the gel pieces, samples were incubated in a sonication bath for 5 min and supernatants were withdrawn. After repeating this step, gel pieces were shrinked with 200 µl of acetonitrile during 5 min incubation in a sonication bath. Subsequently, 100 µl of 10 mM DTT in 50 mM ammonium bicarbonate was added, incubated at 56°C for 60 min and chilled down to room temperature. The supernatants were withdrawn. The samples were then diluted with 100 µl of 55 mM iodoacetamide IAA in 50 mM ammonium bicarbonate and incubated at room temperature in the dark for 1 hour. After adding 100 µl of 100 mM ammonium bicarbonate/acetonitrile (1:1, v/v), samples were incubated in a sonication bath for 5 min. Supernatants were withdrawn and the incubation with ammonium bicarbonate/acetonitrile (1:1, v/v) was repeated once more. The sample was dissolved in 100 µl of acetonitrile and incubated in a sonication bath for 5 min. Subsequently, proteins were digested at 37°C overnight by employing 25 µl of trypsin solution (0.01 µg/µL of trypsin (Serva) in 50 mM ammonium bicarbonate. Samples were diluted with 50 µl of 2% (v/v_{water}) formic acid/acetonitrile (1:1, v/v) and incubated in a sonication bath for 15 min. Supernatants were collected and the step was repeated once with the same buffer and a third time with 100 µl of acetonitrile. The supernatants of all steps were combined and freeze-dryed. The dried peptides were reconstituted in 20 µL of 1% (v/vH2O) formic acid for LC-MS analysis. Samples were analyzed using a NanoAQUITY UPLC system (Waters Corporation, Milford, MA) coupled on-line to a Synapt G2-S high definition mass spectrometer (Waters Corporation) equipped with an electrospray ion

source (Waters Corporation). 2.6 µl (max. vol.) of tryptic peptides were directly loaded onto a LC column (HSS-T3 C18 1.8 µm, 75 µm × 250 mm reversed-phase analytical column, Waters Corporation). Solvent A was 0.1% (v/v) formic acid and 3% (v/v) dimethyl sulfoxide in water and solvent B was 0.1% (v/v) formic acid and 3% (v/v) dimethyl sulfoxide in acetonitrile. A flow rate of 300 nL/min was employed with a solvent gradient of 5-40% (v/v) mobile phase B/A in 90 min. Tandem mass spectra were acquired in ion mobility-enhanced data-independent mode (UDMS^E) according to Distler et *al.* [143]. Raw data were processed using *Symphony v1.0.0.191* (Waters). Database searches were performed using UniProtKB Swiss-Prot Human proteome database (UniProt release 2018_09; 203,894 entries) assuming 2 missed cleavage sites per peptide, carbamidomethylation of cysteines as fixed modification and methionine oxidation as variable modification. . The false discovery rate was estimated by searching a reversed sequence database (target-decoy search strategy). Subsequent label-free quantification was performed with ISOQuant v1.8 as previously described [143]. Briefly, only peptides without missed cleavages and post-translational modifications, a minimum sequence length of 6 amino acids and a identification score of 6 were further considered for quantification. Protein quantities were calculated by averaging the three most intense peptide signals (Top3) for each protein with at least two identified peptides. A false discovery rate of 1% was accepted at the peptide and protein level.

2.3.2 Antibodies

Antibodies for Western Blot and Immunoprecipitation:

Antibodies used in this study recognize human antigens. Phosphorylated CRAF at S338 (rabbit monoclonal, Cat. No. 9427S), total CRAF (rabbit polyclonal, Cat. No. 9422), total ARAF (rabbit polyclonal, Cat. No. 4432), phosphorylated MEK1/2 at S217/S221 (rabbit monoclonal, Cat. No. 9154S), total MEK1/2 (rabbit polyclonal, Cat. No. 9122), phosphorylated ERK1/2 at Tyr202/Tyr204 (rabbit polyclonal, Cat. No. 9101) and total ERK1/2 (rabbit polyclonal, Cat. No. 9102) were purchased by Cell Signaling Technology. Total BRAF (mouse monoclonal, Cat. No. sc-5284) was obtained from Santa Cruz. The antibodies against the housekeeping genes GAPDH (mouse monoclonal, Cat. No. GTX627408) and Tubulin (mouse monoclonal, Cat. No. GTX628802) were purchased from GeneTex. Monoclonal mouse V5 antibody was purchased from Invitrogen (R960-25).

Immunoprecipitations of ARAF and CRAF were performed with mouse monoclonal antibodies purchased from Santa Cruz and BD Transduction Labs (Cat. No. 610151). Mouse IgG1 antibody from SantaCruz (sc3877) was used as IgG control in immunoprecipitation studies.

Antibodies for flow cytometry:

To characterize human moDCs following antibodies for flow cytometry were used and purchased from Biolgend: BV605 anti-human CD14 (Cat. No. 301833), BV605 mouse IgG2a (Cat. No. 400269), BV421 anti-human HLA-DR (Cat. No. 307635), BV421 mouse IgG2a (Cat. No. 400259), FITC anti-human CD80 (Cat. No. 305206), FITC mouse IgG1 (Cat. No. 400107), PerCP/Cy5.5 anti-human CD80 (Cat. No. 305231), PerCP/Cy5.5 mouse IgG1 (Cat. No. 400149), PE anti-human CCR7 (Cat. No. 353204), PE mouse IgG2a (Cat. No. 400213). PE anti-human CD86 (Cat. No. 555665), PE mouse IgG2b (Cat. No. 555743), APC anti-human CD83 (Cat. No. 551073), APC mouse IgG1 (Cat. No. 555751) were purchased from BD Bioscience.

The characterization of mouse bone marrow-derived DCs and of DCs from lymph node and spleen was done with following antibodies (Biolegend): FITC anti-mouse CD11c (Cat. No. 117306), FITC Armenian hamster IgG (Cat. No. 400906), Pacific Blue anti-mouse I-A/I-E (Cat. No. 107620,), Pacific Blue™ rat IgG2b (Cat. No. 400627), APC anti-mouse CD86 (Cat. No. 105012), APC Rat IgG2a (Cat. No. 400512), Brilliant Violet 605™ anti-mouse CD80 (Cat. No. 104729,), Brilliant Violet 605™ Armenian Hamster IgG (Cat. No. 400944), PE anti-mouse CCR7 (Cat. No. 120106), PE Rat IgG2a (Cat. No. 400508), BV510 anti mouse CD45 (Cat. No. 103137), BV510 rat IgG2b (Cat. No. 400645), PE anti-mouse CD11c (Cat. No. 117307), PE hamster IgG (Cat. No. 400907), FITC anti-mouse CD86 (Cat. No. 105109), FITC rat IgG2b (Cat. No. 400633), APC anti-mouse CD80 (Cat. No. 104714), APC hamster IgG (Cat. No. 400911)

2.3.3 SDS-PAGE and Western Blotting

Sodium dodecyl sulfate polyacrylamide gel electrophoresis (SDS-PAGE) is a technique to separate SDS-coated proteins by their molecular masses in an electric field. The electrophoresis is done with polyacrylamide gels, which compose of two layers: a 7.5-

12% separating gel (pH 8.8) and a 5% stacking gel (pH 6.8), to concentrate all proteins in one band before they enter the separating gel.

Cells were either lysed directly in 5x Laemmli buffer or RIPA lysates were diluted with Laemmli buffer. Lysates were boiled at 100°C for 5 min before loading onto polyacrylamide gels. The separated proteins were transferred to nitrocellulose membranes (Cat. No. 10401296, Whatman Protran) using the Wet/Tank Blotting System from Bio-Rad. For immunoblot analysis, membranes were blocked with 3% BSA in PBS with 1% Triton X-100 for 1 h at room temperature. The incubation with primary antibodies was done according to manufacturer's instructions. Horseradish peroxidase (HRP)-coupled secondary antibodies visualized the antigen-antibody complexes by enhanced chemiluminescence (Cat. No. WBKLS0500, Millipore). Quantification of Western Blots was performed by densitometry (ImageJ software). Total protein levels were normalized to the levels of a housekeeping gene or to the Ponceau S staining of the entire membrane. Changes in total protein levels during moDC differentiation are shown in relation to levels detected in monocytes. The amount of phosphorylated protein was quantified by determining the ratio of phosphorylated protein to total protein levels.

2.3.4 Immunoprecipitation

To immunoprecipitate endogenous proteins, 4 - 8 x 10^6 DCs were lysed in 500 - 800 µl IP buffer for 30 min on ice. After clearing the lysates by centrifugation for 15 min at 14000 rpm at 4°C the protein concentration was determined using Pierce 660 nm Protein Assay Reagent (Cat. No. 22660, Thermofisher Scientific). Endogenous CRAF, ARAF or BRAF was immunoprecipitated from 200 - 300 µg total protein, while rotating overnight at 4°C with a target-specific antibody. Antigen-antibody complexes were precipitated by agarose-coupled protein A/G beads (Cat. No. 11-134-515-001 and 11-243-233-001, Roche) while rotating for 3 h at 4°C. Beads were washed with IP buffer and bound proteins were analyzed by SDS-PAGE and subsequent immunoblotting.

V5-tagged ARAF WT and ARAF mutants (ARAF Y301/302D, ARAF R362H, ARAF S257A and ARAF S257D) were immunoprecipitated from 150 - 200 µg total protein by employing the V5 antibody. Immunoprecipitation was performed 48 h after transfecting HEK293T cells with the corresponding constructs (see section 2.2.2).

2.3.5 RAF kinase assay

Endogenous RAF proteins were immunoprecipitated from human immature moDCs and from moDCs stimulated with LPS for 1 h. Alternatively, RAF proteins were immunoprecipitated from DCs treated for 6 h with DMSO or LY3009120. In both cases, IgG control was included. Further, kinase activity of V5-tagged ARAF WT and ARAF mutants (ARAF Y301/302D, ARAF R362H, ARAF S257A and ARAF S257D) was investigated. Constructs were overexpressed in HEK293T cells and immunoprecipitated via the V5 tag. The empty vector served as control. After washing the agarose-coupled protein A/G beads used to pull out the antibody/antigen complexes, a reaction mix of 1x kinase buffer [10x buffer: 100 mM $MgCl_2$, 250 mM β-Glycerophosphate, 250 mM HEPES pH 7.5, 50 mM Benzamidine, 5 mM DTT, 10 mM $NaVO_3$; diluted to 1x with H_2O] and 1 µg of kinase dead His-MEK1 K97A (Cat. No. M02-16H, SignalChem) was added in a total volume of 38 µl. After adding MgATP (Enzo Lifesciences; stock: 20x; diluted to 1x), the reaction was incubated at 30°C for 30 min. For kinase assays with endogenous RAF proteins, each pull down was split into two samples with one receiving MgATP and one receiving H_2O as a control. Kinase assays were stopped by adding 10 µl of Laemmli buffer and were loaded onto a SDS-PAGE gel for immunoblot analysis.

2.3.6 mRNA Isolation, cDNA synthesis and qPCR

RNA from 1 - 2 x 10^6 cells was isolated using either RNA isolation kits (ThermoFisher/Roche) following the manufacturer's instructions or by TRIzol RNA extraction. Therefore, cells were washed with PBS and lysed in 1ml TRIzol (Ambion/ThermoFisher). After adding 200µl Chloroform, the samples were vortexed for 15 s, incubated for 2 min at room temperature and centrifuged at 14000 rpm for 15 min at 4°C. The upper aqueous phase was transferred to a tube containing 0.5 mL isopropanol and incubated for 10 min at room temperature followed by another centrifugation step of 15 min at 14000 rpm at 4°C. The pellet formed by the isolated RNA was washed once with 75% ethanol, air-dried and resuspended in appropriate amount of dH_2O. cDNA was synthesized from 1000 ng of the isolated RNA using the RevertAid First Strand cDNA Synthesis Kit (Cat. No. K1622, Thermo Scientific) and the supplied random hexamer primers.

All real-time PCR reactions were performed at least in triplicates on an iCycler (BioRad cxn96 or connect / Applied Biosystems Step One Plus) using EvaGreen (Cat. No. 27490, Axon). The mRNA levels of the housekeeping gene 18S were used for normalization and relative expression levels were calculated as ΔΔCt.

2.3.7 Cycloheximide chase Assay

Changes in protein stability during the differentiation process from human monocytes to moDCs were analyzed by a cycloheximide chase assay. The assay was performed on day 3 and on day 5 of culture. Cycloheximide (Cat. No. C-7698, Sigma) was added (100 µg/ml) to the cells, which were lysed in RIPA buffer after 1 h, 2 h, 4 h and 6 h. Protein lysates were analyzed by SDS-PAGE and subsequent immunoblotting.

2.4 Phenotypical and functional studies

2.4.1 Flow cytometry

Flow cytometry is a laser-based technique to analyze multiple features of cells at the same time - including cell size, cell shape and marker expression by fluorescent labeling: Single cells pass with high speed through an electronic detection apparatus. The forward scatter (FSC) corresponds to the scattered light detected almost in the direction of the original laser light. The FSC is dependent on the cell volume, thus measuring the cell size. In contrast, the sideward scatter (SSC) signal is recorded in a 90 degree angle to the laser, and thus reflects the cell's size and granularity. Cells with similar scattered light properties are defined as a cell population within a FCS-SSC plot. Additionally, fluorescently labeled antibodies allow the characterization of surface marker expression as well as the detection of intracellular targets.

For surface staining, the *in vitro* generated and treated DCs were washed with PBS and stained for 30 min at 4°C with the fluorescently labeled antibodies listed in section "Antibodies". To discriminate between live and dead cells, cells were simultaneously treated with the Fixable Viability Dye 780 (Cat. No. 65-0865-14, eBioscience). If cells were stained for CCR7 expression the incubation was done for 20 min at room temperature and 10 min at 4°C. After two washing steps with PBS, samples were acquired on a BD FACSCanto II and data were analyzed with BD FACSDiva software (version 6.0) and FlowJo software. The mean fluorescence intensities (MFI) of

independent experiments were quantified relatively to the corresponding controls (DCs treated with DMSO).

2.4.2 Cell Proliferation Assay

Cell proliferation and viability was determined using the Cell Proliferation Kit I (MTT, Cat. No 11465007001 ROCHE, SIGMA-ALDRICH) following the manufacturer's instructions. Cells seeded on 96-well plates were treated for 2 h with MTT. The presence of electron-coupling reagents causes cleavage of the tetrazolium salt MTT to the water-insoluble formazan salt. After solubilizing the formazan salt over night the absorbance at 570 nm was measured by absorbance plate reader.

2.4.3 Transwell migration assay

For transwell migration experiments, *in vitro* generated murine BMDCs were treated for 16 h with LPS or with LPS in presence of the RAF inhibitor LY3009120 or the MEK inhibitor trametinib, along with unstimulated control. In case of the human moDCs the stimulation was done with a combination of LPS and PGE_2 as the addition of PGE_2 led to an increased CCR7 expression.

After two washing steps with PBS, 4×10^5 cells were transferred in serum-free media into a 5 µm transwell migration chamber (Cat. No. 3421, Corning). The lower chamber was filled with serum-free media supplemented with 200 ng/ml recombinant CCL21 (human: Cat. No. 11343180, Immunotools; murine: Cat. No. 250-13, PeproTech) as chemo-attractant. The cells were left to migrate for 3 h and the number of successfully migrated bone-marrow derived DCs were counted using TC 20TM automated cell counter (BioRad #145-0101), while the amount of migrated human DCs was determined with an MTT Assay.

2.4.4 Morphological analysis using Phalloidin

1×10^6 human moDCs were seeded in 12-well plates and were treated for 24 h either with DMSO, LY3009120 or trametinib in the presence or absence of LPS (100 ng/ml). Treated cells were resuspended and 200 µl of the cell suspension were transferred into a 12-well plate assembled with Poly-L-lysine (Cat. No. P6282, Sigma) coated cover slips. The cells were allowed to adhere for 6 h. Subsequently, cells were washed twice with

PBS, fixed with 4% PFA (Roti histofix) for 10 min and permeabilized with 0.1% Triton-X100 in PBS for 5 min at room temperature. After two additional washing steps, cells were blocked with 1% BSA in PBS for 1 h at room temperature. F-actin was stained using the high affinity probe phalloidin conjugated to green fluorescent Oregon Green 488 dye (Cat. No. 07466, ThermoFisher). Staining was done with 4 U/ml phalloidin in blocking buffer for 20 min in the dark. After staining the nuclei with 2 µg/ml Hoechst dye for 5 min, cells were washed and mounted with Mowiol on cover slides. Cells were imaged using a Leica SP8 confocal microscope (63x, oil immersion objective, Oregon Green, excitation at 488 nm). The circularity of the cells was determined with ImageJ.

2.4.5 Enzyme-linked immunosorbent assay (ELISA)

The secretion of the pro-inflammatory cytokines IL-12p70, IL-6, IL-8, TNFα by human moDCs was measured by ELISA according to the manufacturer's instructions (BD Bioscience). After treating the DCs for 48 h with DMSO, LY3009120 or trametinib in presence of LPS, the supernatant was harvested and centrifuged for 10 min, at 15000 rpm (4°C). The supernatant of DCs treated just with DMSO served as a negative control.

2.4.6 Mixed lymphocyte reaction

The property of DCs to induce T cell proliferation was investigated with a mixed lymphocyte reaction. Human moDCs were treated with DMSO or LY3009120 in the presence or absence of LPS for 48 h. The treated DCs were harvested, washed with PBS and resuspended in X-VIVO-15 medium at a density of 0.5 x 10^6 cells/ml.

Simultaneously, $CD4^+$ T cells were isolated from PBMCs or purified buffy coats from a different donor. The isolation of CD4+ T cells was accomplished by employing human CD4 microbeads (Cat. No. 130-045-101, Miltenyi Biotec) following the manufacturer's instructions. CD4 microbeads were added in a ratio of 1 µl per 10^7 cells. The isolation was performed by using MACS separation columns 25 LS and a Milenyi magnet according to the manufacturer's instructions. The enriched $CD4^+$ cells were washed with PBS and resuspended in X-VIVO-15 medium (1 x 10^6/ml).

The mixed lymphocyte reactions were done in triplicates in a 96-well plate. The highest DC:T cell ratio was 1:2 (5 x 10^4 DCs : 1 x 10^5 $CD4^+$ cells). A two fold serial dilution was

performed with DCs, which resulted in DC:T cell ratios from 1:2 – 1:256. Controls containing just DCs or only $CD4^+$ cells were included. On day 4, ^3H-thymidine was added to each well (37 kBq/well) and cells were cultured for an additional 16 h. DC-induced T cell proliferation was measured by ^3H-thymidine incorporation using a liquid β-scintillation counter and was done in collaboration with Helmut Jonuleit's group (Department of Dermatology of the University Medical Center of the Johannes Gutenberg-University Mainz,).

2.4.7 T cell proliferation assay

The assay to investigate the influence of RAF or MEK1/2 inhibition on the proliferation of human $CD4^+$ cells was done in collaboration with Helmut Jonuleit's group (Department of Dermatology of the University Medical Center of the Johannes Gutenberg-University Mainz). Briefly, $CD4^+$ cells were isolated as described in chapter 2.4.8 and stained with CFSE staining buffer. After washing, CFSE-labeled T cells were seeded and stimulated with 0.5 µg/ml anti-human CD3 mAb (clone OKT3, Bio X Cell) and 1 µg/ml anti-human CD28 mAb (clone: CD28.2, BD Pharmingen™). Stimulation was done in presence of LY3009120 (1 µM) or trametinib (1 µM). DMSO treated cells served as negative control. The dilution of CFSE fluorescence was recorded in the FITC channel on day 4.

2.4.8 *In vivo* effect of LY3009120 on DCs

LY3009120 (15 mg/kg, dissolved in 0.5% carboxymethylcellulose) was i.p. injected into C57Bl/6J on d 0 and d 1. LPS injection (10 µg/mouse) was done on d 2. One control group received exclusively the vehicle carboxymethylcellulose. The other control group received no inhibitor, but was treated with LPS alone. In each group four mice were treated. 6 h after LPS injection, mice were sacrificed and spleen and inguinal lymph nodes were isolated. Organs were digested for 1 h at 37°C in 1 mg/ml Collagenase D (Cat. No. 11088866001, Sigma). After stopping the reaction with 0.5 mM EDTA, cells were passed through a cell strainer (40 µm) and stained for flow cytometric analyses.

2.4.9 Statistic analysis

P values were obtained by t-test in GraphPad Prism and if not stated otherwise $p<0.05$ was considered as a significant difference. Statistical significance levels are annotated as *P < 0.05; **P < 0.01; ***P < 0.001.

2.5 Buffers, Solutions and Chemicals

Chemicals:

Acrylamide/Bis solution, 40%	BioRad
APS	Applichem
Albumine bovine fraction V	Sigma, Taufkirchen, Germany
Bromphenolblue	Roth, Karlsruhe, Germany
β-mercaptoethanol	Applichem
DTT	Sigma, Taufkirchen, Germany
Ethanol	Roth, Karlsruhe, Germany
HEPES	Roth, Karlsruhe, Germany
Glycerol	Roth, Karlsruhe, Germany
Glycine	Applichem
Magnesium chloride ($MgCl_2$)	Applichem
NP-40	Applichem
Protease inhibitor Cocktail Set	Calbiochem
SDS	Sigma, Taufkirchen, Germany
Sodium chloride (NaCl)	Roth, Karlsruhe, Germany
Sodium orthovanadate ($NaVO_3$)	Sigma, Taufkirchen, Germany
Sodium fluoride (NaF)	Sigma, Taufkirchen, Germany
Sodium hydroxide (NaOH)	Riedel-de-Haën
T-EDTA, 10x	Sigma, Taufkirchen, Germany
Temed	Sigma, Taufkirchen, Germany
Tris-base	Applichem
Trypsin/EDTA	PAA Laboratories, Austria
Triton X-100	Applichem

Solution and buffers:

LB medium	10 g/L Bacto-tryptone, 10 g/L NaCl, 5 g/L yeast extract, pH 7.5 For plates, 15 g Bacto-agar per liter was added
RIPA buffer	50 mM Tris-HCl (pH 7.5), 250 mM NaCl, 10% glycerol, 1% Triton X-100, 1 mM $NaVO_3$, 1 mM NaF, 1 x Protease inhibitor Cocktail Set
IP buffer	100mM NaCl, 50mM Tris-HCl, 1% NP40, 1 mM $NaVO_3$, 1 mM NaF, and 1 x Protease inhibitor Cocktail Set
10x kinase buffer	100 mM $MgCl_2$, 250 mM β-glycerolphosphate, 250 mM HEPES pH 7.5, 50 mM benzamidine, 5 mM DTT, 10 mM $NaVO_3$
5X SDS-loading Buffer, Laemmli (for SDS-PAGE)	0.125 M Tris-HCl (pH 6.8), 4% SDS, 10% Glycerin, 19 mM DTT, 0.05 % bromophenol blue
10X Running Buffer (for SDS-PAGE)	192 mM Glycine, 25 mM Tris, 0.1% SDS, pH 8.3
10X Blotting Buffer	2 M Glycine, 250 mM Tris
1X Blotting Buffer	10% of 10X Blotting Buffer, 10% of 99.9% Ethanol, ad 1l dH_2O
FACS buffer	PBS, 2 mM EDTA, 0.5 % BSA, 0.01% NaN_3
MACS buffer	PBS, 3 mM EDTA, 0.5% BSA

3 Results

3.1 Regulation of RAFs in human monocyte-derived DCs

3.1.1 Phosphoproteome analysis of monocytes and monocyte-derived DCs

The success of targeted therapeutics against "oncogenic" kinases with ATP competitive and non-competitive inhibitors led to numerous studies focusing on the role of kinases in tumorigenesis. In contrast, relatively less is known on the physiological role of these kinases in the regulation of the immune system. As DCs play a central role in the induction and maintenance of anti-tumor immune responses, we were initially interested, if their immune function could potentially be influenced by certain targeted therapeutics. A well-established *in vitro* model to study DC functions is the isolation of human blood monocytes and the subsequent generation of moDC through the addition of GM-CSF and IL-4. Using these *in vitro* generated DCs a phosphoproteomic analysis was performed in collaboration with Bernd Thiede's lab (Biotechnology Centre of Oslo) to compare monocytes with moDCs and to identify regulated phospho-proteins possibly required for DC differentiation or DC function **(Fig. 3.1)**. Phosphopeptides from three independent experiments with a minimum peptide count of 1 were used for the subsequent analysis. As shown in **Fig. 3.1A**, of 2319 identified phosphopeptides, 16 phosphopeptides were exclusively detected in all biological replicates of monocytes and under the same criteria 40 phosphopeptides were assigned to moDC. In this setting regulated phosphopeptides, which were detected in both monocytes and moDC, were not considered. Corresponding proteins of phosphopeptides only detected in DCs were classified using Panther Classification System with the settings "GO:Slim Molecular Function" **(Fig. 3.1B)**. Within the protein class possessing "catalytic activity", ARAF was identified as a regulated phosphopeptide. Focusing on phosphopeptides from ARAF as well as from CRAF and BRAF revealed **(Fig. 3.1C)**, that only the phosphorylation site ARAF S257 was significantly enriched in moDC (p-value = 0.017). In case of CRAF, a mono- and di-phosphorylated peptide with the potential phosphorylation sites S295, S296 and S301 was highly represented in moDCs (p-value = 0.17). According to the PhosphoSitePlus database, ARAF S257 was correlated to an induced enzymatic activity of ARAF, while the sites identified in CRAF are corresponding to both an induced and

inhibited enzymatic activity of CRAF. The identified phosphorylation sites in ARAF and CRAF are located between the CR2 and CR3 region **(Fig. 3.1D)**.

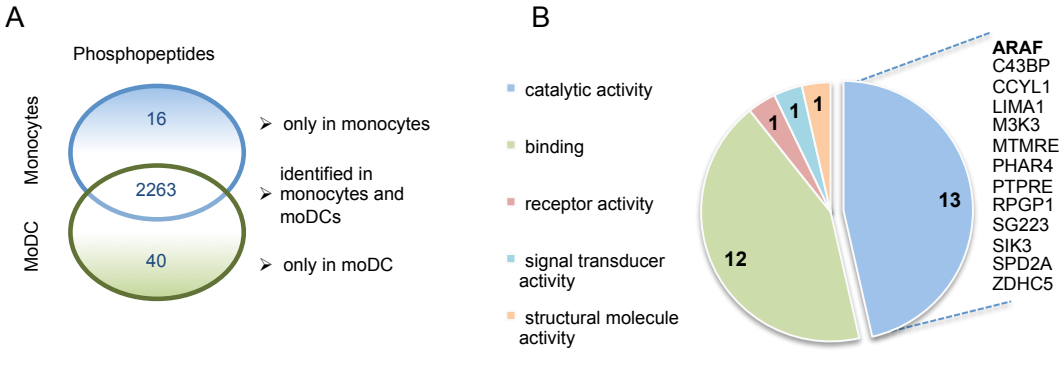

C

Protein	Sequence	p-value	Fold Change	Function (phosphosite.org)
ARAF	$_{248}$GGSDGTPRG**S^{ph}**PSPASVSSGR$_{267}$	0.017	INF	S257: enzymatic activity, induced
ARAF	$_{210}$IRSTSTPNVHMV**STT**APMDSNLIQLTGQSFSTDAAGSR$_{247}$	0.61	1.2	unknown
CRAF	$_{283}$SHSESASPSALS**SS**PNNL**S**PTGWSQPK$_{309}$	0.17	4.4	S296, S301: regulation of enzymatic activity
CRAF	$_{257}$QR**STS**TPNVHMVSTTLPVDSR$_{275}$	0.59	0.9	S259: enzymatic activity, inhibited
BRAF	$_{361}$DR**SSS**APNVHINTIEPVNIDDLIR$_{384}$	0.30	2.1	S365, T373: enzymatic activity, inhibited
BRAF	$_{444}$RD**SS**DDWEIPDGQITVGQR$_{462}$	0.92	0.9	S446: enzymatic activity, induced

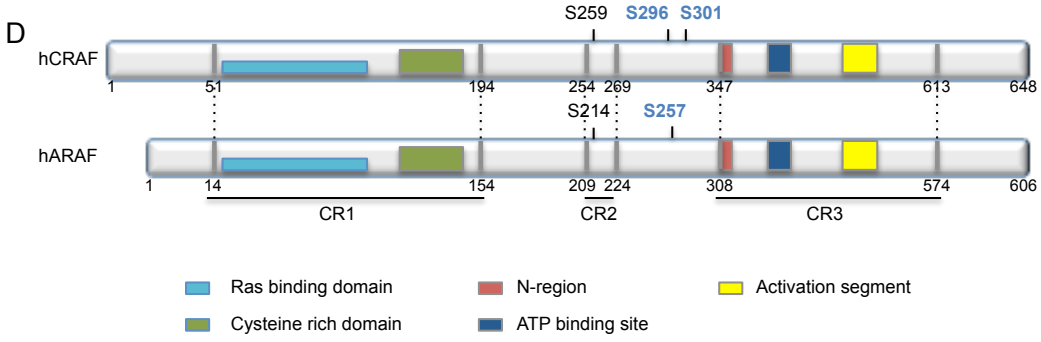

Figure 3.1 Phosphoproteomics on human monocytes and moDCs. (A) Mass spectrometry-based proteome analysis was performed to compare monocytes (isolated from buffy coats; cultured for 24 h in X-VIVO-15 supplemented with 1% heat-inactivated plasma) with moDCs (differentiation of monocytes with GM-CSF/IL-4 for five days). Phosphopeptides were identified with a minimum peptide count of 1. The Venn diagram shows phosphopeptides attributed to monocytes or moDCs detected in all three biological replicates of the respective samples. (B) The corresponding proteins of the phosphopeptides, which were detected only in moDCs, were classified using Panther Classification System with the settings "GO:Slim Molecular Function" leading to the identification of ARAF among other enzymes within the protein class "catalytic activity". (C) Phosphopeptides of ARAF, BRAF and CRAF are presented, which were identified in all three replicates of either monocytes or moDCs. Potential phosphorylation sites of the phosphorylated peptides are shown in bold. Among the identified phosphopeptides, the ARAF phosphopeptide covering amino acids 248-267 was the only one being significantly upregulated in moDCs. The CRAF phosphopeptide covering amino acids 283-309, which was found to be mono- and di-phosphorylated, was higher in moDCs, but not significantly enriched. (D) The RAF proteins general consist of three conserved regions (CR1, CR2 and CR3). The schematic structure of CRAF and ARAF displays that the ARAF phosphorylation site S257 and CRAF phosphorylation sites S296/S301 are located between the CR2 and CR3 domain

The influence of the identified phosphorylation sites on the MAPK pathway was validated by generating mutants, which carried instead of the serine either an alanine to prevent phosphorylation at this site or an aspartic acid to mimic the negative charge of a

phosphorylated residue. Thus, the two ARAF mutants ARAF S257A and ARAF S257D were generated, overexpressed in HEK293T cells and the kinase activity of the immunoprecipitated mutants was determined by a kinase assay using an inactive MEK1 mutant MEK K97A as a substrate. A kinase-dead mutant (ARAF R362H) and a kinase-active mutant (ARAF Y301/302D) were included as a control. As shown in **Fig. 3.2A**, ARAF S257A as well as ARAF S257D were still capable to phosphorylate the substrate MEK1, although the kinase activity of ARAF S257A was lower compared to the kinase activity seen with ARAF WT. ARAF S257D mutant revealed a comparable kinase activity to ARAF WT. In case of CRAF, the double mutants CRAF S296/301A and CRAF S296/301D were created. MAPK signaling was studied after overexpressing the new CRAF mutants as well as wild type CRAF and the kinase-dead mutant (CRAF R401H) in HEK293T cells. Mutating CRAF S296/301 to aspartic acid resulted in a higher phosphorylation of MEK1/2 compared to the corresponding alanine mutant (**Fig. 3.2B)**. Further, CRAF S296/301D induced a higher MEK1/2 phosphorylation compared to CRAF WT.

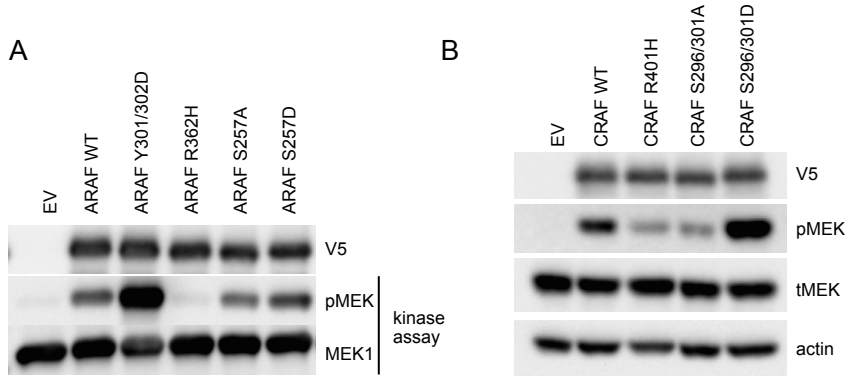

Figure 3.2: Influence of RAF mutations on MAPK signaling in HEK293T cells (A) The phosphorylation site ARAF S257, identified in the phosphoproteome analysis and enriched in moDCs, was mutated to either alanine [A] or aspartic acid [D]. ARAF WT and ARAF mutants (ARAF S257A and ARAF S257D) were overexpressed in HEK293T cells, immunoprecipitated via their V5 tag and kinase activity was studied as mentioned in the methods. Phosphorylation of the MEK1 K97A substrate at S217/221 was investigated by Western Blot. The kinase active mutant (ARAF Y301/302D) and kinase dead mutant (ARAF R362H) were included as controls. (B) The phosphorylation sites CRAF S296 and S301 were mutated to either alanine [A] or aspartic acid [D] and double mutants were generated. CRAF mutants were transfected into HEK293T cells. Wild type CRAF and a kinase dead mutant (CRAF R401H) were included as a control. Phosphorylation of MEK1/2 (S217/221) was analyzed by immunoblot.

3.1.2 Increasing RAF levels during differentiation of DCs

MAPK signaling was further characterized during moDC differentiation through immunoblot analysis to monitor changes in RAF levels as well as in MAPK signaling components. The representative immunoblots in **Fig. 3.3A** show a steady increase in

protein level of all RAF proteins during the differentiation process. Quantifying the ARAF **(Fig. 3.3B),** BRAF **(Fig. 3.3C)** and CRAF **(Fig. 4.4D)** levels in relation to the levels detected in monocytes revealed a 2 to 138-fold increase in the protein amount of ARAF, a 1.5 to 26-fold increase of BRAF and a 7 to 72-fold increase of CRAF in immature moDCs (day 5 of differentiation). While MEK1/2 phosphorylation shows high deviation during moDC differentiation **(Fig. 4.4E)**, phosphorylation of ERK1/2 rather describes an oscillating pattern **(Fig. 4.4F)**. Although the dynamics of kinase activation from six independent experiments are not exactly matching, it can be observed that ERK1/2 phosphorylation is high at the beginning of differentiation, which declines and increases again.

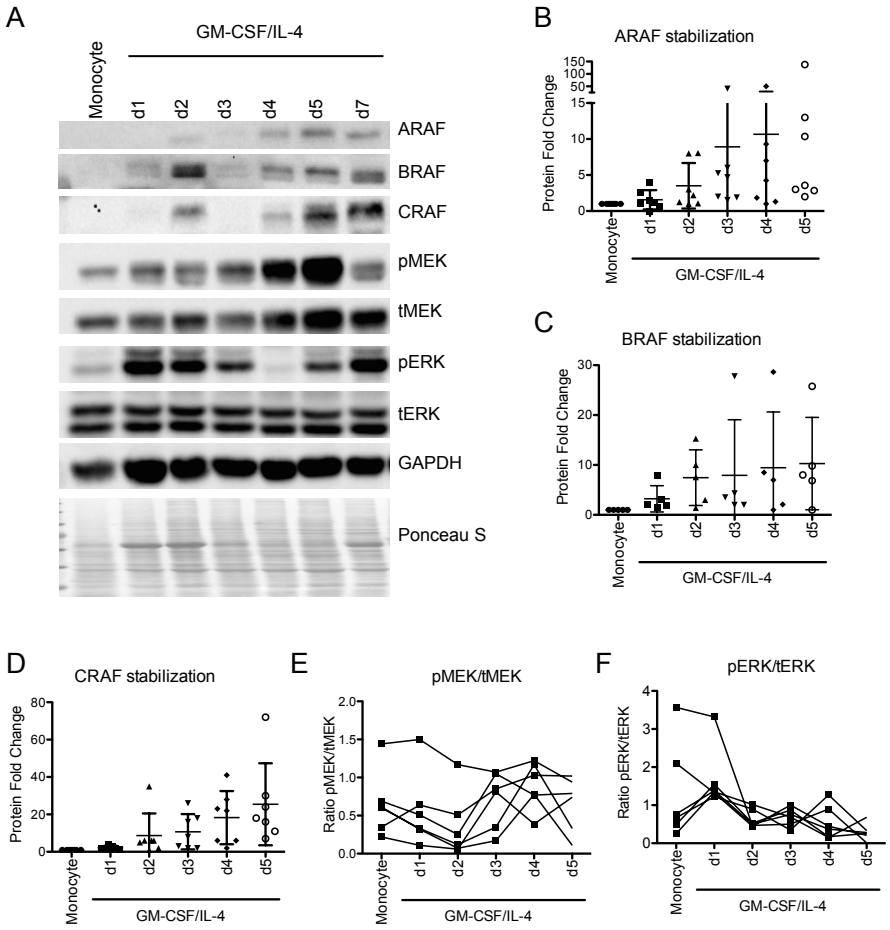

Figure 3.3 RAF expression levels in monocytes during their differentiaton into moDCs. (A) Representative Western Blot monitoring RAF protein levels and the MAPK signaling during the differentiation of monocytes to moDCs induced by GM-CSF/IL-4. (B) The change in total ARAF (n = 7) (C) BRAF (n = 5) and (D) CRAF levels (n = 7) was quantified during the progressive differentiation to moDCs. Total protein levels are shown relatively to levels detected in monocytes. (E) MEK1/2 (S217/221) (n = 6) and (F) ERK1/2 (Y202/Y204) phosphorylation (n = 6) during the differentiation process was quantified by determining the ratio of phosphorylated protein to total protein.

3.1.3 Enhanced RAF stability in immature DCs

Because of the observed increase in RAF protein levels during the differentiation of human monocytes to moDCs, possible underlying regulatory mechanisms influencing protein levels were analyzed. Determining the mRNA expression of ARAF, BRAF and CRAF relatively to the mRNA level of monocytes revealed no changes in the mRNA levels **(Figure 3.4A)**. In case of CRAF, mRNA expression was even slightly reduced during differentiation. Cycloheximide chase experiments were performed with cells on day 3 of culture and with immature moDCs (day 5 of culture). The representative immunoblots in **Figure 3.4B** revealed a change in the protein stability of ARAF and CRAF with RAF proteins being more stable in immature moDCs. The quantification of three independent experiments illustrated an enhanced half-life of ARAF and CRAF in differentiated moDCs **(Figure 3.4C)**. On day 3 of culture, CRAF had a half-life of around 3.5 h, which increases to more than 6 h in immature moDCs. ARAF was a short-lived protein during the differentiation process having a half-life of around 0.5 h. In immature moDCs, the half-life of ARAF increased to approximately 6 h. The observed enhanced protein stability points to a regulatory mechanism involving the proteostasis of ARAF and CRAF.

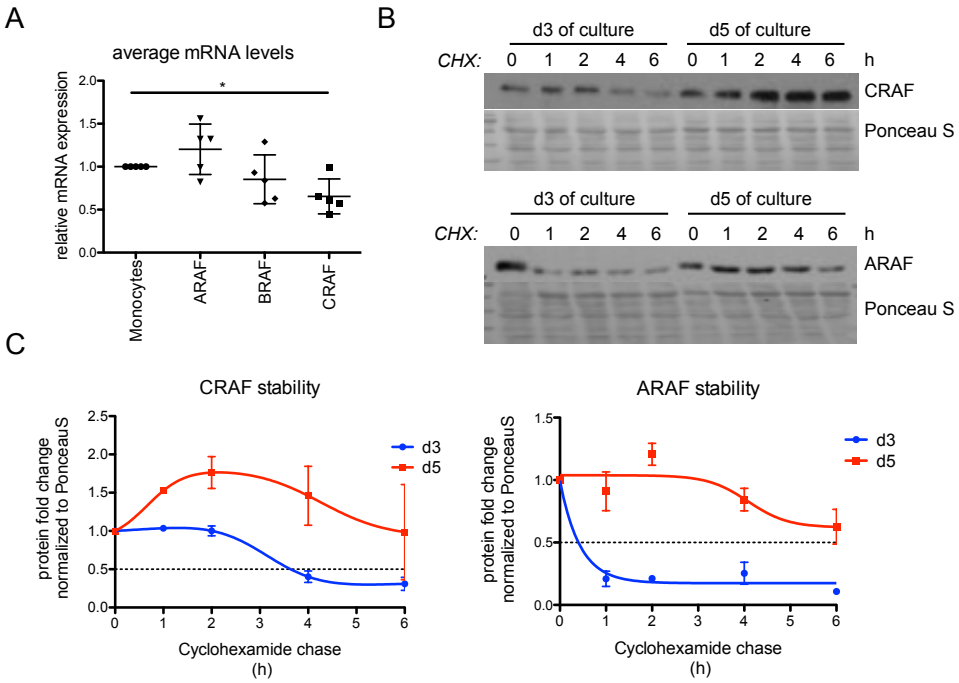

Figure 3.4 RAF stability in immature moDCs. (A) Real time PCR analysis was performed to compare mRNA levels of A-/B- and CRAF from monocytes with immature moDCs (n = 5). (B) Protein stability of CRAF and ARAF in cells on day 3 and day 5 of differentiation was investigated by cycloheximide (CHX) chase experiments and subsequent Western Blot analysis. (C) The half-life of CRAF and ARAF was determined by quantifying the decrease in total protein levels observed in the cycloheximide chase experiments relative to Ponceau S staining (n = 3).

Protein degradation is often regulated by the ubiquitin-proteasome system. Therefore, ubiquitination of proteins, mostly on lysine (K) 48, serves as a label for the proteasomal degradation [144]. Since degradation by the proteasome is especially well described for CRAF, it was tested if RAF proteins are targets for ubiquitination. Cells on day 3 of differentiation were treated with the proteasome inhibitor MG132, which leads to the accumulation of ubiquitinated proteins. The atypical MAPK ERK3 served as positive control because of its low protein stability. Indeed there was an increase of ERK3 detected after MG132 treatment **(Figure 3.5A)**. In comparison to ERK3, ARAF and CRAF showed only a minor increase in protein level, while BRAF levels were unchanged, which was confirmed by the quantification of relative RAF levels **(Figure 3.5B)**.

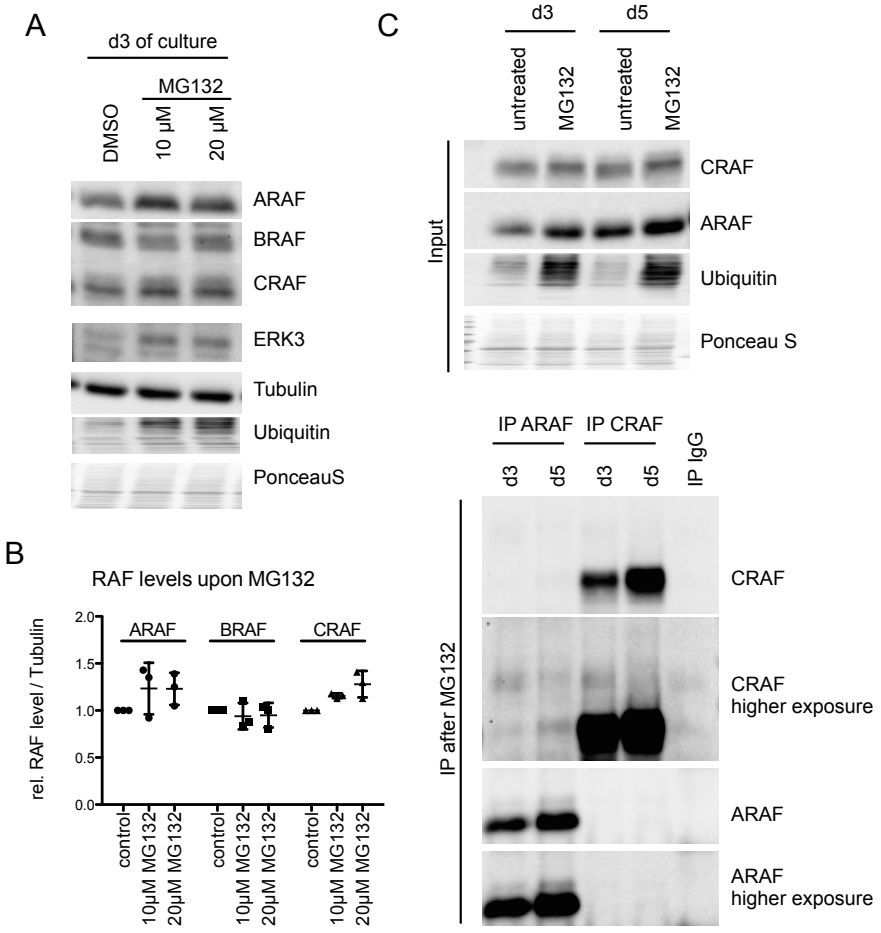

Figure 3.5 Ubiquitination of RAF proteins during moDC differentiation. (A) Differentiation of human monocytes was initiated by GM-CSF/IL-4 and 3 days later cells were treated with MG132 (10 µM and 20 µM) for 6 h. RAF protein levels were analyzed by Western Blot. ERK3 was used as a positive control. (B) The change in RAF protein levels after MG132 treatment (10 µM, 6 h) was quantified relatively to the housekeeping gene tubulin (n = 3). (C) Cells on day 3 and day 5 of differentiation were treated with 10 µM MG132 for 6 h. ARAF and CRAF were immunoprecipitated and analyzed by Western Blot.

Western Blot analysis of precipitated ARAF and CRAF from MG132-treated cells on day 3 of culture exhibited a typical polyubiquitination smear suggesting that the RAF proteins were targets for ubiquitination **(Figure 3.5C)**. Precipitated ARAF and CRAF from MG132-treated immature DCs (day 5 of culture) displayed a similar ubiquitination pattern.

3.2 MAPK signaling and RAF activation in human DCs

3.2.1 Activation of MAPK signaling in DCs by LPS

DCs can exhibit an immature and mature phenotype. The immature status is typically remained during steady-state conditions and contributes to the maintenance of the tolerance to self-antigens. In response to danger signals, DCs undergo a maturation process, which equips them with T cell activating properties to regulate adaptive immunity. A well known, DC maturation inducing ligand is LPS, a common component of gram-negative bacterial wall, which signals through TLR4 receptors. Besides detecting the protein stabilization of RAF proteins during moDC differentiation, we investigated if MAPK signaling was further involved in the translation of the LPS-induced signals in moDCs.

Consistent with the published observations [145, 146], we confirmed, that LPS induced the phosphorylation of MEK1/2 and ERK1/2 in human moDCs **(Fig. 3.6A)**. The quantification of phosphorylated MEK1/2 in relation to the total protein levels illustrated a strong induction after 1 h of LPS stimulation, which decreased after 24 h **(Fig. 3.6B)**. In contrast, ERK1/2 phosphorylation was just slightly induced 1 h after LPS stimulation, but was clearly activated 24 h after LPS stimulation **(Fig. 3.6C)**.

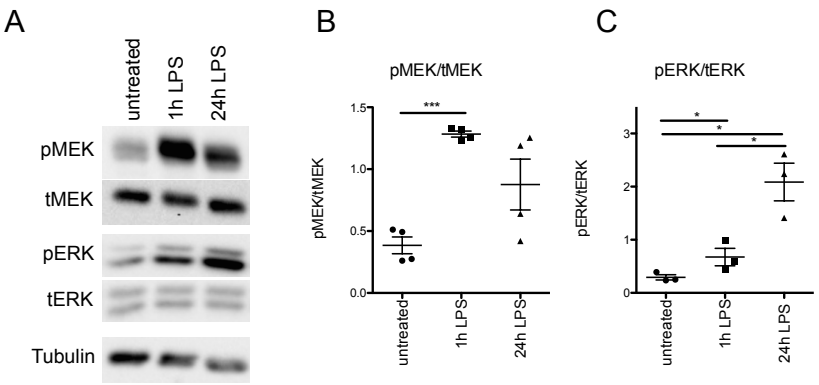

Figure 3.6 LPS-induced MAPK signaling in moDCs. (A) Immature dendritic cells were stimulated for 1 h and 24 h with LPS (100 ng/ml) and phosphorylation of MEK1/2 (S217/221) and ERK1/2 (Y202/Y204) was determined by Western Blot analysis. (B) The relative level of MEK1/2 (n = 4) and (C) ERK1/2 (n = 3) phosphorylation was determined by the ratio of phosphorylated protein to total protein.

3.2.2 RAF interactions in human DCs

As LPS induced the activation of MEK1/2 and ERK1/2 kinases in moDCs, RAF activation was investigated in immature moDCs and moDCs stimulated with LPS. RAF dimerization is a required step for RAF activation. Therefore, interactions between the RAF proteins were examined through immunoprecipitation studies. The representative immunoblot in **Figure 3.7A** shows the immunoprecipitates of ARAF, BRAF and CRAF from untreated moDCs. We detected BRAF in ARAF and CRAF immunoprecipitates demonstrating a complex formation of BRAF with ARAF and CRAF. Under stimulating conditions, BRAF was still found in complex with ARAF and CRAF, although the interaction between BRAF and ARAF was stronger after 24 h of LPS stimulation **(Figure 3.7B)**. In three out of four independent experiments, the protein amount of co-immunoprecipitated BRAF with ARAF was 1.6 - 4.6 times higher after stimulation with LPS for 24 h compared to the amount detected in the ARAF immunoprecipitates from unstimulated moDCs. The interaction between CRAF and BRAF was detected in all four independent experiments as well. But the yield of precipitated CRAF showed high variation between the experiments so that changes in the intensity of BRAF-CRAF interactions could not be quantified. In two out of four independent experiments, ARAF was detected in CRAF precipitates from moDCs stimulated for 24 h with LPS. Interestingly, just in one replicate, MEK1/2 was identified exclusively in CRAF immunoprecipitates.

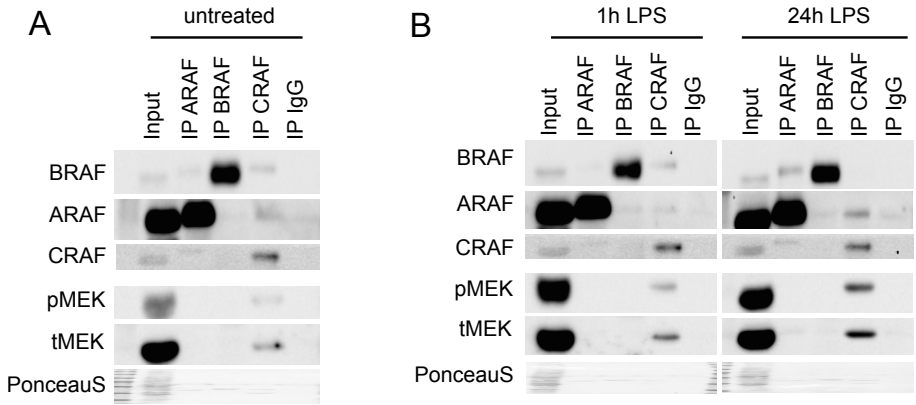

Figure 3.7 RAF interactions in LPS-stimulated moDCs. (A) Endogenous RAF proteins were immunoprecipitated from immature moDCs and (B) from LPS-stimulated moDCs (1 h and 24 h, 100 ng/ml). Immunoprecipitates were analyzed by Western Blot. The data are representative for 4 independent experiments.

3.2.3 Activation of RAF kinases in human DCs

Efficient activation of ARAF and CRAF requires the phosphorylation of S299 and S338, respectively. While the phosphorylation of these sites is induced upon activation, BRAF carries a constitutive phosphorylation at the corresponding serine. As shown in **Fig. 3.8A**, LPS stimulation of moDCs induces phosphorylation of CRAF. The quantification of phosphorylated CRAF in relation to the total protein levels illustrated a slight induction after 1 h of LPS stimulation **(Fig. 3.8B)**. But determining the ratio of the shifted CRAF pS338 band to the total CRAF pS338 band demonstrated that LPS stimulation significantly induced a band shift of CRAF **(Fig. 3.8C)**. In contrast, no increased phosphorylation of S299 upon LPS stimulation was detected in case of ARAF **(Fig. 3.8D)**.

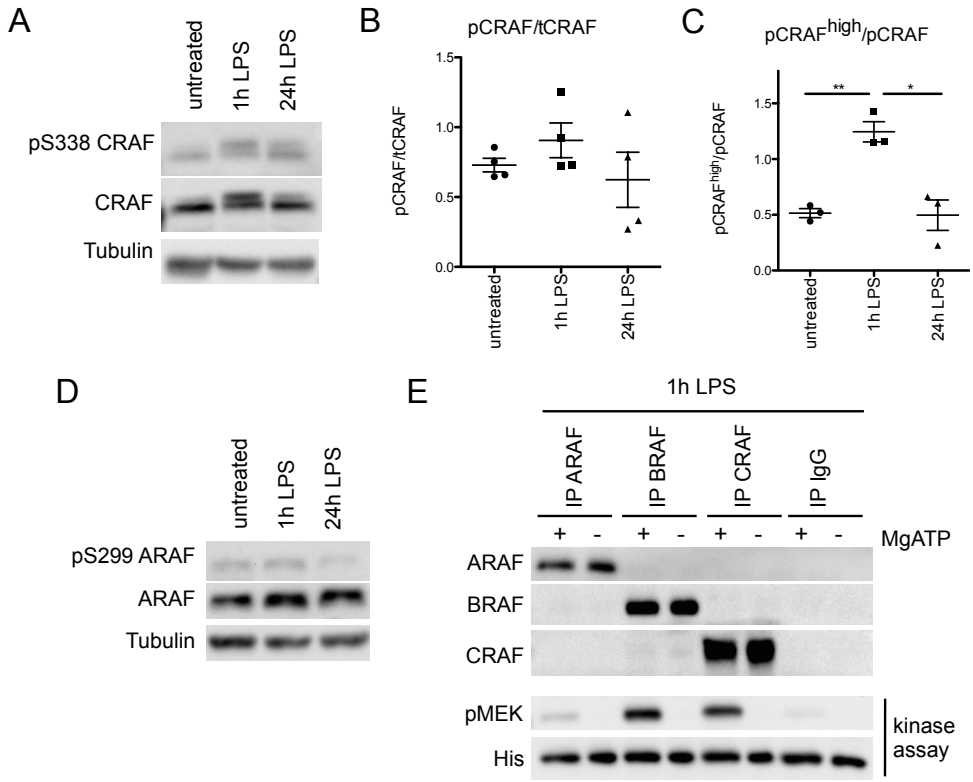

Figure 3.8 RAF activity in moDCs. (A) Representative Western Blot of immature moDCs stimulated with LPS (100 ng/ml) for 1 h and 24 h. Phosphorylation of CRAF (S338) was analyzed. (B) The relative level of CRAF (n = 4) phosphorylation was determined by the ratio of phosphorylated protein to total protein. (C) The band shift of CRAF was determined by the quantification of the shifted CRAF pS338 band to the total CRAF pS338 (n = 4). (D) Western Blot analysis of ARAF phosphorylation (S299) after stimulating moDCs for 1 h and 24 h with LPS (100 ng/ml). (E) Kinase activity of RAF proteins immunoprecipitated from LPS-stimulated moDCs (1 h) was studied as mentioned in the methods. Phosphorylation of the MEK K97A substrate at S217/221 was investigated by Western Blot.

Another approach to investigate RAF activity is to perform *in vitro* kinase assays with RAFs precipitated from cells. Therefore, endogenous RAF proteins were

immunoprecipitated from moDCs and a kinase assay was performed using an inactive MEK1 mutant K97A as substrate. As shown in **Fig. 3.8E**, moDCs were stimulated for 1 h with LPS. While BRAF and CRAF clearly phosphorylated the MEK1 substrate, ARAF induced phosphorylation of MEK1 was just slightly higher compared to the phosphorylation observed in the IgG background control.

3.3 Role of RAF kinases in the maturation of human DCs

3.3.1 Validating the efficiency of RAF inhibitor LY3009120 for the analysis of DC function

Results thus far showed that RAF proteins were stabilized during the differentiation from monocytes to moDCs and that especially BRAF and CRAF were active in LPS-stimulated moDCs. To further investigate whether RAF kinases contribute to DC function itself, RAF and MEK inhibitors were employed in order to block the MAPK pathway at different levels. RAF inhibitors are already successfully used as targeted therapeutics against cancer. Despite their initial clinical success, difficulties came up as RAF inhibitors can paradoxically activate the MAPK pathway in patients with RAS mutations. While RAF inhibitors like PLX4032 inhibited the MAPK pathway driven by mutant BRAF, Poulikakos *et al.* demonstrated paradoxical activation through a drug-induced transactivation of RAF dimers when MAPK pathway was dependent on RAS activation [91]. Thus, efforts were made to generate next generation RAF inhibitors like LY3009120 to circumvent this issue. These inhibitors are characterized through their equal affinity to monomeric and dimeric RAF proteins, thus avoiding negative cooperativity, which reduces the affinity to the second protomer after RAF-dimerization. First, the activity of the inhibitor LY3009120 on the MAPK signaling and on the proliferation of various cancer cell lines was analyzed **(Fig. 3.9A)**. The working concentration of LY3009120 was determined by treating HeLa cells with increasing inhibitor concentrations. Phosphorylation of MEK1/2 and ERK1/2 was inhibited in HeLa cells after 6 h using 1 µM of LY3009120 **(Fig. 3.9B)**. The inhibitory effect on MEK1/2 and ERK1/2 phosphorylation was demonstrated with the cancer cell lines Calu1 and MDA-MB231 as well **(Fig. 3.9C)**. Calu1 cells carry a K-RAS G12D mutation and were derived from a lung epidermoid carcinoma. MDA-MB231 is a cell line derived from breast adenoma carcinoma with K-RAS G13D mutation. Since HeLa cells have no *k-ras* mutation, LY3009120 inhibited the MAPK pathway independent of mutated *kras*. It is

worth mentioning, that under EGF-stimulation LY3009120 still inhibited MAPK signaling, but there was no complete block in MEK1/2 and ERK1/2 phosphorylation.

The effect of LY3009120 on the proliferation of the cancer cell lines HeLa, Calu1 and MDA-MB-231 as well as on the K-RAS G13D mutated, colon carcinoma derived HCT-116 cell line and *ras* wild type, lung squamous cell carcinoma derived NCI-H226 cell line was investigated by using a MTT-assay, which measures the metabolic activity of cells. As illustrated in **Fig. 3.9D**, the determined metabolic activity of cells treated with LY3009120 (LY) was diminished in all cancer cell lines after 72 h treatment displaying a reduced cell number. There are two possible explanations for the detected lower cell numbers: either the cells had a reduced cellular proliferation or they underwent apoptosis. The MEK inhibitor trametinib had similar effects on the proliferation and viability of the cancer cell lines tested.

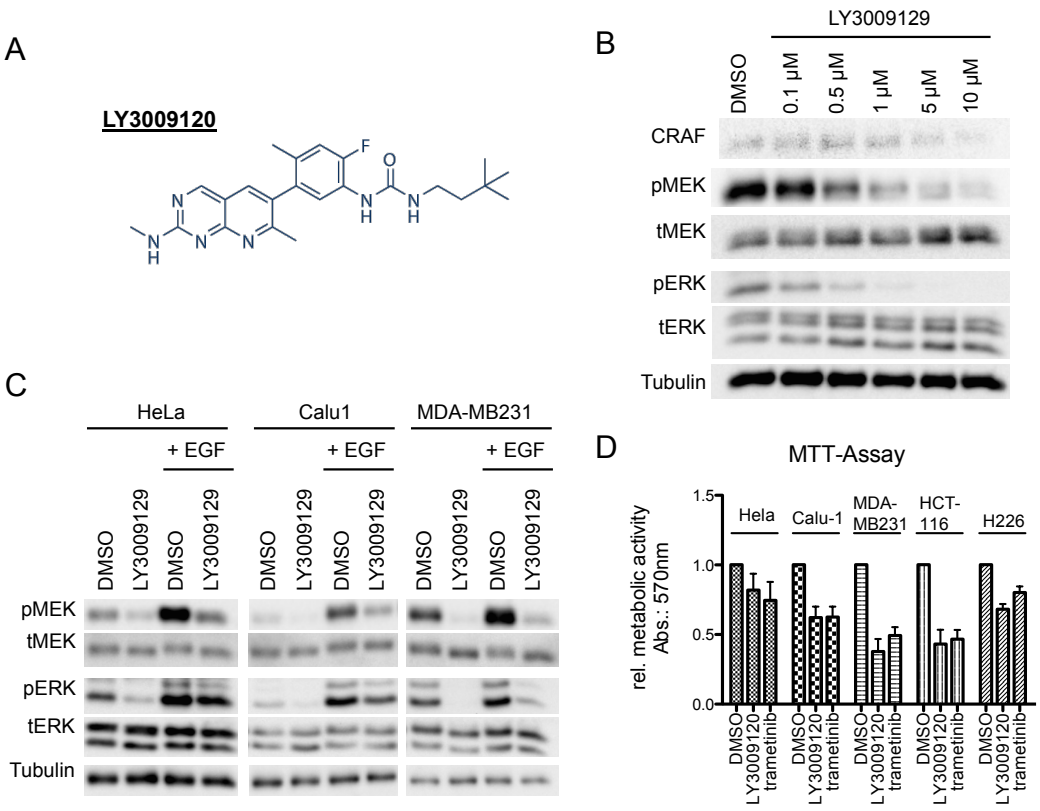

Figure 3.9 Activity of LY3009120 in different cancer cell lines. (A) The pan-RAF-Inhibitor LY3009120 is a new generation RAF inhibitor with an equal affinity to monomeric and dimeric RAF proteins. Shown is the chemical structure of LY3009120. (B) HeLa cells were treated with increasing concentrations of LY3009120 (0.1 µM to 10 µM). After 6 h treatment MEK1/2 (S217/221) and ERK1/2 (Y202/204) phosphorylation was investigated by Western Blot analysis. (B) Cancer cell lines (HeLa, Calu1, MDA-MB231) were treated with the RAF inhibitor LY3009120 (1 µM) for 6 h in starvation. Optionally, they were stimulated for 5 min with EGF. MEK1/2 (S217/221) and ERK1/2 (Y202/204) phosphorylation was investigated by Western Blot. (D) Metabolic activity of various cancer cell lines was measured by MTT assay after treating cells for 72h with 1 µM LY3009120 and 1 µM trametinib. LY3009120 showed a comparable inhibitory effect on proliferation and viability of several cancer cell lines like the MEK-Inhibitor trametinib (n = 3).

As the RAF inhibitor should later be employed on moDCs to investigate the role of RAF kinases in DC function, it was further examined if LY3009120 is inhibiting RAF kinases in moDCs as well. Immature moDCs were treated with LY3009120 for 6 h and RAF proteins were subsequently immunoprecipitated. The activity of RAFs was determined in a kinase assay using the inactive MEK1 mutant MEK K97A as a substrate. **Fig. 3.10A** demonstrates, that the treatment with LY3009120 inhibited CRAF activity as the phosphorylation of the substrate was reduced when compared to the phosphorylation detected in the vehicle control. BRAF activity was attenuated after LY3009120 treatment as well **(Fig. 3.10B)**. Interestingly, in the kinase assay with precipitated BRAF an induced RAF dimerization upon LY3009120 treatment was observed. RAF inhibitors inducing RAF dimerization is a well known phenomena.

As shown in 3.2.3, ARAF exhibited hardly a detectable activity in the kinase assay pointing to a low kinase activity towards the substrate MEK1. Because of this it was not possible to demonstrate the inhibitory effect of LY3009120 on ARAF (data not shown).

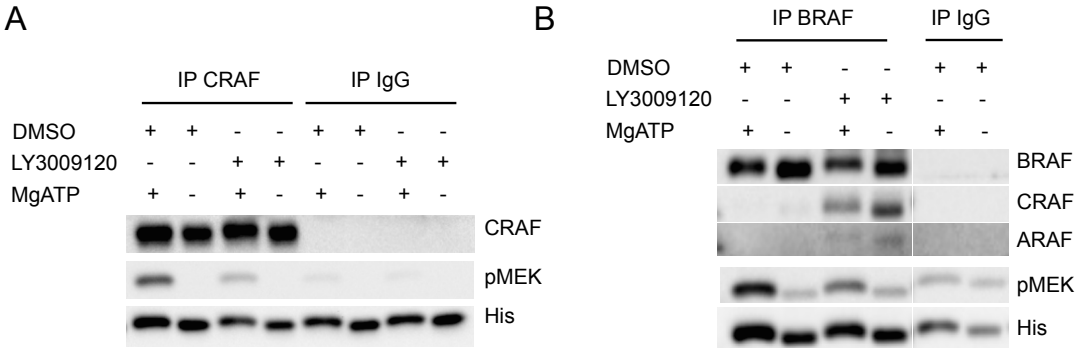

Figure 3.10 LY3009120 inhibiting CRAF and BRAF in moDCs. (A) Immature moDC were treated for 6 h with LY3009120 (1µM) or with the vehicle (DMSO). Kinase activity of CRAF and (B) BRAF precipitated from the treated DCs was determined by a kinase assay using MEK K97A as a substrate. Shown is a representative experiment.

3.3.2 Influence of RAF and MEK inhibitors on the surface marker expression in moDCs

Initially, the role of MAPK signaling during the differentiation from monocytes to moDCs was investigated after inhibiting RAF or MEK1/2 by addition of the inhibitors LY3009120 or trametinib, respectively. Culturing the cells in the presence of LY3009120 resulted in a reduced MEK1/2 phosphorylation, which did not influence ERK1/2 phosphorylation **(Fig. 3.11A)**. In contrast, the MEK inhibitor trametinib clearly blocked ERK1/2 phosphorylation. *In vitro* generated moDCs were identified by the absence of the monocytic marker CD14 and the expression of MHC-II in flow cytometric analyses. Five days after starting the differentiation, moDCs showed a moderate expression of

MHC-II **(Fig. 3.11B)**. Inhibition of RAF as well as MEK1/2 resulted in slightly increased MHC-II and CD86 expression, which was confirmed through the quantification of four independent experiments **(Fig. 3.11C)**.

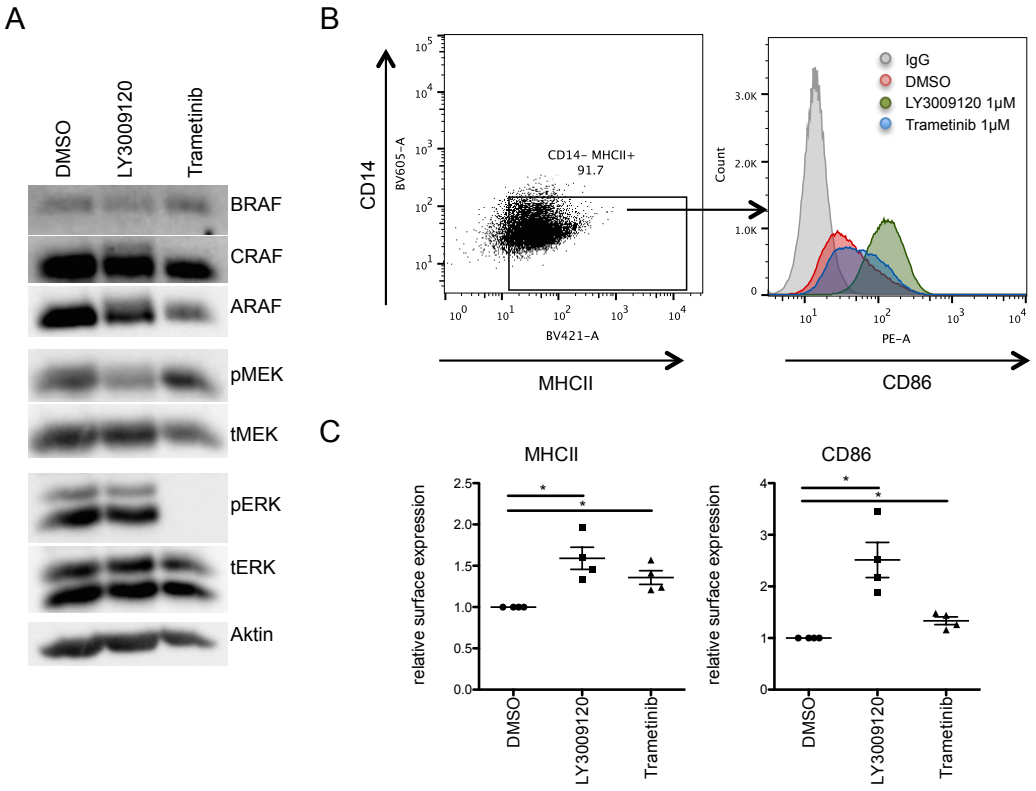

Figure 3.11 Effect of MAPK signaling on moDC differentiation determined by surface marker expression. (A) MAPK signaling was analyzed by Western Blot after differentiating monocytes to moDCs in presence of the RAF inhibitor LY3009120 (1 µM) or MEK inhibitor trametinib (1 µM) for 5 days. Shown is a representative Western Blot. (B) Surface marker expression (CD14, MHCII and CD86) was determined by flow-cytometry after a 5 days differentiation of monocytes to moDCs in presence of LY3009120 (1 µM) or trametinib (1 µM). (C) The mean fluorescence of MHCII and CD86 relatively to the DMSO control was quantified (n = 4).

Besides the impact on differentiation itself, it was tested whether MAPK signaling directly interfered with moDC function. Therefore, immature moDCs were first generated and subsequently treated with the inhibitors for 48 h. The scatter plots shown in **Fig. 3.12A** illustrate, that unstimulated moDCs (DMSO control) are positive for CD86, but have a low expression of CD83 and CD80. The treatment with LY3009120 for 48 h did not affect surface marker expression in immature moDCs, but the treatment with the MEK inhibitor trametinib resulted in a slightly enhanced surface marker expression of especially CD83 (1.24-2.51 fold increase).

As already described earlier, treatment of DCs with LPS induces a maturation process, which leads to a number of phenotypical and functional changes. Generally, this process involves the redistribution of MHC molecules from intracellular endocytic

compartments to the DC surface, the upregulation of co-stimulatory molecules and the induction of cytokine and chemokine secretion. In line with this, inducing moDC maturation by LPS stimulation for 48 h led to a 1.04-1.57 fold higher CD86, 1.57-2.77 fold higher CD83 and a 1.54-4.24 fold higher CD80 surface marker expression **(Fig. 3.12B)**. While the treatment with the MEK inhibitor did not impede LPS-induced moDC maturation, treatment with LY3009120 under stimulating conditions had a negative effect on the surface marker expression.

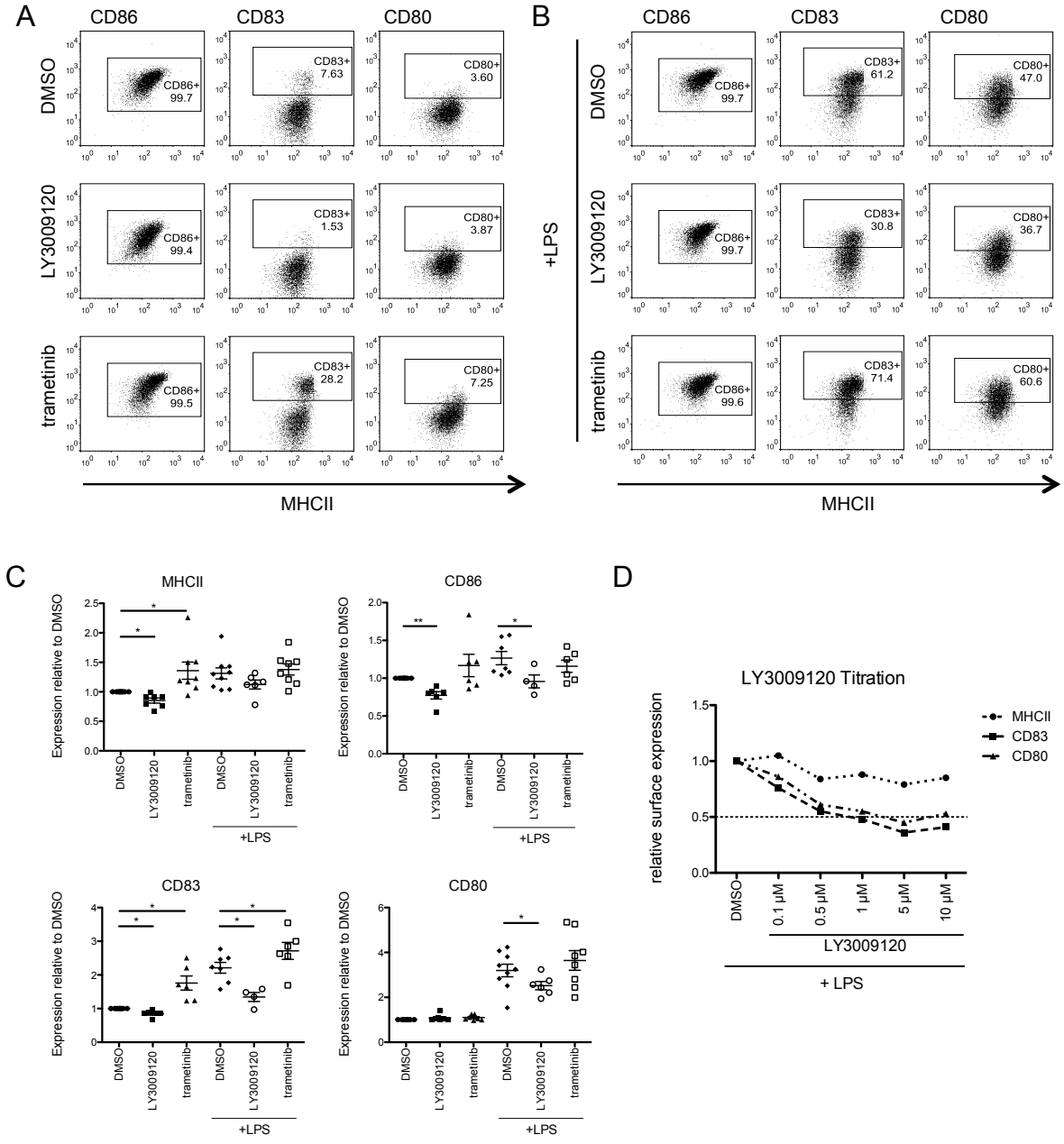

Figure 3.12 Effect of RAF kinases in moDC surface marker expression. (A) Surface markers of moDCs (MHC-II, CD86, CD83 and CD80) were analyzed by flow cytometry after a 48 h treatment with trametinib (1 µM) or with LY3009120 (1 µM) in absence (B) or presence of LPS (100 ng/ml). One representative experiment is depicted. (C) The relative mean fluorescence of the surface markers of multiple independent experiments was quantified. (D) Immature moDCs were treated with increasing LY3009120 concentrations under LPS stimulating conditions and surface marker expression (MHCII, CD83 and CD80) was analyzed 48 h after treatment.

The quantification of the relative mean fluorescence of multiple experiments in **Fig. 3.12C** suggests that LY3009120 treatment in presence of LPS resulted in a significant lower surface marker expression of CD86, CD80 and CD83. CD86 showed an average 26 ± 10%, CD80 an average 41 ± 10% and CD83 an average 20 ± 12% lower signals as compared to the corresponding LPS-treated moDCs. LY3009120 concentrations higher than 1 µM did not further decrease surface marker expression **(Fig. 3.12D)**.

To minimize the possibility of unspecific effects of the RAF inhibitor LY3009120 on moDC maturation, multiple RAF inhibitors were employed under LPS stimulating conditions. The treatment with all of the RAF inhibitors listed in **Fig. 3.13A** resulted in a significantly reduced surface marker expression of CD83 and CD80 as compared to moDCs only stimulated with LPS **(Fig. 3.13B)**. Interestingly, PLX4720 had no effect on CD80 surface marker expression.

A

Inhibitor	Mechanism
LY3009120	potent pan-RAF inhibitor for ARAF, BRAF, and CRAF
GDC-0879	selective BRAF inhibitor with activity against CRAF
Raf265	inhibitor of CRAF/BRAF/BRAF V600E , exhibits potent inhibition on VEGFR2
Kobe 0065	H-Ras-CRAF interaction inhibitor
PLX4720	inhibitor of BRAF_V600E, 10-fold selectivity for BRAF_V600E than wild-type BRAF

B

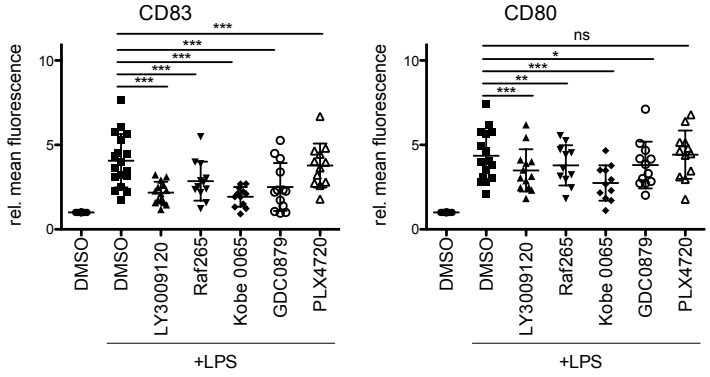

Figure 3.13 Effect of multiple RAF inhibitors on moDC surface marker expression. (A) Complete list of all RAF inhibitors used in this study. (B) CD80 and CD83 surface expression was determined by flow cytometry after treating moDCs for 48 h with the in (A) listed RAF-Inhibitors (Raf265: 0.5 µM, n = 12, Kobe: 10 µM, n = 12, GDC0879: 1 µM, n = 13, PLX4720: 10 µM, n = 12) in presence of LPS. The relative mean fluorescence was quantified.

Since the effect of the RAF and MEK inhibitor on surface marker expression was only seen in the presence of the stimulating agent LPS, it was further investigated whether other TLR ligands such as Poly(I:C) and Pam3CSK4 had similar effects **(Fig. 3.14A)**. Comparable to LPS stimulation, Poly(I:C) and Pam3CSK4 treatment caused an

upregulation of CD80 and CD83 surface marker expression **(Fig. 3.14B)**. Subsequently, the RAF inhibitor LY3009120 was employed under these stimulating conditions **(Fig. 3.14B)**. The quantification of the mean fluorescence relatively to the corresponding control of multiple independent experiments is illustrated in **Fig. 3.14C**. LY3009120 treatment resulted in a significantly reduced surface expression of CD83 - independent of the TLR ligand used. In case of CD80, the inhibiting effect on surface expression was significant when combined with LPS and Poly(I:C). Under Pam3CSK4 stimulation, LY3009120 diminished CD80 surface marker expression, but this effect was not significant.

A

Stimuli	Receptor	Description
LPS	TLR4	Lipopolysaccharide in outer membrane of gram-negative bacteria
Poly-I:C	TLR3	Poly I:C is a double-stranded homopolymer resembling RNA
Pam3CSK4	TLR1/TLR2	synthetic, triacylated lipopeptide; used as analogue of naturally occurring lipoproteins

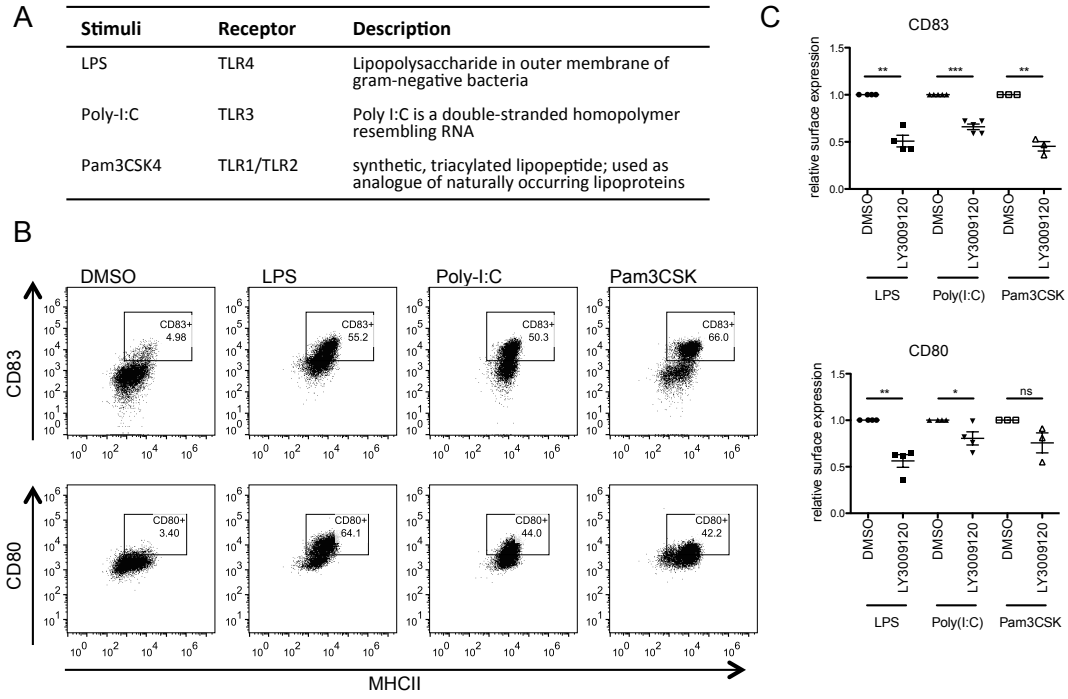

Figure 3.14 Effect of other TLR ligands in combination with LY3009120 on surface marker expression. (A) The RAF inhibitor LY3009120 was combined with the listed TLR ligands to investigate the influence on surface marker expression of moDCs. (B) Flow cytometer analysis of CD83 and CD80 after stimulating moDCs for 48 h with LPS (100 ng/ml), Poly(I:C) (50 µg/ml) or Pam3Cys (1 µg/ml) (C) CD80 and CD83 surface expression was determined by flow cytometry after treating moDCs for 48 h with LPS (100 ng/ml), Poly(I:C) (50 µg/ml, n = 4) or Pam3Cys (1 µg/ml, n = 3) in presence of LY3009120. Shown is the relative mean fluorescence.

3.3.3 Cytokine secretion of human DCs upon RAF and MEK blockade

The maturation of moDCs does not just include altered surface marker expression, but it also leads to the induction of cytokine release. The cytokine profile is usually dependent on the stimulus and it is decisive for the triggered T cell differentiation. It is known, that LPS induces the secretion of inflammatory cytokines such as IL-12p70, IL-6, IL-8 and TNFα [147]. These cytokines were selected to investigate if the RAF inhibitor LY3009120 or the MEK inhibitor trametinib had an impact on the cytokine secretion

profile. The cytokine secretion was determined by ELISA and the viability of the cells was additionally controlled by flow cytometry. **Fig. 3.15A** displays the secreted cytokines relative to the cytokine secretion from LPS stimulated moDCs. The RAF inhibitor LY3009120 reduced under stimulating conditions the secretion of all cytokines, although IL-12p70 secretion was inhibited the most (78 ± 17%). The MEK inhibitor trametinib in presence of LPS had a comparable reducing effect on IL-6 and IL-8 secretion like LY3009120, but caused a more pronounced reduction of TNFα secretion (67 ± 28%). In contrast to the negative effect of LY3009120 on IL-12p70 secretion, trametinib rather promoted its secretion, even though there was a higher deviation in the cytokine secretion.

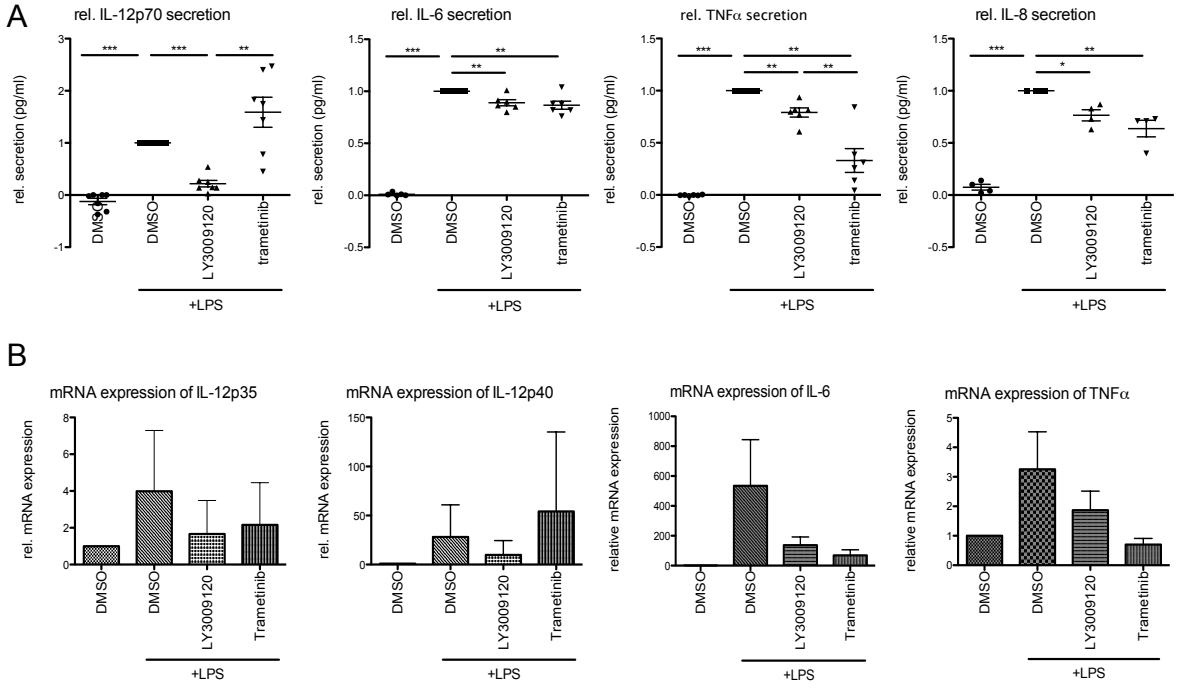

Figure 3.15 Effect of LY3009120 and trametinib on moDC cytokine secretion. (A) The secretion of the inflammatory cytokines IL-12p70 (n = 7), IL-6 (n = 6), TNFα (n = 6) and IL-8 (n = 4) was studied by ELISA after treating moDCs for 48 h with trametinib (1 μM) or LY3009120 (1 μM) in presence of LPS (100 ng/ml). (B) Real time PCR analysis was performed to investigate the mRNA expression of IL-12A, IL-12B, IL-6 and TNFα after treating moDCs with LY3009120 (1 μM) or trametinib (1 μM) in presence of LPS (100 ng/ml) for 48 h (n = 4).

The reduced IL-6 and TNFα secretion was probably due to reduced expression of the cytokines on the mRNA level **(Fig. 3.15B)**. IL-12p70 is a heterodimeric cytokine consisting of IL-12p35 and IL-12p40. LY3009120 treatment diminished mRNA levels of both subunits. While trametinib treatment slightly reduced the mRNA levels of IL-12p35, its effect on IL-12p40 mRNA levels was very inconsistent.

3.3.4 siRNA-mediated loss of function studies on human DCs

Although, the attenuating effect of RAF inhibition on moDC surface marker expression was demonstrated with multiple RAF inhibitors, a specific knockdown of RAF proteins by employing siRNAs should further confirm the specificity of the observed phenotype. As all three RAF kinases were stabilized and as RAF kinases are functioning as heteromers, double knockdowns were performed in moDCs cells (siARAF+siBRAF, siARAF+siCRAF and siBRAF+siCRAF). As shown in **Fig. 3.16A**, siRNA treatment leads to a decrease of RAF proteins in moDCs. The efficiency of the knockdown is illustrated in **Fig. 3.16B**. The reduction of RAF proteins was determined by normalizing the RAF levels to the corresponding actin level or to the PonceauS staining in relation to the respective cells treated with control siRNA. The knockdown resulted only in a moderate reduction of RAF protein levels. Determining the surface expression of CD83 and CD80 of siRNA-treated and LPS-stimulated moDCs revealed no significant differences on the surface expression **(Fig. 3.16C)**. Further, cytokine secretion of IL-12p70 was investigated. The double knockdown of ARAF and CRAF resulted in 29 ± 8 % and the knockdown of BRAF and CRAF in a 36 ± 22,5 % reduced IL-12p70 secretion **(Fig. 3.16D)**.

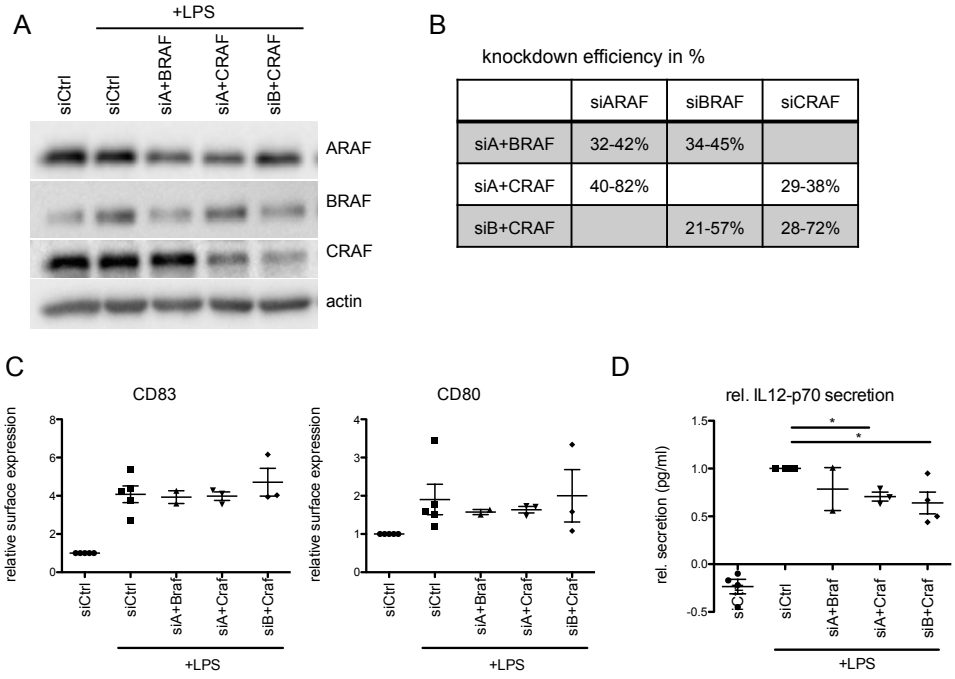

Figure 3.16 siRNA induced double knockdown of RAF proteins in moDCs. (A) By transfecting the corresponding siRNAs a double knockdown of two RAF proteins was achieved (siA+BRAF, siA+CRAF and siB+CRAF). One day after siRNA transfection medium was exchanged and LPS (100 ng/ml) stimulation was started. The knockdown of RAF proteins was investigated by Western Blot at 30 h after stimulation. (B) The knockdown of RAF proteins was determined after normalizing the RAF levels to the corresponding actin or to the ponceauS staining. The reduction of RAF proteins was put in relation to the corresponding siControl. (C) Surface marker expression of CD80 and CD83 and (D) cytokine secretion of IL-12p70 was analyzed 54 h after siRNA transfection including a 30 h stimulation with LPS.

3.4 Role of RAF kinases in the functional maturation of human DCs

3.4.1 Morphological changes upon RAF and MEK1/2 blockade

Together with the alterations observed in surface marker expression and cytokine secretion, morphological changes become apparent during moDC maturation: Cells are forming dendrites and veils in order to enlarge their cellular surface to improve interaction with T cells. Additionally, the coordination of cytoskeletal rearrangements required for the formation of polarized protrusions, formation of new adhesion points or for detachment is necessary for the migration of DCs through tissues and endothelial barriers towards lymphoid tissues.

As shown in the study of Burns *et al*., *in vitro* derived, immature DCs are usually non-adherent, floating cells, while the addition of LPS causes a rapid alteration in morphology. Stimulated DCs rapidly become adherent, develop polarity and assemble actin-rich structures known as podosomes. With progressive maturation, a large proportion of DCs become again more rounded lacking podosomes. Thus, Burns *et al*. concluded, that early maturation favors polarized cell movement and later the formation of ruffles [148]. It is well known, that MAPK signaling is involved in the regulation of cell migration. Published data from our lab demonstrated a modulation of MAPK signaling and cell migration by the regulation of the turnover of CRAF [149]. Further, Ehrenreiter *et al*. showed that CRAF deficiency in keratinocytes and fibroblasts resulted in morphological changes, which were accompanied by migratory defects [70]. Although there is less known about ARAF and its role in migration, published data from our lab showed a role of ARAF in promoting MAPK activity and cell migration in a cell type-dependent manner [150].

To get first insights, if RAF kinases and MAPK signaling are involved in the regulation of moDC morphology and migration, phalloidin staining was performed to analyze the morphology of LPS-stimulated moDCs. The recorded microscopic images in **Fig. 3.17A** illustrate, that LPS-stimulated moDCs, grown on poly-L-lysine coated coverslips, had an elongated morphology, while the treatments with LY3009120 as well as trametinib under stimulating conditions caused a more rounded morphology. Determining the circularity index of the cells confirmed that cells were more rounded after RAF and

MEK1/2 inhibition, although MEK1/2 inhibition resulted in a more pronounced change in cell circularity **(Fig. 3.17B)**.

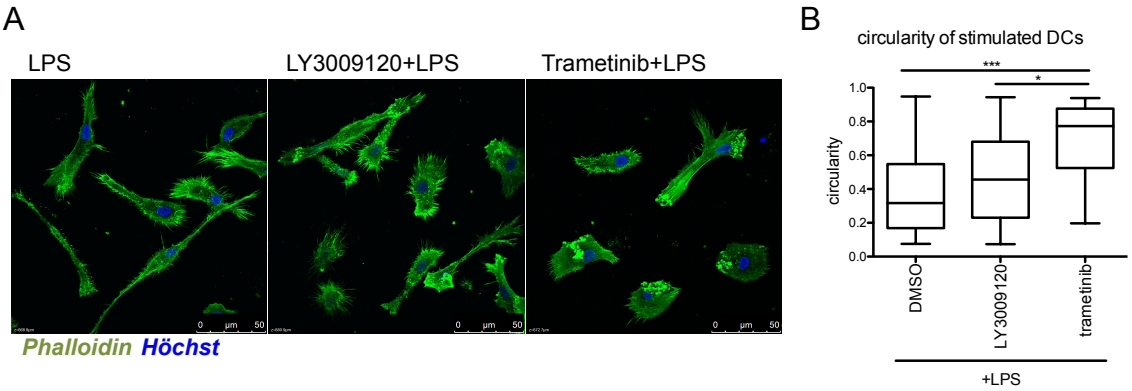

Figure 3.17 Influence of RAF and MEK1/2 inhibition on moDC morphology. (A) F-actin of LPS-stimulated DCs, which were simultaneously treated with LY3009120 (1 µM) or trametinib (1 µM), was stained by phalloidin-rhodamine and visualized by a Leica SP8 confocal microscope using a 63X objective. (B) Morphology was analyzed by determining the circularity index of 26-60 cells per condition.

3.4.2 Influence of RAF and MEK inhibitors on directed DC migration *in vitro*

Another feature of activated DCs is the up-regulation of the chemokine receptor CCR7, which directs the DCs from peripheral tissue to the draining lymph nodes where they find a pool of naïve T cells. The known ligands of CCR7 are CCL19 and CCL21. Both ligands are expressed in the T cell zones of secondary lymphoid organs [151, 152], while CCL21 is additionally expressed by endothelial cells of lymphatic vessels and by high endothelial venules [153].

Due to the central role of CCR7 in directing DCs to the lymph nodes, it was tested whether RAF kinases and MAPK signaling influence the CCR7 expression, which is induced upon moDC stimulation. Analysis of the mRNA confirmed the up-regulation of CCR7 after stimulating moDCs with LPS for 48 h **(Fig. 3.18A)**. Treatment with the MEK inhibitor trametinib alone already enhanced CCR7 expression. But under stimulating conditions, MEK1/2 inhibition did not further enhance CCR7 mRNA levels compared to LPS-induced mRNA levels. In accordance to the observed contrary effect of RAF and MEK1/2 inhibition on surface marker expression shown in section 3.3.2, inhibition of RAF kinases by the inhibitor LY3009120 restricted the LPS induced up-regulation of CCR7 mRNA levels. In order to perform transwell migration experiments, enhanced surface marker expression should be confirmed as well. Despite the augmented CCR7 mRNA level after LPS stimulation, just moderate surface marker expression of CCR7 was detected **(Fig. 3.18B)**. The study from Bruckner *et al.* identified prostaglandine E_2

(PGE_2) as a critical factor for DC migration and further demonstrated enhanced CCR7 expression upon the addition of PGE_2 [154]. In agreement to this, CCR7 surface expression was clearly enhanced after concurrent stimulation of moDCs with LPS and PGE_2. Further, the combined stimulation did not affect the observed reduction of CCR7 surface expression after blocking RAF kinases by LY3009120 **(Fig. 3.18C)**. In contrast, MEK1/2 inhibition while stimulating moDCs with LPS and PGE_2 even enhanced CCR7 surface expression compared to the stimulated control cells. Thus, transwell migration experiments were carried out with LPS- and PGE_2-stimulated moDCs treated with LY3009120 or trametinib and CCL21 was employed as the chemoattractant. **Fig. 3.18D** displays the number of cells migrated to the lower chamber relatively to the corresponding stimulated control. Consistent with the reduction in CCR7 expression, inhibition of RAF kinases resulted in a significantly reduced directed migration towards CCL21. No conclusion can be drawn about the effect of MEK1/2 inhibition on moDC migration, as the obtained results were highly inconsistent.

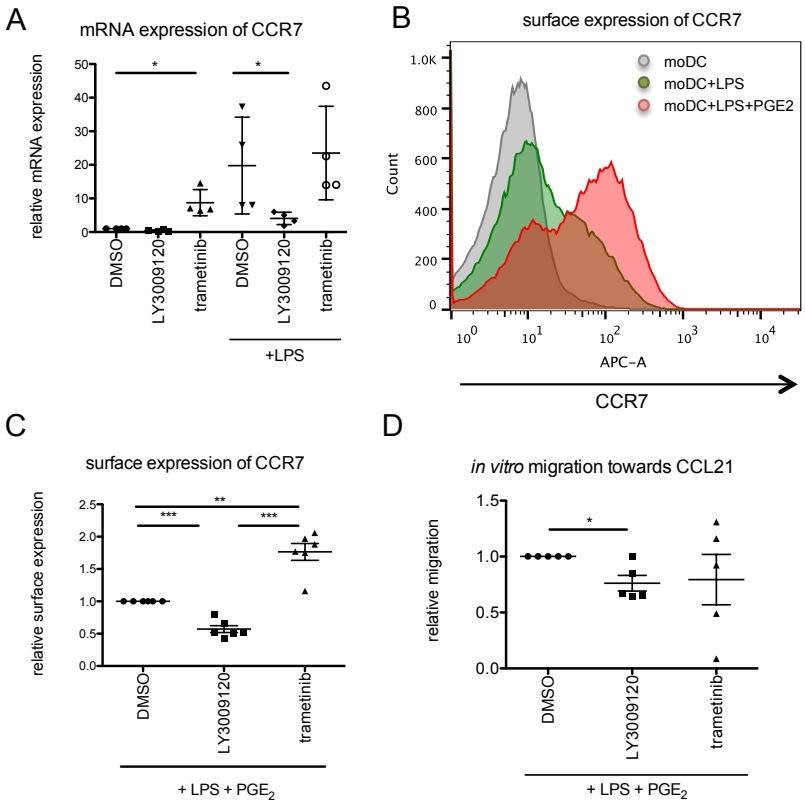

Figure 3.18 Influence of RAF and MEK1/2 inhibition on moDC migration. (A) CCR7 mRNA levels were measured by real time PCR after treating moDCs with LY3009120 (1 µM) or trametinib (1 µM) in presence or absence of LPS for 48 h. (B) Flow cytometric analysis of CCR7 surface marker expression of immature moDCs (grey) and moDCs stimulated with LPS (100 ng/ml, green) or with a combination of LPS and PGE_2 (PGE_2: 1 µg/ml, red) for 48 h. (C) Analysis of the CCR7 surface marker expression after LY3009120 (1 µM) or trametinib (1 µM) treatment while stimulating with LPS (100 ng/ml) and PGE_2 (1 µg/ml) (n = 6). (D) Directed migration of moDCs towards the cytokine CCL21 (200 ng/ml) was determined in transwell migration experiments by counting successfully migrated DCs after 3 h (n = 5).

3.4.3 DCs treated with RAF inhibitors inhibit T cell activation

DCs have the unique property of integrating multiple signals from the environment in order to induce an appropriate adaptive immune response through the induction and differentiation of naïve T cells into helper and effector T cells. The activation state of the DC is crucial for the final outcome of the induced T cell response. Thus, a series of independent parameters commit to the priming of naïve T cells including the concentration of peptides presented to the T cells, the duration and frequency of DC-T cell interaction, the commitment of T cell co-stimulatory molecules and the secretion of cytokines [155, 156].

A commonly used technique to evaluate the functional activity of DCs is a mixed lymphocyte reaction (MLR), in which the DC-induced T cell proliferation is determined. By the usage of DCs and T cells from different donors, allogeneic antigens serve as stimulant. The experiments were done in collaboration with Helmut Jonuleit's group (Department of Dermatology of the University Medical Center of the Johannes Gutenberg-University Mainz). As shown by a representative MLR in **Fig. 3.19A**, DCs stimulated with LPS clearly induced the proliferation of $CD4^+$ T cells compared to immature DCs resulting in an average 227 ± 114% enhanced T cell proliferation. The concurrent treatment of LPS-stimulated DCs with the RAF inhibitor LY3009120 did not just result in reduced surface marker expression, but also in a diminished functional activity as the efficiency of inducing $CD4^+$ T cell proliferation was reduced as well. Thereby, the difference in functional activity between LPS-stimulated DCs and DCs treated with LY3009120 was significant when DCs were cultured with $CD4^+$ T cells in a ratio between 1:4 and 1:32 displaying the range in which the induced T cell proliferation was the highest. Within this range, seven of the nine independently performed MLRs showed a 10-37% reduction in T cell proliferation, while two of them did not show a significant difference **(Fig. 3.19B)**.

The influence of the MEK inhibitor trametinib on the functional activity of moDCs could not be determined by allogeneic MLRs as the treated moDCs generally died shortly after starting the co-culture with the $CD4^+$ T cells, thus not being able to induce a proper T cell proliferation.

After showing that RAF inhibitor treated moDCs led to a reduction in T cell proliferation, it was additionally tested in collaboration with Helmut Jonuleit's group whether the RAF

inhibitor itself has an effect on T cell proliferation. Therefore, CFSE-labeled, human CD4+ T cells were stimulated with CD3 and CD28 in presence of LY3009120. After four days, dividing cells were identified by flow cytometry. **Fig. 3.19C** illustrates that stimulation of CD4+ T cells with CD3 and CD28 induced T cell proliferation. In contrast, T cell proliferation was completely blocked in the presence of LY3009120. The same result was obtained with the MEK inhibitor trametinib. Further, ERK1/2 phosphorylation was blocked in CD4+ T cells by the RAF as well as by the MEK inhibitor **(Fig. 3.19D).**

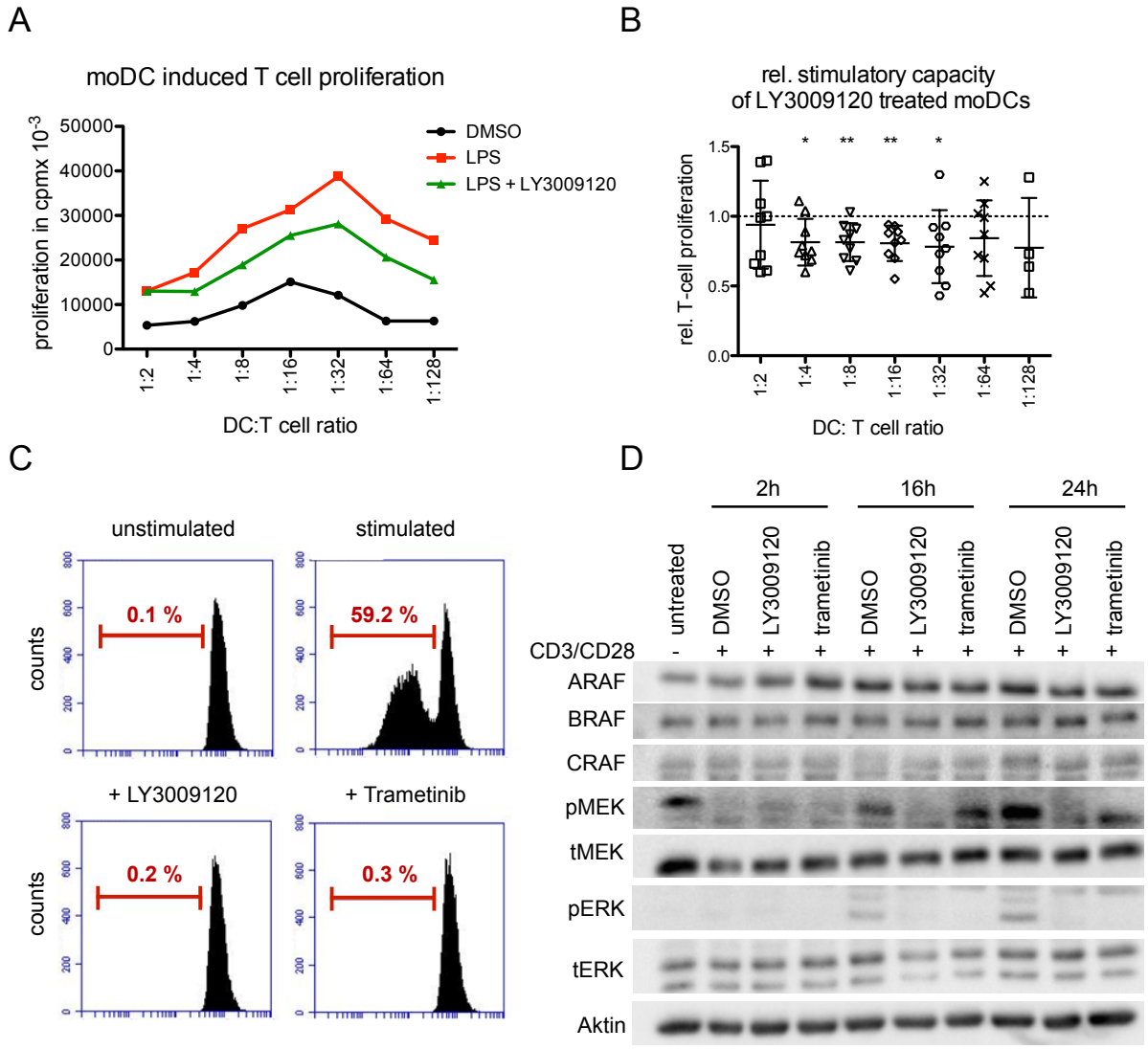

Figure 3.19 Attenuating effect of LY3009120 on the functional activity of moDC in allogeneic MLR. (A) To evaluate moDC-induced T cell proliferation a MLR with moDCs stimulated with LPS in presence of LY3009120 (1 µM) and allogeneic CD4+ cells was performed. T cell proliferation was determined via ^{3}H-thymidine incorporation. Shown is a representative experiment. (B) The induced T cell proliferation of moDCs treated with LY3009120 (1 µM) was determined relatively to the corresponding stimulated control (n = 9). (C) CFSE labeled CD4+ T cells stimulated with 0.5 µg/ml anti-CD3 mAb and 1 µg/ml anti-CD28 mAb were simultaneously treated with LY3009120 (1 µM) or trametinib (1 µM). Dividing cells were identified by flow cytometry. (D) Western Blot analysis of anti-CD3/CD28 stimulated CD4+ T cells treated for 0 h, 2 h, 16 h and 24 h was performed to analyze MAPK signaling after LY3009120 (1 µM) or trametinib (1 µM) treatment.

3.5 RAF kinases and murine DCs

3.5.1 Effect of RAF and MEK inhibitors on bone-marrow derived DCs

In order to perform *in vivo* studies, we tested for the effects of RAF inhibitors on murine BMDCs. Therefore, surface marker expression of the co-stimulatory molecules CD86 and CD80 was analyzed after treating BMDCs with LY3009120 or trametinib in the presence or absence of LPS. While MEK1/2 inhibition alone induced a higher surface marker expression of CD86 and CD80, MEK1/2 inhibition under stimulating conditions did not further increase the expression levels of the tested markers. In contrast, LY3009120 treatment significantly reduced the LPS-induced up-regulation of CD86 and CD80 **(Fig. 3.20A)**. The treatments of BMDCs with LY3009120 or trametinib under stimulating and non-stimulating conditions had a similar outcome on the surface marker expression level of the chemokine receptor CCR7 **(Fig. 3.20B)**. The migratory properties of treated BMDCs were investigated by transwell migration experiments. Reflecting the CCR7 surface marker expression, BMDCs treated with LY3009120 during LPS stimulation revealed a significantly reduced directed migration **(Fig. 3.20C)**. The data obtained with trametinib-treated BMDCs were inconsistent.

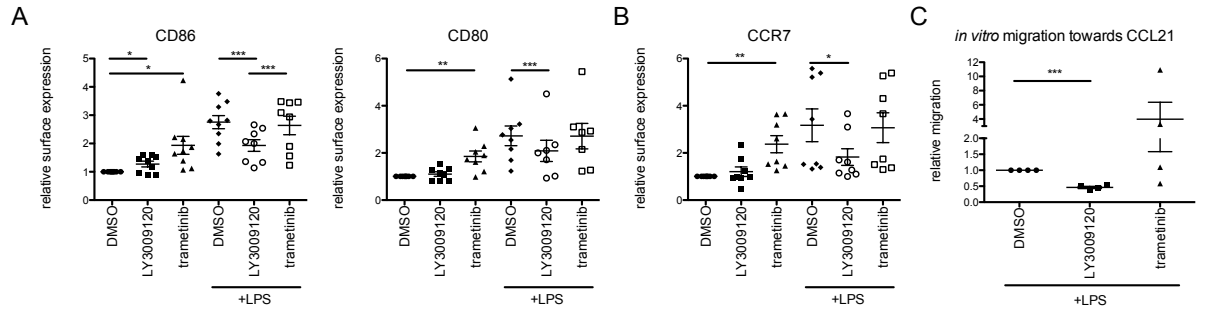

Figure 3.20: Influence of RAF and MEK inhibitor on mouse bone marrow-derived DCs. (A) Bone marrow-derived DCs from C57BL/6J mice were treated with 1 µM trametinib or with 1 µM LY3009120 in presence or absence of 100 ng/ml LPS for 48 h and surface marker expression of CD86 and CD80 (B) as well as of the chemokine receptor CCR7 was analyzed by flow cytometry. Shown is the relative mean fluorescence of multiple independent experiments. (C) The directed migration of BMDCs, treated for 16 h with LY3009120 (1 µM) or trametinib (1 µM) in presence of LPS, was investigated in transwell migration experiments using CCL21 (200 ng/ml) as chemoattractant. Successfully migrated BMDCs were determined after 3 h by MTT assay.

In summary, similar effects of the tested inhibitors LY3009120 and trametinib were observed in human and murine DCs *in vitro*.

3.5.2 Influence of the pan-RAF inhibitor LY3009120 on murine DCs activation *in vivo*

The aforementioned studies clearly suggest a critical role for RAF kinases for DC activation and function both in mice and human. To further evaluate the physiological significance of RAF inhibitors on DC function *in vivo*, the LPS-induced surface marker expression of splenic DCs and DCs from lymph node was investigated after treating C57BL/6J mice with LY3009120 as described in the section 2.4.8. The employed RAF inhibitor concentration has been selected based on published observations, showing tumor growth inhibition in NU/NU mice [100].

We first tested the appropriate LPS concentration that is required to activate DCs as measured by the expression of surface markers CD80 and CD86. Six hours after administering 10 µg LPS, the surface marker expression was clearly enhanced in splenic and lymph node DCs **(Fig. 3.21A-B)**. To investigate the physiological role of LY3009120 on DC activation, C57BL/6J mice were pre-treated with the inhibitor. After administering the inhibitor for two consecutive days, LPS was injected in order to induce an immune response. While the treatment with LY3009120 did not affect the surface marker expression of DCs isolated from lymph nodes, splenic DCs had a slightly decreased expression of MHCII, CD80 and CD86 after RAF inhibitor treatment.

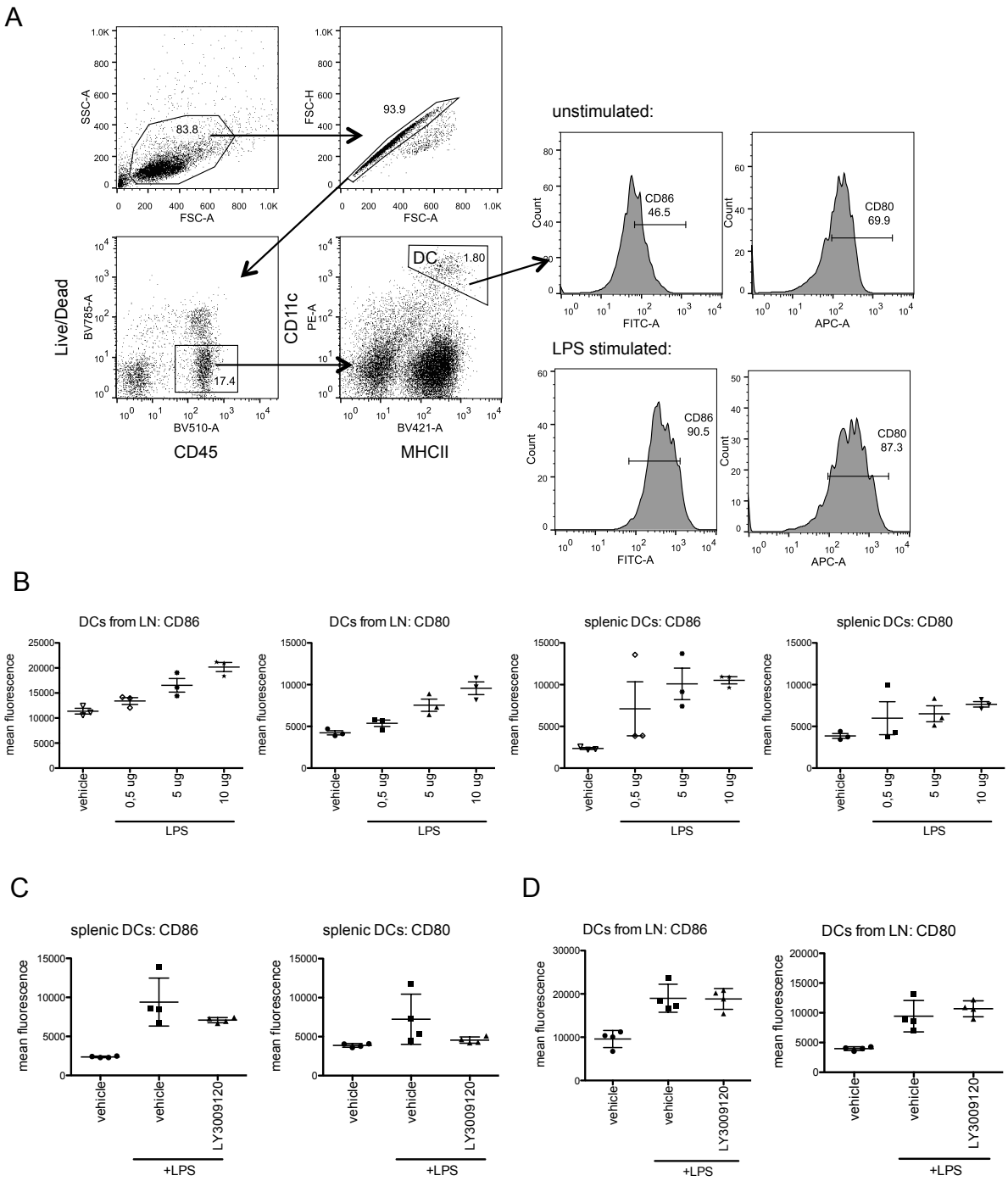

Figure 3.21: ***In vivo*** **role of RAF kinases on mouse DCs from lymph node and spleen** (A) Gating strategy to identify splenic DCs. Expression of CD86 and CD80 from $CD11c^{high}MHC^{high}$ cells was investigated. The histograms are representative for CD86 and CD80 expression of control mice (unstimulated) and LPS-treated mice. (B) LPS concentrations ranging from 0.5 µg to 10 µg were injected i.p. and after 6 h expression of CD86 and CD80 from DCs isolated from LN or (C) spleen was investigated. (D) The *in vivo* effect of LY3009120 was investigated on DCs from lymph node and (C) on splenic DCs from C57BL/6J mice. The inhibitor (15 mg/kg; solved in 0.5% carboxymethylcellulose) was administered i.p. on day 0 and day 1. LPS (10 µg/mouse) was injected i.p. on day 2. Control mice received the corresponding vehicle. 6 h after LPS administration, mice were sacrificed, inguinal lymph nodes and spleens were isolated and surface expression of DCs (CD86 and CD80) was analyzed by flow cytometry.

3.6 Identification of proteins interacting with CRAF in DCs

3.6.1 A mass spectrometric-based approach to identify CRAF interactome

We aimed to identify potential interaction partners and substrates of CRAF by employing crosslinking experiments coupled to mass spectrometry. In short, cross-linked RAF proteins were precipitated from LPS-stimulated human moDCs and co-immunoprecipitated proteins were then identified by mass-spectrometry.

Initially, DTME cross-linking was established on moDCs stimulated for 24 h with LPS. DTME is a maleimide cross-linker, which conjugates between sulfhydryl groups (-SH). Because of a disulfide bond in its spacer arm DTME can be cleaved after adding reducing agents like DTT. Different DTME concentrations were supplied on stimulated moDCs and cross-linking was investigated using CRAF as first RAF kinases to be studied. Cross-linking of CRAF was achieved with a 0.2 mM DTME concentration and it resulted in a high molecular weight complex of more than 245 kDa, which was cleaved after adding DTT **(Fig. 3.22A)**. The complex, which was precipitated through cross-linked CRAF, had the same size like the one detected in the input sample **(Fig. 3.22B)**. By adding DTT, the complex was again cleaved and CRAF was detected with its known molecular weight.

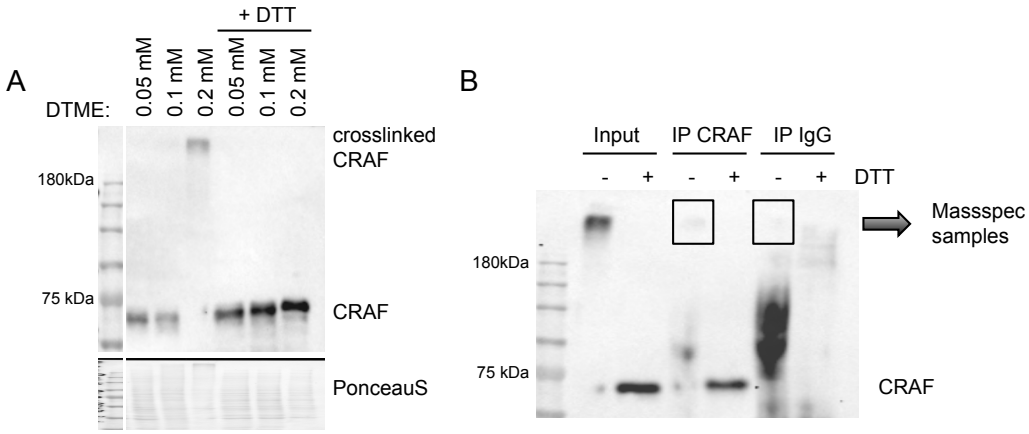

Figure 3.22: Crosslinking CRAF by using DTME. (A) LPS-stimulated moDCs (24 h) were incubated with different DTME concentrations for 30 min at 37°C. The reaction was stopped by incubating the cells for 10 min in Tris buffer pH = 8. Western Blot analysis was performed to analyze the efficiency of the crosslinking. (B) The high molecular weight complex, which was obtained after cross-linking, was precipitated by using a CRAF specific antibody. The precipitated complex was cleaved after adding DTT.

Subsequently, mass-spectrometric analysis was performed in collaboration with Stefan Tenzer's group in order to examine the precipitate of cross-linked CRAF. In a second approach, cross-linked CRAF was first precipitated and then loaded on an acrylamide gel. At the size of the detected high molecular weight complex the gel was cut out and

send for mass spectrometry. In both cases an immunoprecipitation using a corresponding IgG antibody served as a control.

3.6.2 Identified proteins in CRAF precipitates from stimulated moDCs

The proteins, which were identified by mass-spectrometry in precipitates of cross-linked CRAF, were validated by a log2 ratio between the CRAF precipitates and the precipitates obtained with the corresponding IgG control. Proteins with a log2 ratio higher than 1 were defined as enriched in CRAF precipitates. Comparing the results obtained with two biological replicates revealed, that 47 proteins of the first replicate and 41 proteins of the second replicate were enriched in the CRAF precipitates **(Fig. 3.23A)**. Of the identified, enriched proteins 8 proteins were detected in both replicates **(Fig. 3.23B)**. In both samples CRAF was exclusively detected in the CRAF immunoprecipitates proving the precipitation of CRAF itself. Besides several 14-3-3 proteins, which are known to interact with RAF proteins and being involved in RAF regulation, ATP-citrate synthase was a protein, which was detected only in CRAF precipitates.

A

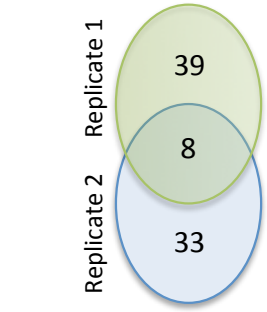

B

		Replicate 1			Replicate 2		
description	entity	reported peptides	log2(01/02)	ttest 01 vs 02	reported peptides	log2(01/02)	ttest(01vs02)
RAF proto-oncogene serine/threonine-protein kinase	**RAF1_Human**	**12**	**3.43**	**1.28E-03**	**9**	**10.66**	**1.00E-06**
ATP-citrate synthase	ACLY_HUMAN	39	3.10	1.47E-04	45	12.35	1.00E-06
14-3-3 protein beta/alpha	1433B_HUMAN	14	1.29	7.12E-04	6	2.72	4.79E-06
14-3-3 protein epsilon	1433E_HUMAN	12	1.12	2.16E-02	6	2.41	3.24E-03
14-3-3 protein eta	1433F_HUMAN	13	1.77	3.20E-03	7	7.58	1.00E-06
14-3-3 protein gamma	1433G_HUMAN	14	1.44	1.19E-03	8	2.22	8.58E-05
14-3-3 protein theta	1433T_HUMAN	10	1.04	2.28E-04	5	8.39	1.00E-06
Acylamino-acid-releasing enzyme	ACPH_HUMAN	9	3.46	1.42E-04	3	9.54	1.00E-06

Figure 3.23: Mass-spectrometry analysis of CRAF precipitates from stimulated moDCs. (A) LPS-stimulated moDCs (24 h) were treated with 0.2 mM DTME for 30 min at 37°C. After stopping the reaction by incubating the cells for 10 min in Tris buffer pH = 8, CRAF was precipitated. An IgG control was included. For the replicate 1, proteins immobilized on beads were sent for mass-spectometry. For the replicate 2, immunoprecipitates were loaded on an acrylamide gel and the high molecular complex with cross-linked CRAF was cut out and analyzed. For both replicates, three technical replicates were prepared. Proteins from CRAF and IgG precipitates were compared and proteins with a log2 > 1 were defined as enriched in CRAF precipitates. Of the enriched proteins, 8 proteins were detected in both replicates and are listed in (B) together with their log 2 ratio. The t-test was applied on the technical replicates itself.

Further studies are warranted to validate the interaction of CRAF with the identified proteins and to demonstrate a physiological relevance of the interaction.

4 Discussion

4.1 RAF kinases are stabilized during moDC differentiation

The development of selective ATP competitive and non-competitive inhibitors against kinases had gained much interest because of their clinical success in treating a wide variety of malignancies. For instance, mTOR inhibitors were shown to be effective to treat solid tumors, such as breast and kidney cancer [157], the inhibitor of epidermal growth factor receptor gefitinib has been employed with success in treating non small cell lung cancer and the inhibitor of vascular epidermal growth factor receptor sorafenib was approved for the treatment of renal cancer [158]. Targeting RAF and MEK1/2 kinases are of substantial clinical interest, as the MAPK pathway is deregulated in many human cancers with the upstream activator RAS [72] as well as BRAF [75] being among the most frequent oncogenes. Already in 2011, vemurafenib was approved by the FDA for the treatment of unresectable or metastatic melanoma with BRAF V600E mutation [159]. Currently, there are 18 ongoing phase II clinical trials with vemurafenib as listed in the database of ClinicalTrials.gov. In case of dabrafenib, another FDA approved BRAF inhibitor, 27 phase II clinical trials with melanoma patients are active [ClinicalTrials.gov [160]]. Despite extensive studies focusing on uncovering the role of the RAF kinases in tumorigenesis, relatively little is known on their physiological role in the regulation of the immune system. The RAF-MEK1/2-ERK1/2 signaling cascade regulates multiple basic cellular processes, like proliferation, migration, differentiation and cell death [2]. Inhibition of such a basic cell signaling pathway systemically may not only hamper tumor growth, but may have unexpected side effects like dampening of the anti-tumor immune response.

In the tumor-immune interface, a series of events must take place in order to generate an efficient anti-cancer immune response resulting in effective killing of cancer cells [161]. Tumor-associated cDCs capture cancer-associated antigens and transport them to the draining lymph nodes, where they present the antigens on MHC-I and MHC-II molecules to T cells. Subsequently, primed and activated T cells traffic to the tumor, specifically recognize cancer cells and mediate their killing [161]. Each step is critical to develop an effective anti-cancer immune response in order to destroy immunologically vulnerable cancer cells. Nonetheless, cancer cells can evade immune elimination due to

genetic instability and constant cell division, which can result in a reduced immunogenicity by gaining immune suppressive effects or by the loss of target antigen expression. Immune suppressive effects by the tumor also include the production of immune suppressive mediators [162]. For instance, the secretion of cytokines like transforming growth factor (TGF)-β [163] or the recruitment of regulatory T cells to the tumor microenvironment contribute to the tumor immune escape mechanisms [164].

One of the key issues in targeted therapeutics is to evaluate whether the drug treatment elicits adverse effects in the immune system. In this case, we focused initially on DCs, which are necessary for T cell mediated-cancer immunity as they are the central regulators of the adaptive immune system. We worked with a well-established *in vitro* culture model, in which human monocytes were differentiated to moDCs in the presence of GM-CSF and IL-4 [129]. During this *in vitro* culture the influence of various drugs, including kinase inhibitors, on the differentiation, maturation and functions of DCs can be evaluated.

The hypothesis free phospho-proteome analysis described in chapter 3.1 compared the phospho-proteome of monocytes and moDCs to provide information on proteins and pathways, which might be phosphorylated or dephosphorylated during the differentiation process. Phospho-peptides, which were exclusively detected in moDCs, were of special interest as their regulation is possibly important for moDC differentiation or function. As we discovered a phosphopeptide of ARAF exclusively in moDCs, we analyzed the phosphopeptides of all three RAF isoforms more in detail. But it should be mentioned, that unmodified RAF proteins were not detected by LC-MS. Consequently, differences seen in the phosphoproteome analysis are either the result of enhanced phosphorylation of the detected phosphorylation site or they are the result of changes in protein translation. In case of ARAF, the phosphopeptide identified in moDCs carried the phosphorylation site S257. This phosphorylation site was first identified by a mass spectrometry based approach and further characterized by Baljuls *et al*. in an attempt to identify novel phosphorylation sites in ARAF. Together with seven novel phosphorylation sites, the site S257 was identified within a regulatory domain, which they designated as isoform-specific hinge segment (IH-segment), which is located between the CR2 and CR3 domains. In their study, a single point mutation replacing S257 by alanine resulted in a significantly diminished catalytic activity of ARAF in an *in vitro* kinase assay [165]. Our own kinase assay-based data confirmed a lower kinase

activity of ARAF S257D compared to wild type ARAF (Fig. 3.2). Further the study by Baljuls *et al*. claims, that S257 might be involved in ERK-mediated feedback phosphorylation as S257 revealed an ERK-directed phosphorylation motif (SP) and treatment with a MEK inhibitor decreased the kinase activity of ARAF wild type. Interestingly, the amino acid sequence of the IH-segment in ARAF and CRAF have a very low degree of similarity with the exception of the site S257 in ARAF, which corresponds to the site S296 in CRAF [165]. In our own phospho-proteome analysis, we found that the phosphopeptide of CRAF with the phosphorylation sites S296 and S301 was highly detected in moDCs. These sites are associated with ERK-mediated feedback regulation, but phosphorylation at these positions has been correlated with both reduced [61, 166] and enhanced CRAF activity [36]. Differences in the observed CRAF activity can be explained by the fact, that these studies were employing different RAF mutants to investigate ERK-mediated feedback regulation: While Balan *et al*. analyzed CRAF activity after mutating S289/296/301 [36], Doughtery *et al*. characterized a CRAF mutant with six substituted, ERK-targeted SP sites (S29, S43, S289, S296, S301 and S642) [61]. Both studies validated CRAF activity with a kinase assay. The triple mutants resulted in sustained CRAF activity, while mutation of the six residues had the opposite effect. In contrast, Hekman *et al*. analyzed the kinase activity of single mutants by a kinase assay using recombinant MEK and ERK as substrates. By determining the phosphorylation of ERK they showed an enhanced kinase activity of CRAF S296A or CRAF S301A [166]. Because of these aforementioned discrepancies, we wanted to determine the kinase activity of CRAF S296 mutants in our study as well. We revealed that overexpression of CRAF S296/301D mutant in HEK293T cells increased MEK1/2 activation, which suggests that these phosphorylation sites might enhance the enzymatic activity of CRAF (Fig. 3.2).

Since the phosphoproteome data point to a differential regulation of ARAF and CRAF in moDCs compared to monocytes, we further investigated the expression of RAF kinases during the differentiation of monocytes to moDCs. We found a strong up-regulation of RAF proteins (Fig. 3.3) during differentiation, which we attributed to increased protein stability in moDCs since we couldn't detect any changes in the mRNA levels (Fig. 3.4). Altered RAF expression levels during cellular differentiation were already found in erythroblasts, in which CRAF expression was down-regulated during the differentiation of erythroblasts to mature erythrocytes [167]. In contrast to our study, which showed

altered protein levels because of altered protein stability, the decrease during erythroid differentiation was due to reduced mRNA levels [168]. Most of the studies have been focusing on CRAF and BRAFV600E protein stability. It is known that CRAF or activated BRAFV600E forms a complex with heat shock protein Hsp90 and disruption of these complexes significantly reduces their protein levels [169-171]. Subsequently, CRAF and BRAF V600E, but not wild type BRAF, are degraded by the proteasomes [171-173]. For proteasomal degradation, proteins are usually covalently conjugated with multiple ubiquitin molecules [174]. A known ubiquitin ligase for CRAF is CHIP [175]. A study from our lab further showed an involvement of X-linked inhibitor of apoptosis protein and cellular inhibitor of apoptosis protein in promoting CRAF degradation by supporting the binding of CHIP to the Hsp90-CRAF complex [149].

In our study we demonstrated, that three days after initiating moDC differentiation the treatment with the proteasome inhibitor MG132 caused only a slight accumulation of ubiquitinated CRAF as well as ARAF, but not of BRAF (Fig. 3.5). Precipitated ARAF and CRAF after MG132 treatment showed a smear in the subsequent western blot analysis, which is an indicator for ubiquitinated proteins. Comparing the smear of ubiquitinated ARAF and CRAF from cells on day 3 of culture and from immature moDCs on day 5 of culture revealed no major differences in the polyubiquitination pattern. Since there was anyway no substantial increase in ARAF and CRAF levels after MG132 treatment, it is possible that the turn over of RAF proteins is additionally mediated through other protein quality control machineries. An alternative pathway for protein turn over is lysosomal proteolysis. It has been reported that autophagy, a lysosomal pathway that degrades damaged organelles and cytoplasmic material [176], is induced when monocytes were differentiated with M-CSF or with GM-CSF and IL-4 and that it is essential for monocyte-macrophage differentiation [176]. Thus, it would be interesting to study the effect on RAF degradation after blocking autophagy with inhibitors like chloroquine or 3-methyladenine [177, 178].

Because of the observed steady increase in RAF protein levels during moDC differentiation the downstream signaling was investigated as well (Fig 3.3). Despite the increase in RAF proteins, we failed to detect any consistent changes in MEK1/2 protein levels as well as in the phosphorylation of MEK1/2. The activation of ERK1/2 followed an oscillating pattern, while total ERK1/2 levels largely remained unchanged during the differentiation process. Although the ERK1/2 phosphorylation pattern itself was

comparable within six independent replicates, the kinetics of ERK1/2 activation and phosphorylation were shifted and did not correlate to a certain day of culture reflecting a higher deviation. However, despite undetectable RAF levels at the beginning of moDC differentiation, ERK1/2 phosphorylation was still sufficiently induced. These observations suggest a possible involvement of alternative ERK1/2 activating mechanisms apart from the classical RAS-RAF-MEK1/2 cascade. It is reported, that oscillations can occur as a result of negative feedback loops [179]. In line with this, oscillating ERK1/2 activity was observed in FGF-stimulated NIH3T3 cells, which was caused by an ERK mediated negative-feedback phosphorylation [180]. Further, in the study by Waters *et al.* the oscillating ERK1/2 signal has been translated to an altered gene regulation pattern [181]. Consequently, it is possible that the oscillating ERK1/2 signal during moDC differentiation is potentially required to regulate the dynamic expression of a unique subset of genes.

4.2 Activation of RAF kinases in moDCs

TLR stimulation activates and regulates several intracellular signaling pathways including MAPK and NFκB [182, 183]. TLR signaling can activate the three main MAPK signaling cascades including ERK1/2, JNK and p38 [145]. Initially it was speculated, that TLR4 signaling does not stimulate ERK1/2 in DCs [184], but the study by Kaiser *et al.* demonstrated LPS-induced ERK1/2 phosphorylation in BMDCs [146]. In our study we confirmed LPS-mediated activation of ERK1/2 in moDCs (Fig. 3.6).

There are studies demonstrating that TLR4 signaling utilizes the tumor progression locus 2 (Tpl-2) as MAP3K for MEK1/2 in innate immune cells [185]. In line with this, LPS-induced ERK1/2 phosphorylation was blocked in BMDCs from tpl-2$^{-/-}$ mice [146]. However, RAF kinases are implicated in LPS induced MEK1/2-ERK1/2 signaling as well [186, 187]. In line with these studies, we observed that LPS-mediated stimulation induced CRAF S338 phosphorylation, dimerization in moDCs, which paralleled activation of the downstream kinase MEK1/2 (Fig. 3.8). Phosphorylation of S338 is a critical event in the activation cycle of CRAF and is essential for the biological and enzymatic activities of CRAF [51]. In ARAF, Baljuls *et al.* demonstrated that phosphorylation of the corresponding S299 residue was crucial for its kinase activity [52]. In our study stimulation of moDCs with LPS did not promote ARAF S299 phosphorylation (Fig. 3.8). Further, ARAF precipitated from LPS-stimulated moDCs

showed only a low kinase activity in an *in vitro* kinase assay. However, one needs to indicate that ARAF has the least kinase activity among the RAF isoforms [188]. In contrast, substantial kinase activity of precipitated CRAF as well as BRAF was seen (Fig. 3.8). A quantitative comparison of the kinase activities of BRAF and CRAF was not possible in the conducted experiments: in the presented experimental settings different antibodies were used to precipitate the protein of interest, which led to varying amounts of precipitated proteins. Furthermore, a direct comparison of ARAF, BRAF and CRAF kinase activity is hampered by their different activities, with BRAF exhibiting the highest and ARAF the lowest kinase activity [52]. However, based on the qualitatively determined kinase activities, our data suggest that BRAF and CRAF are the primary RAF kinases in moDCs after LPS stimulation.

Another crucial step in RAF activation is RAF dimerization, which leads to the allosteric activation of the binding partners and to the stabilization of the activated conformation [54]. Additionally, it has been reported that kinase activity of isolated CRAF/BRAF heterodimers is relatively higher in comparison with the respective homodimers [55]. Compared to BRAF and CRAF, dimerization of ARAF is less well studied. Freeman *et al.* showed that EGF stimulation induced only a low level of binding between ARAF and BRAF and little to no interaction between ARAF and CRAF [79]. Thus, weak dimerization of ARAF is likely to be the reason for the focus on BRAF and CRAF dimerization. Under basal conditions, we observed binding of ARAF and CRAF to BRAF (Fig. 3.7). Interestingly, 24h after LPS stimulation an increased binding of ARAF and BRAF was seen. Further, two out of four independent experiments revealed binding of CRAF to ARAF at this time point post LPS stimulation. The study by Rebocho *et al.* also showed ARAF binding to BRAF as well as to CRAF. Further, they revealed a role of ARAF in stabilizing BRAF-CRAF complexes in some cells, which were treated with RAF inhibitors. But surprisingly, the destabilization of the BRAF-CRAF complex after the loss of ARAF did not attenuate the RAF inhibitor induced paradoxical activation [189]. In contrast, the study by Mooz *et al*., revealed a drug-induced and cell-type dependent ARAF homodimerization contributing to MAPK activity and tumor cell invasion. They showed that BRAF-CRAF heterodimers triggered in the absence of ARAF were unable to activate MEK1/2. Additionally, the study uncovered a competition among the RAF isoforms for MEK1/2 binding and suggested RAF competition as a general feature of MAPK signaling [150]. Accordingly, it would be worth investigating if the heterodimers

differ in their ability to bind and activate MEK1/2. Within our immunoprecipitation studies we could detect MEK1/2 only in one out of four independent experiments, but in this experiment MEK1/2 was exclusively detected in CRAF immunoprecipitates. Since the RAF proteins showed a diverse affinity in MEK1/2 binding in moDCs, it is possible that their contribution to promote MAPK signaling differs as well. It would be especially interesting to determine the ARAF activity in more detail as the data obtained until now are contradictory to some extent. While the phosphoproteome data as well as the interaction studies suggest a possible that ARAF is active in moDCs, we detected only a low ARAF activity in the kinase assay. As RAF dimerization is not necessarily linked to catalytic activity [190], it is possible that ARAF functions rather as a scaffold to stabilize BRAF:CRAF heterodimers as described by Rebocho *et al.* [189] or that it is involved in the regulation of the MAPK signaling by a RAF competition mechanism described by Mooz *et al.* [150]. Since it is often shown that ARAF and CRAF cannot compensate for each other in certain conditions, distinct functions of the RAF kinases with ARAF exhibiting non-catalytic roles is another possibility.

4.3 Targeting MAPK signaling in moDC

Although the FDA approved RAF inhibitors vemurafenib and dabrafenib showed remarkable clinical success in melanomas with mutant BRAF V600E [85-88], concerns about the fast developing drug resistance and the occurrence of secondary malignancies were limiting the excitement [85, 88, 89]. Extensive studies on RAF inhibitors revealed that paradoxical activation of ERK1/2 occurred in the absence of BRAF-activating mutations [90]. MAPK signaling driven by RAS relies on RAF dimerization. In this case, paradoxical activation of the pathway is caused through a drug-induced RAF dimerization and transactivation of the dimers [91]. Consequently, next generation RAF inhibitors were developed to prevent the paradoxical ERK1/2 activation. Among others are the so-called pan-RAF inhibitor LY3009120, which inhibits both the monomeric and dimeric RAF proteins with equal efficiency [99].

The inhibitory effect of LY3009120 on MAPK signaling was confirmed with various tumor cells showing that a 1 µM concentration was sufficient to inhibit MEK1/2 and ERK1/2 phosphorylation as well as to reduce the proliferation and viability of the tested cancer cell lines (Fig. 3.9). Inhibition of RAF kinases in human moDCs after LY3009120 treatment was confirmed by an in vitro kinase assay (Fig. 3.10). Since LY3009120

concentrations higher than 1 µM did not further reduce surface marker expression of LPS-stimulated moDCs (Fig. 3.12), we conclude that the defined working concentration is sufficient to study the effect of RAF inhibition on moDC function.

Interestingly, there was a substantial difference in the inhibition of the MAPK signaling through LY3009120 treatment in moDCs compared to the tested cancer cell lines as well as in $CD4^+$ T cells. While RAF inhibition in the cancer cell lines and in $CD4^+$ T cells (Fig. 19B) translated to a reduced MEK1/2 and ERK1/2 phosphorylation, RAF inhibition during the differentiation from monocytes to moDCs resulted in less MEK1/2 phosphorylation, but ERK1/2 phosphorylation was not affected (Fig. 3.11). MEK1/2 inhibition by trametinib completely abrogated ERK1/2 phosphorylation in moDCs thus verifying MEK1/2 as the essential kinase to phosphorylate and activate ERK1/2. Since MEK1/2 phosphorylation is not completely blocked after RAF inhibition it is possible that partially activated MEK1/2 kinases are still able to induce sufficient ERK1/2 phosphorylation in moDCs. In this context it is worth reminding, that the observed ERK1/2 activation during the differentiation from monocytes to moDCs did not correlate to the detected RAF levels since a strong ERK1/2 phosphorylation was observed even at the beginning of the culture when RAF levels were still undetectable. It is possible that ERK1/2 activation may be regulated through other signaling pathways not depending on RAFs. There are several regulatory mechanisms already described for RAF-independent MEK1/2-ERK1/2 activation. For instance, protein kinase C α is required for TPA-triggered ERK1/2 phosphorylation in hepatoma cells, which is prevented by MEK- but not RAF-inhibition [191]. As already mentioned, another kinase, which is able to activate MEK1/2 and ERK1/2 independent of RAF is Tpl2, which had been shown to drive resistance to RAF inhibition in BRAF V600E mutated cell lines [192]. Tpl2 is further considered as the main MAP3K for MEK1/2 in innate immune cells [185]. Another possibility to achieve sustained ERK1/2 activation in cells can be mediated by the down-regulation of specific phosphatases. It is reported that in macrophages, which are exposed to hyperoxia, prolonged ERK1/2 signaling is beneficial for their survival and that it is mediated through decreased activity of the two ERK-directed phosphatases PP2A and MAPK phosphatase 3 [193].

4.4 Role for RAF kinases in regulating the moDC phenotype

DCs are described as professional antigen presenting cells, which form the interface between the innate and adaptive immune response. In steady state, DCs exhibit an immature phenotype, which is characterized by high antigen capture and low surface expression of MHC and of the co-stimulatory molecules [110]. Despite the demonstrated increase in RAF protein level during the differentiation from monocytes to moDCs, there was no considerable impact of RAF or MEK inhibitors on the differentiation of monocytes to moDCs. Only a slight increase in MHCII and CD86 surface marker expression was observed upon RAF or MEK1/2 inhibition (Fig. 3.11). These observations are in contrast with the studies by Xie *et al.* showing that MEK inhibition retarded the differentiation of moDCs and induced cell death [194]. The different outcome may be explained by how cells were differentiated and treated. While Xie *et al.* cultured the cells for seven days with medium changes every other day, we performed differentiation of moDCs with only one medium change during the 5 days of culture. Further, in the study of Xie *et al.* the immature DCs have a higher expression of CD80 compared to CD86. In line with the study by Hubo *et al.* immature DCs obtained after five days of differentiation are positive for CD86 but negative for CD80 [110].

Inflammatory conditions cause DC maturation resulting in an increased surface expression of MHC as well as induction of co-stimulatory molecules and release of key cytokines. Further, DCs start migrating to the lymph node in a CCR7-dependent manner, where they present processed antigens to T cells. The cytokine profile of DCs is essential to trigger the differentiation of T cells into different effector T cell types [113]. We confirmed that LPS stimulation of immature DCs resulted in enhanced MHCII and CD86 surface marker expression as well as significant induction of CD80 and CD83 expression (Fig. 3.12). Previous studies have shown that LPS stimulation of human moDCs induced the secretion of inflammatory cytokines such as IL-12p70, IL-6, IL-8 and TNFα [147], which is in accordance with our own data (Fig. 3.15). The significant up-regulation of the chemokine receptor CCR7 further proves the successful maturation of moDCs (Fig. 3.17).

While inhibition of MEK1/2 in immature moDCs partially led to spontaneous maturation indicated by a small $CD83^+$ population, trametinib treatment did not interfere with LPS-induced maturation (Fig. 3.12). In contrast, inhibition of the upstream kinase RAF by LY3009120 had a negative effect on the surface marker expression of especially CD86,

CD80 and CD83. Such a contrary effect was further observed on the secretion of the pro-inflammatory cytokine IL-12p70 (Fig. 3.15) and on the expression of the chemokine receptor CCR7 (Fig. 3.17). In case of IL-12p70 and CCR7, MEK1/2 inhibition under stimulating conditions even promoted their secretion and expression, respectively (Fig. 3.15 and 3.17). Consequently, the data suggest that RAF proteins may have MEK1/2 independent functions through which they contribute to the moDC phenotype. Previous studies investigating the impact of MAPK signaling pathway on DCs mostly applied MEK inhibitors for pharmacological inhibition of ERK1/2. Thus, consistent with our data Agarwal *et al*. as well as Puig-Kröger *et al.* reported an increase in IL-12p70 secretion in human moDCs after ERK1/2 inhibition [132, 135]. In line with this, Dillon *et al.* demonstrated that the induction of IL-12p70 upon LPS stimulation was enhanced in splenic DCs isolated from *erk1*$^{-/-}$ deficient mice [195]. Initially, it was demonstrated that LPS-induced ERK1/2 phosphorylation was impaired in Tpl-2 deficient macrophages, while p38 and JNK activation was unaffected [196]. But Kaiser *et al.* revealed that Tpl-2 deficiency inhibits LPS-induced ERK1/2 activation in BMDCs as well. Further, *tpl-2*$^{-/-}$ BMDMs as well as *tpl-2*$^{-/-}$ BMDCs produced elevated levels of IL-12p40 and IL-12p70 protein [146] confirming the data obtained by pharmacological inhibition of ERK1/2. It is tempting to speculate that MAPK signaling is primarily promoted through Tpl-2 and thus RAF proteins are not required for MAPK signaling but may be required for MEK1/2-independent functions. This may further explain why MEK1/2 and ERK1/2 phosphorylation were just slightly and inconsistently impaired in moDCs after RAF inhibitor treatment compared to the tested cancer cells and CD4^{+} cells. Nevertheless, secretion of IL-6, TNFα and IL-8 were reduced by the treatment with the RAF as well as MEK inhibitor (Fig. 3.15) indicating that RAF proteins do not act exclusively in a MEK1/2-independent manner. It has been already reported that MEK1/2 inhibition attenuates the secretion of these cytokines [196, 197].

We wanted to confirm our RAF inhibitor based studies by employing validated siRNAs to specifically knockdown different RAF proteins in moDCs. Because of the observed RAF interactions among the three RAF isoforms (Fig. 3.7), we wanted to generate a double knockdown by combining siRNAs targeting RAF proteins with each other generating a knockdown of ARAF+BRAF, ARAF+CRAF and BRAF+CRAF in moDCs. The knockdown efficiency was rather modest resulting in an approx. 30% reduction of RAF proteins (Fig. 3.16). Further, no impact on LPS-induced surface marker expression after

siRNA transfection was observed (Fig. 3.16). Although the negative impact of LY3009120 treatment was significant on the LPS induced surface marker expression, the reduction was less than 50% (Fig. 3.12: CD86: 26 ± 10%, CD80: 41 ± 10%, CD83: 20 ± 12%). Assuming that the RAF inhibitor LY3009120 blocks RAF activity more efficiently, it is possible that the knockdown efficiency was too low to reproduce the inhibitor based data. Besides surface marker expression, IL-12p70 secretion was investigated after siRNA transfection, since LY3009120 treatment efficiently decreased IL-12p70 secretion (Fig. 3.15: IL-12p70: 78 ± 17%). The double knockdown of ARAF and CRAF led to a significant reduction of IL-12p70 secretion by 29 ± 8 % and the double knockdown of BRAF and CRAF reduced IL12-p70 secretion by 26 ± 22,5 % (Fig. 3.16). These data suggest that RAF kinases may cooperate to accomplish their influence on the moDC phenotype. This hypothesis is further supported by our data concerning the RAF stabilization during moDC differentiation and the interaction studies. Since the siRNA data are still only indicative for the role of RAF proteins in the regulation of the moDC phenotype, it is advisable to confirm these data with a conditional knockout mouse where one shall bypass the technical difficulties of manipulating dendritic cells *in vitro*. Therefore, we detected that the RAF inhibitor LY3009120 affects murine BMDCs in a comparable way as RAF inhibition in BMDCs attenuated LPS-induced CD86 and CD80 surface expression and reduced the induction of CCR7 expression (Fig. 3.20). A DC-specific knockout of RAF allows the analysis of RAF deficient DCs. Therefore, CD11c-Cre transgenic mice are commonly used and a conditional knock down can be induced in conventional $CD11c^{high}$ DCs both from lymphoid and non-lymphoid tissues such as lung and epidermis, and in plasmacytoid DCs. However, we wanted to minimize the possibility of unspecific effects caused by the RAF inhibitor LY3009120 by employing several different RAF inhibitors (Fig. 3.13). Three of the four RAF inhibitors showed similar effects to LY3009120 reducing the expression of CD83 and CD80. This leads to the conclusion that the observed impact on the moDC phenotype is not exclusively for the RAF inhibitor LY3009120. Interestingly, PLX4720 had the smallest impact on CD83 expression and showed no effect on CD80 expression. PLX4720 is a PLX4032 progenitor designed as a potent and selective BRAF V600E inhibitor. The study by Ott *et al.* demonstrated that the BRAF inhibitor PLX4032 did not exhibit any detrimental effects on human moDC function [198], thus somehow confirming what we observed with

BRAFV600E inhibitor PLX4720. In contrast to the others, the activity of this inhibitor is stated to be exclusive for BRAF, BRAF V600E and CRAF Y340/341D, respectively
Finally, it should be mentioned that the inhibitory effect of LY3009120 on surface marker expression of especially CD83 was not restricted to LPS treatment but was also seen with other innate immune stimuli (Fig. 3.14). Taken together, these data confirm that RAF kinases are required for the proper activation of DCs in response to innate immune stimuli. This further underlines the possibility that RAF inhibitors may impede an effective anti-tumor immune response by inhibiting DC activation.

4.5 Physiological role of RAF kinases in regulating moDC function

Inhibition of RAF kinases by multiple RAF inhibitors impaired LPS-induced DC maturation. A successful maturation is required to enable DCs to migrate to T cell rich zones in lymph nodes to finally induce the clonal expansion of antigen-specific naïve T cells [113]. Since several studies reported about cell migration regulated by MAPK signaling [70, 149, 150], we addressed the question if RAF or MEK1/2 inhibition interferes with moDC migration. Indeed, we detect that moDCs exhibited a more rounded morphology after inhibiting MEK1/2 or RAF by trametinib or LY3009120, respectively (Fig. 3.17). It remains to be elucidated what functional consequences are entailed because of the transition to more amoeboid morphology. In general, changes in the cytoskeletal rearrangements can influence the formation of polarized protrusions, formation of adhesion points and the detachment. Consequently, it would be interesting to test whether the morphological changes have an influence on the migratory properties of moDCs. Burns *et al.* showed that DCs were highly migratory during the first 4h of maturation. At later time points, cells had largely lost their podosomes and did not spread or achieve significant polarity, although the ability to migrate on a fibronectin substrate was retained [148]. A time-lapse-experiment monitoring the undirected migration of moDCs especially during the first hours of maturation would allow us to determine whether RAF or MEK1/2 inhibition affects the migratory speed of moDCs. Further insights about a functional role of the observed morphological changes in moDCs may be obtained by studying the attachment to fibronectin, which is part of the extracellular matrix, or to endothelial cells after RAF or MEK1/2 inhibition. Whether RAF-MAPK signaling contributes to the activation dynamics of RhoGTPases to control cell shape, polarity and migration in DCs deserves further investigations.

As already mentioned above, besides the morphological changes we observed a reduced induction of the chemokine receptor CCR7, when moDCs were stimulated with LPS in the presence of LY3009120 (Fig. 3.18). The CCR7 ligands CCL19 and CCL21 are expressed in the T cell zones of secondary lymphoid organs [151, 152], thus directing the migration of activated DCs from peripheral tissue to the draining lymph nodes. Indeed, the reduced CCR7 expression after LY3009120 treatment translated to a reduction in directed migration towards CCL21 in a transwell migration experiment. The RAF inhibitor LY3009120 had a comparable effect on the *in vitro* migration towards CCL21 of murine BMDCs (Fig. 3.20). So the *in vivo* migration could be further tested by injecting labeled and treated BMDCs subcutaneously into the ear fold of mice to detect later the successfully migrated BMDCs in the auricular lymph nodes. By doing so, directed migration of activated BMDCs towards lymphoid tissue can be determined. Moreover, it can be investigated if the altered DC phenotype observed after RAF inhibitor treatment impedes with the *in vivo* migration as well.

In the T cell area of secondary lymphoid organs, DCs initiate the activation and differentiation of naïve T lymphocytes. The intensity of T cell stimulation depends on the concentration of peptide-MHC complexes as well as on the level of co-stimulatory molecules provided by DCs [199]. While the T cell receptor (TCR) complex recognizes the antigens presented by MHC molecules, the costimulatory molecule CD28 is simultaneously engaged with its ligands CD80 or CD86. It is known, that CD28 costimulation increases the T cell response and this is mediated by recruiting membrane rafts containing a concentrated amount of kinases and adapters [200]. Since the upregulation of the costimulatory molecules CD80 and CD86 during DC maturation ensures an efficient amplification of signaling in naïve T cells, we validated how the negative impact of the RAF inhibitor on DC surface marker expression affects the capability to induce T cell activation. In our study, we employed allogeneic $CD4^+$ T cells which suggest that the DC phenotype obtained after RAF inhibition led to a reduced allostimulatory capacity (Fig. 3.19).

As we obtained significant, reproducible effects advocating for an indispensable role of RAF kinases for the activation and migration of DCs and subsequent T cell stimulation, we attempted further experiments *in vivo* by administering the inhibitor through i.p. injection to the mice. The administered inhibitor dose of 15 mg/kg LY3009120 was chosen based on published studies, which employed the inhibitor to investigate tumor

growth. The study by Zhao *et al.* confirmed the anti-tumor activity of LY3009120 within a xenograft model using a pancreatic carcinoma cell line [100]. The ability to suppress tumor growth was further demonstrated in the study by Wei *et al*., who employed a xenograft model with thyroid carcinoma cells [101]. Based on these studies we resorted to the aforementioned concentration as this concentration inhibited tumor growth in mice.

In a pre-experiment, we demonstrated that maturation of DCs located in spleen and lymph nodes was successfully induced by i.p. injection of LPS (Fig. 3.21). Pretreating mice with LY3009120 did not affect the maturation of DCs from lymph nodes. However, it resulted in a minor but not significant reduction in the expression of the co-stimulatory molecules CD80 and CD86 of splenic DCs. It would be interesting if a prolonged treatment with the LY3009120 inhibitor causes more substantial effects on the DC maturation *in vivo*. A good tolerance of prolonged treatment is likely, since no systemic toxicity was reported, when mice were treated with the LY3009120 inhibitor for 31 days in order to investigate its anti-tumor activity [100]. Although we were working with a tumor-inhibiting dose, the bioavailability of the inhibitor has to be clarified in more detail to ensure the drug effects to the time point when DC maturation is induced. Moreover, it could be possible that the impact on surface marker expression seen *in vitro* is too small to detect the difference *in vivo*. With regard to the initial question of our study it would be interesting to investigate the impact of LY3009120 treatment on DC activation in a tumor setting. The study by Preynat-Seauve *et al.* identified tumor-infiltrating cells with a DC phenotype in the mouse melanoma model using the B16F10 or K17-35 cell lines [201]. But the tumor-infiltrating dendritic cells had characteristics of immature DCs *in vivo*, which only fully matured *ex vivo*, making it to a not suitable model for us to investigate the activation of tumor-infiltrating dendritic cells after RAF inhibitor treatment. Other aspects, which have to be encountered for the choice of a suitable mouse model, are the observed effects of the RAF inhibitor on moDC cytokine secretion of especially IL-12p70 (Fig. 3.15) and the direct impact on proliferation of $CD4^+$ T cells (Fig. 3.19). First of all, it is important to determine if RAF-inhibitor treated DCs induce an altered T helper response. As already mentioned above, the differentiation of T cells into different effector T cell types is dependent on the cytokine production by DCs [113]. The cytokine IL-12p70 belongs to the Th1-polarizing cytokines [202] and is elicited by most pathogens. TLR4 activation is also known to

induce Th1 polarization [203]. Since IL-12p70 secretion is significantly reduced in the presence of the RAF inhibitor, it is possible that the outcome of the inhibitor treatment also affects T cell differentiation. However, it is challenging to confirm the relevance of the altered DC phenotype after RAF inhibition *in vivo,* since the RAF inhibitor directly inhibits $CD4^+$ T cell priming. Consequently, we are now in the process to investigate if the capability of naïve $CD4^+$ T cells to differentiate into different effector T cells is impaired upon RAF inhibition. Dependent on the pattern of stimuli $CD4^+$ T cells give rise to a set of effector T cells like the Th1, Th2, Th17 and regulatory T cells [204]. Abnormal activation and differentiation of T cells are linked to certain diseases. For instance, organ-specific autoimmune diseases are attributed to Th1 cells, while Th2 cells are rather responsible for allergic inflammatory diseases and asthma [204]. If RAF inhibitors would directly influence T cell differentiation and/or affect the DC-induced T cell differentiation it would be tempting to consider a disease model, in which RAF inhibitors could elicit a beneficial effect. Additionally, the better understanding of how RAF inhibition potentially affects immune cells can help to develop better strategies for cancer treatment. In line with this, Ebert *et al.* showed that MEK1/2 inhibition in tumor-bearing mice blocked naïve $CD8^+$ T cell priming. But their study revealed that MEK1/2 inhibition protected tumor-infiltrating $CD8^+$ T cells from death and durable tumor regression was achieved by the combination of MEK inhibitors with anti-programmed death-ligand 1 (PD-L1) [205]. The relevance of combining targeted therapeutics with suitable immune checkpoint inhibitors was also already shown in the clinics. For instance, it was proven that the overall survival of patients with advanced melanoma was enhanced by a combined treatment of BRAF or MEK inhibitors with inhibition of the immune checkpoint regulator lymphocyte associated-protein-4 (CTLA4) [206].

4.6 Outlook and future prospects

Because of the contrary effects of the RAF inhibitor LY3009120 and the MEK inhibitor trametinib on the expression of the co-stimulatory molecules, of the chemokine receptor CCR7 as well as on the IL-12p70 secretion we were considering that RAF proteins might have MEK1/2 independent functions in moDCs. Considering this scenario, RAF proteins probably recruit or regulate other substrates to fulfill their function. Alternative RAF targets are already described in the literature [65, 66, 69], although MEK1/2 is the only commonly accepted substrate. Consequently, we are now following two approaches to

discover how RAF proteins could be involved in the regulation of moDCs activation in a MEK1/2-independent manner. First, we wanted to identify new RAF substrates through a mass-spectrometric approach after precipitating cross-linked RAF proteins from stimulated moDCs (Fig. 3.22 and 3.23). Therefore, we started with the identification of proteins in the precipitates of cross-linked CRAF displaying targets, which can potentially interact with CRAF (Fig. 3.23). We further want to extent the study to determine possible substrates of ARAF since both RAF proteins were regulated in a comparable way in our study. Further, we are planning to characterize promising targets to finally elucidate how RAF proteins could play a role in their regulation. On the other side, we want to perform RNA-sequencing of RAF inhibitor treated moDCs under stimulating and non-stimulating conditions to get more insights about transcriptional changes.

Beside this, it deserves further studies to investigate how RAF proteostasis is regulated in moDCs. Although we found that RAF kinases are stabilized during moDC differentiation, we were not able to link the increase in protein stability to any significant alteration in the polyubiquitination. As already mentioned, we want to investigate whether other protein degradation pathways are involved in regulating RAF stability in moDCs. We are further interested how RAF kinases are activated in moDCs. With RAS being the classical activator of the RAF-MEK1/2-ERK1/2-pathway we want to test if activation of RAF proteins is dependent on RAS in moDCs.

Most importantly the clinical implication of pan-RAF inhibitors has to be studied in more detail. Previous studies have shown that BRAF inhibitors like vemurafenib or dabrafenib did not have immunomodulatory effects on human moDCs [198, 207]. But due to dimerization-induced paradoxical MAPK activation, the next generation of pan-RAF inhibitors was developed and our study suggests that pan-RAF inhibitors may indeed have adverse effects on DC function. Since T cell proliferation was further blocked by pan-RAF inhibition we additionally want to address the question whether other T cell functions are impaired upon pan-RAF inhibition. Consequently, it is of greatest importance to investigate in more detail how pan-RAF inhibitors affect distinct immune cell subsets and whether pan-RAF inhibitors might impair the anti-tumor immunity.

5 References

1. Coulombe, P. and S. Meloche, *Atypical mitogen-activated protein kinases: structure, regulation and functions.* Biochim Biophys Acta, 2007. **1773**(8): p. 1376-87.
2. Yang, S.H., A.D. Sharrocks, and A.J. Whitmarsh, *MAP kinase signalling cascades and transcriptional regulation.* Gene, 2013. **513**(1): p. 1-13.
3. Krishna, M. and H. Narang, *The complexity of mitogen-activated protein kinases (MAPKs) made simple.* Cell Mol Life Sci, 2008. **65**(22): p. 3525-44.
4. Yang, S.H., A.D. Sharrocks, and A.J. Whitmarsh, *Transcriptional regulation by the MAP kinase signaling cascades.* Gene, 2003. **320**: p. 3-21.
5. Kolch, W., *Coordinating ERK/MAPK signalling through scaffolds and inhibitors.* Nat Rev Mol Cell Biol, 2005. **6**(11): p. 827-37.
6. Owens, D.M. and S.M. Keyse, *Differential regulation of MAP kinase signalling by dual-specificity protein phosphatases.* Oncogene, 2007. **26**(22): p. 3203-13.
7. Pearson, G., et al., *Mitogen-activated protein (MAP) kinase pathways: regulation and physiological functions.* Endocr Rev, 2001. **22**(2): p. 153-83.
8. Wood, K.W., et al., *ras mediates nerve growth factor receptor modulation of three signal-transducing protein kinases: MAP kinase, Raf-1, and RSK.* Cell, 1992. **68**(6): p. 1041-50.
9. Papin, C., et al., *Identification of signalling proteins interacting with B-Raf in the yeast two-hybrid system.* Oncogene, 1996. **12**(10): p. 2213-21.
10. Pritchard, C.A., et al., *Conditionally oncogenic forms of the A-Raf and B-Raf protein kinases display different biological and biochemical properties in NIH 3T3 cells.* Mol Cell Biol, 1995. **15**(11): p. 6430-42.
11. Wellbrock, C., M. Karasarides, and R. Marais, *The RAF proteins take centre stage.* Nat Rev Mol Cell Biol, 2004. **5**(11): p. 875-85.
12. Mason, C.S., et al., *Serine and tyrosine phosphorylations cooperate in Raf-1, but not B-Raf activation.* EMBO J, 1999. **18**(8): p. 2137-48.
13. Bromberg-White, J.L., N.J. Andersen, and N.S. Duesbery, *MEK genomics in development and disease.* Brief Funct Genomics, 2012. **11**(4): p. 300-10.
14. Eblen, S.T., et al., *Mitogen-activated protein kinase feedback phosphorylation regulates MEK1 complex formation and activation during cellular adhesion.* Mol Cell Biol, 2004. **24**(6): p. 2308-17.
15. Park, E.R., S.T. Eblen, and A.D. Catling, *MEK1 activation by PAK: a novel mechanism.* Cell Signal, 2007. **19**(7): p. 1488-96.
16. Catalanotti, F., et al., *A Mek1-Mek2 heterodimer determines the strength and duration of the Erk signal.* Nat Struct Mol Biol, 2009. **16**(3): p. 294-303.
17. Scholl, F.A., et al., *Mek1/2 MAPK kinases are essential for Mammalian development, homeostasis, and Raf-induced hyperplasia.* Dev Cell, 2007. **12**(4): p. 615-29.
18. Belanger, L.F., et al., *Mek2 is dispensable for mouse growth and development.* Mol Cell Biol, 2003. **23**(14): p. 4778-87.
19. Giroux, S., et al., *Embryonic death of Mek1-deficient mice reveals a role for this kinase in angiogenesis in the labyrinthine region of the placenta.* Curr Biol, 1999. **9**(7): p. 369-72.

20. Cruzalegui, F.H., E. Cano, and R. Treisman, *ERK activation induces phosphorylation of Elk-1 at multiple S/T-P motifs to high stoichiometry.* Oncogene, 1999. **18**(56): p. 7948-57.
21. Sears, R., et al., *Ras enhances Myc protein stability.* Mol Cell, 1999. **3**(2): p. 169-79.
22. Scheid, M.P., K.M. Schubert, and V. Duronio, *Regulation of bad phosphorylation and association with Bcl-x(L) by the MAPK/Erk kinase.* J Biol Chem, 1999. **274**(43): p. 31108-13.
23. Allan, L.A., et al., *Inhibition of caspase-9 through phosphorylation at Thr 125 by ERK MAPK.* Nat Cell Biol, 2003. **5**(7): p. 647-54.
24. Roux, P.P. and J. Blenis, *ERK and p38 MAPK-activated protein kinases: a family of protein kinases with diverse biological functions.* Microbiol Mol Biol Rev, 2004. **68**(2): p. 320-44.
25. Shaul, Y.D. and R. Seger, *The MEK/ERK cascade: from signaling specificity to diverse functions.* Biochim Biophys Acta, 2007. **1773**(8): p. 1213-26.
26. Roskoski, R., Jr., *ERK1/2 MAP kinases: structure, function, and regulation.* Pharmacol Res, 2012. **66**(2): p. 105-43.
27. Lloyd, A.C., *Distinct functions for ERKs?* J Biol, 2006. **5**(5): p. 13.
28. Pages, G., et al., *Defective thymocyte maturation in p44 MAP kinase (Erk 1) knockout mice.* Science, 1999. **286**(5443): p. 1374-7.
29. Yao, Y., et al., *Extracellular signal-regulated kinase 2 is necessary for mesoderm differentiation.* Proc Natl Acad Sci U S A, 2003. **100**(22): p. 12759-64.
30. Lefloch, R., J. Pouyssegur, and P. Lenormand, *Single and combined silencing of ERK1 and ERK2 reveals their positive contribution to growth signaling depending on their expression levels.* Mol Cell Biol, 2008. **28**(1): p. 511-27.
31. Caunt, C.J. and S.M. Keyse, *Dual-specificity MAP kinase phosphatases (MKPs): shaping the outcome of MAP kinase signalling.* FEBS J, 2013. **280**(2): p. 489-504.
32. Lake, D., S.A. Correa, and J. Muller, *Negative feedback regulation of the ERK1/2 MAPK pathway.* Cell Mol Life Sci, 2016. **73**(23): p. 4397-4413.
33. Alessi, D.R., et al., *Inactivation of p42 MAP kinase by protein phosphatase 2A and a protein tyrosine phosphatase, but not CL100, in various cell lines.* Curr Biol, 1995. **5**(3): p. 283-95.
34. Pulido, R., A. Zuniga, and A. Ullrich, *PTP-SL and STEP protein tyrosine phosphatases regulate the activation of the extracellular signal-regulated kinases ERK1 and ERK2 by association through a kinase interaction motif.* EMBO J, 1998. **17**(24): p. 7337-50.
35. Brummer, T., et al., *Identification of novel ERK-mediated feedback phosphorylation sites at the C-terminus of B-Raf.* Oncogene, 2003. **22**(55): p. 8823-34.
36. Balan, V., et al., *Identification of novel in vivo Raf-1 phosphorylation sites mediating positive feedback Raf-1 regulation by extracellular signal-regulated kinase.* Mol Biol Cell, 2006. **17**(3): p. 1141-53.
37. Rapp, U.R., et al., *Structure and biological activity of v-raf, a unique oncogene transduced by a retrovirus.* Proc Natl Acad Sci U S A, 1983. **80**(14): p. 4218-22.
38. Jansen, H.W., et al., *Two unrelated cell-derived sequences in the genome of avian leukemia and carcinoma inducing retrovirus MH2.* EMBO J, 1983. **2**(11): p. 1969-75.
39. Jansen, H.W., et al., *Homologous cell-derived oncogenes in avian carcinoma virus MH2 and murine sarcoma virus 3611.* Nature, 1984. **307**(5948): p. 281-4.
40. Kyriakis, J.M., et al., *Raf-1 activates MAP kinase-kinase.* Nature, 1992. **358**(6385): p. 417-21.

41. Huebner, K., et al., *Actively transcribed genes in the raf oncogene group, located on the X chromosome in mouse and human.* Proc Natl Acad Sci U S A, 1986. **83**(11): p. 3934-8.
42. Ikawa, S., et al., *B-raf, a new member of the raf family, is activated by DNA rearrangement.* Mol Cell Biol, 1988. **8**(6): p. 2651-4.
43. Matallanas, D., et al., *Raf family kinases: old dogs have learned new tricks.* Genes Cancer, 2011. **2**(3): p. 232-60.
44. Luo, Z., et al., *An intact Raf zinc finger is required for optimal binding to processed Ras and for ras-dependent Raf activation in situ.* Mol Cell Biol, 1997. **17**(1): p. 46-53.
45. Morrison, D.K., et al., *Identification of the major phosphorylation sites of the Raf-1 kinase.* J Biol Chem, 1993. **268**(23): p. 17309-16.
46. Light, Y., H. Paterson, and R. Marais, *14-3-3 antagonizes Ras-mediated Raf-1 recruitment to the plasma membrane to maintain signaling fidelity.* Mol Cell Biol, 2002. **22**(14): p. 4984-96.
47. Michaud, N.R., et al., *14-3-3 is not essential for Raf-1 function: identification of Raf-1 proteins that are biologically activated in a 14-3-3- and Ras-independent manner.* Mol Cell Biol, 1995. **15**(6): p. 3390-7.
48. Morrison, D.K. and R.E. Cutler, *The complexity of Raf-1 regulation.* Curr Opin Cell Biol, 1997. **9**(2): p. 174-9.
49. Abraham, D., et al., *Raf-1-associated protein phosphatase 2A as a positive regulator of kinase activation.* J Biol Chem, 2000. **275**(29): p. 22300-4.
50. Chong, H., J. Lee, and K.L. Guan, *Positive and negative regulation of Raf kinase activity and function by phosphorylation.* EMBO J, 2001. **20**(14): p. 3716-27.
51. Diaz, B., et al., *Phosphorylation of Raf-1 serine 338-serine 339 is an essential regulatory event for Ras-dependent activation and biological signaling.* Mol Cell Biol, 1997. **17**(8): p. 4509-16.
52. Baljuls, A., et al., *Unique N-region determines low basal activity and limited inducibility of A-RAF kinase: the role of N-region in the evolutionary divergence of RAF kinase function in vertebrates.* J Biol Chem, 2007. **282**(36): p. 26575-90.
53. Zhang, B.H. and K.L. Guan, *Activation of B-Raf kinase requires phosphorylation of the conserved residues Thr598 and Ser601.* EMBO J, 2000. **19**(20): p. 5429-39.
54. Baljuls, A., B.N. Kholodenko, and W. Kolch, *It takes two to tango--signalling by dimeric Raf kinases.* Mol Biosyst, 2013. **9**(4): p. 551-8.
55. Rushworth, L.K., et al., *Regulation and role of Raf-1/B-Raf heterodimerization.* Mol Cell Biol, 2006. **26**(6): p. 2262-72.
56. Hu, J., et al., *Allosteric activation of functionally asymmetric RAF kinase dimers.* Cell, 2013. **154**(5): p. 1036-1046.
57. von Kriegsheim, A., et al., *Regulation of the Raf-MEK-ERK pathway by protein phosphatase 5.* Nat Cell Biol, 2006. **8**(9): p. 1011-6.
58. Park, S., et al., *Regulation of RKIP binding to the N-region of the Raf-1 kinase.* FEBS Lett, 2006. **580**(27): p. 6405-12.
59. Rath, O., et al., *The RKIP (Raf-1 Kinase Inhibitor Protein) conserved pocket binds to the phosphorylated N-region of Raf-1 and inhibits the Raf-1-mediated activated phosphorylation of MEK.* Cell Signal, 2008. **20**(5): p. 935-41.
60. Yeung, K., et al., *Suppression of Raf-1 kinase activity and MAP kinase signalling by RKIP.* Nature, 1999. **401**(6749): p. 173-7.
61. Dougherty, M.K., et al., *Regulation of Raf-1 by direct feedback phosphorylation.* Mol Cell, 2005. **17**(2): p. 215-24.

62. Ding, Q., et al., *Raf kinase activation of adenylyl cyclases: isoform-selective regulation.* Mol Pharmacol, 2004. **66**(4): p. 921-8.
63. Beazely, M.A., J.K. Alan, and V.J. Watts, *Protein kinase C and epidermal growth factor stimulation of Raf1 potentiates adenylyl cyclase type 6 activation in intact cells.* Mol Pharmacol, 2005. **67**(1): p. 250-9.
64. Wang, S., R.N. Ghosh, and S.P. Chellappan, *Raf-1 physically interacts with Rb and regulates its function: a link between mitogenic signaling and cell cycle regulation.* Mol Cell Biol, 1998. **18**(12): p. 7487-98.
65. Broustas, C.G., et al., *Phosphorylation of the myosin-binding subunit of myosin phosphatase by Raf-1 and inhibition of phosphatase activity.* J Biol Chem, 2002. **277**(4): p. 3053-9.
66. Jette, C. and A. Thorburn, *A Raf-induced, MEK-independent signaling pathway regulates atrial natriuretic factor gene expression in cardiac muscle cells.* FEBS Lett, 2000. **467**(1): p. 1-6.
67. Chien, K.R., et al., *Regulation of cardiac gene expression during myocardial growth and hypertrophy: molecular studies of an adaptive physiologic response.* FASEB J, 1991. **5**(15): p. 3037-46.
68. Pearson, G., et al., *Uncoupling Raf1 from MEK1/2 impairs only a subset of cellular responses to Raf activation.* J Biol Chem, 2000. **275**(48): p. 37303-6.
69. Chen, J., et al., *Raf-1 promotes cell survival by antagonizing apoptosis signal-regulating kinase 1 through a MEK-ERK independent mechanism.* Proc Natl Acad Sci U S A, 2001. **98**(14): p. 7783-8.
70. Ehrenreiter, K., et al., *Raf-1 regulates Rho signaling and cell migration.* J Cell Biol, 2005. **168**(6): p. 955-64.
71. Prior, I.A., P.D. Lewis, and C. Mattos, *A comprehensive survey of Ras mutations in cancer.* Cancer Res, 2012. **72**(10): p. 2457-67.
72. Cooper, G., *Oncogenes*, in *The Cell: A Molecular Approach,, 2nd edition*. 2000, Sinauer Associates: Sunderland (MA).
73. Downward, J., *Targeting RAS signalling pathways in cancer therapy.* Nat Rev Cancer, 2003. **3**(1): p. 11-22.
74. Forbes, S.A., et al., *COSMIC: somatic cancer genetics at high-resolution.* Nucleic Acids Res, 2017. **45**(D1): p. D777-D783.
75. Davies, H., et al., *Mutations of the BRAF gene in human cancer.* Nature, 2002. **417**(6892): p. 949-54.
76. Durrant, D.E. and D.K. Morrison, *Targeting the Raf kinases in human cancer: the Raf dimer dilemma.* Br J Cancer, 2018. **118**(1): p. 3-8.
77. Garnett, M.J., et al., *Wild-type and mutant B-RAF activate C-RAF through distinct mechanisms involving heterodimerization.* Mol Cell, 2005. **20**(6): p. 963-9.
78. Dankner, M., et al., *Classifying BRAF alterations in cancer: new rational therapeutic strategies for actionable mutations.* Oncogene, 2018. **37**(24): p. 3183-3199.
79. Freeman, A.K., D.A. Ritt, and D.K. Morrison, *Effects of Raf dimerization and its inhibition on normal and disease-associated Raf signaling.* Mol Cell, 2013. **49**(4): p. 751-8.
80. Lee, J.W., et al., *Mutational analysis of the ARAF gene in human cancers.* APMIS, 2005. **113**(1): p. 54-7.
81. Emuss, V., et al., *Mutations of C-RAF are rare in human cancer because C-RAF has a low basal kinase activity compared with B-RAF.* Cancer Res, 2005. **65**(21): p. 9719-26.
82. Karreth, F.A., et al., *C-Raf is required for the initiation of lung cancer by K-Ras(G12D).* Cancer Discov, 2011. **1**(2): p. 128-36.

83. Blasco, R.B., et al., *c-Raf, but not B-Raf, is essential for development of K-Ras oncogene-driven non-small cell lung carcinoma.* Cancer Cell, 2011. **19**(5): p. 652-63.
84. Wu, P., T.E. Nielsen, and M.H. Clausen, *Small-molecule kinase inhibitors: an analysis of FDA-approved drugs.* Drug Discov Today, 2016. **21**(1): p. 5-10.
85. Chapman, P.B., et al., *Improved survival with vemurafenib in melanoma with BRAF V600E mutation.* N Engl J Med, 2011. **364**(26): p. 2507-16.
86. Lee, J.T., et al., *PLX4032, a potent inhibitor of the B-Raf V600E oncogene, selectively inhibits V600E-positive melanomas.* Pigment Cell Melanoma Res, 2010. **23**(6): p. 820-7.
87. Sosman, J.A., et al., *Survival in BRAF V600-mutant advanced melanoma treated with vemurafenib.* N Engl J Med, 2012. **366**(8): p. 707-14.
88. Hauschild, A., et al., *Dabrafenib in BRAF-mutated metastatic melanoma: a multicentre, open-label, phase 3 randomised controlled trial.* Lancet, 2012. **380**(9839): p. 358-65.
89. Cseh, B., E. Doma, and M. Baccarini, *"RAF" neighborhood: protein-protein interaction in the Raf/Mek/Erk pathway.* FEBS Lett, 2014. **588**(15): p. 2398-406.
90. Su, F., et al., *RAS mutations in cutaneous squamous-cell carcinomas in patients treated with BRAF inhibitors.* N Engl J Med, 2012. **366**(3): p. 207-15.
91. Poulikakos, P.I., et al., *RAF inhibitors transactivate RAF dimers and ERK signalling in cells with wild-type BRAF.* Nature, 2010. **464**(7287): p. 427-30.
92. Solit, D. and N. Rosen, *Oncogenic RAF: a brief history of time.* Pigment Cell Melanoma Res, 2010. **23**(6): p. 760-2.
93. Downward, J., *Targeting RAF: trials and tribulations.* Nat Med, 2011. **17**(3): p. 286-8.
94. Hatzivassiliou, G., et al., *RAF inhibitors prime wild-type RAF to activate the MAPK pathway and enhance growth.* Nature, 2010. **464**(7287): p. 431-5.
95. Jin, T., et al., *RAF inhibitors promote RAS-RAF interaction by allosterically disrupting RAF autoinhibition.* Nat Commun, 2017. **8**(1): p. 1211.
96. Lavoie, H., et al., *Inhibitors that stabilize a closed RAF kinase domain conformation induce dimerization.* Nat Chem Biol, 2013. **9**(7): p. 428-36.
97. Baljuls, A., et al., *Single substitution within the RKTR motif impairs kinase activity but promotes dimerization of RAF kinase.* J Biol Chem, 2011. **286**(18): p. 16491-503.
98. Karoulia, Z., et al., *An Integrated Model of RAF Inhibitor Action Predicts Inhibitor Activity against Oncogenic BRAF Signaling.* Cancer Cell, 2016. **30**(3): p. 485-498.
99. Peng, S.B., et al., *Inhibition of RAF Isoforms and Active Dimers by LY3009120 Leads to Anti-tumor Activities in RAS or BRAF Mutant Cancers.* Cancer Cell, 2015. **28**(3): p. 384-98.
100. Zhao, X., et al., *A combinatorial strategy using YAP and pan-RAF inhibitors for treating KRAS-mutant pancreatic cancer.* Cancer Lett, 2017. **402**: p. 61-70.
101. Wei, W.J., et al., *Obatoclax and LY3009120 Efficiently Overcome Vemurafenib Resistance in Differentiated Thyroid Cancer.* Theranostics, 2017. **7**(4): p. 987-1001.
102. Vakana, E., et al., *LY3009120, a panRAF inhibitor, has significant anti-tumor activity in BRAF and KRAS mutant preclinical models of colorectal cancer.* Oncotarget, 2017. **8**(6): p. 9251-9266.
103. Thota, R., D.B. Johnson, and J.A. Sosman, *Trametinib in the treatment of melanoma.* Expert Opin Biol Ther, 2015. **15**(5): p. 735-47.

104. Weart, T.C., K.D. Miller, and C.B. Simone, 2nd, *Spotlight on dabrafenib/trametinib in the treatment of non-small-cell lung cancer: place in therapy.* Cancer Manag Res, 2018. **10**: p. 647-652.
105. Depenni, R., et al., *Dabrafenib-trametinib combination in 'field-practice': an Italian experience.* Future Oncol, 2018. **14**(20): p. 2045-2052.
106. Gotwals, P., et al., *Prospects for combining targeted and conventional cancer therapy with immunotherapy.* Nat Rev Cancer, 2017. **17**(5): p. 286-301.
107. Steinman, R.M. and Z.A. Cohn, *Identification of a novel cell type in peripheral lymphoid organs of mice. I. Morphology, quantitation, tissue distribution.* J Exp Med, 1973. **137**(5): p. 1142-62.
108. Steinman, R.M. and M.D. Witmer, *Lymphoid dendritic cells are potent stimulators of the primary mixed leukocyte reaction in mice.* Proc Natl Acad Sci U S A, 1978. **75**(10): p. 5132-6.
109. Nussenzweig, M.C., et al., *Dendritic cells are accessory cells for the development of anti-trinitrophenyl cytotoxic T lymphocytes.* J Exp Med, 1980. **152**(4): p. 1070-84.
110. Hubo, M., et al., *Costimulatory molecules on immunogenic versus tolerogenic human dendritic cells.* Front Immunol, 2013. **4**: p. 82.
111. Mahnke, K., et al., *Immature, but not inactive: the tolerogenic function of immature dendritic cells.* Immunol Cell Biol, 2002. **80**(5): p. 477-83.
112. Raker, V.K., M.P. Domogalla, and K. Steinbrink, *Tolerogenic Dendritic Cells for Regulatory T Cell Induction in Man.* Front Immunol, 2015. **6**: p. 569.
113. Dalod, M., et al., *Dendritic cell maturation: functional specialization through signaling specificity and transcriptional programming.* EMBO J, 2014. **33**(10): p. 1104-16.
114. Akira, S., S. Uematsu, and O. Takeuchi, *Pathogen recognition and innate immunity.* Cell, 2006. **124**(4): p. 783-801.
115. Belz, G.T. and S.L. Nutt, *Transcriptional programming of the dendritic cell network.* Nat Rev Immunol, 2012. **12**(2): p. 101-13.
116. Collin, M. and V. Bigley, *Human dendritic cell subsets: an update.* Immunology, 2018. **154**(1): p. 3-20.
117. Swiecki, M. and M. Colonna, *The multifaceted biology of plasmacytoid dendritic cells.* Nat Rev Immunol, 2015. **15**(8): p. 471-85.
118. Jongbloed, S.L., et al., *Human CD141+ (BDCA-3)+ dendritic cells (DCs) represent a unique myeloid DC subset that cross-presents necrotic cell antigens.* J Exp Med, 2010. **207**(6): p. 1247-60.
119. Villadangos, J.A. and K. Shortman, *Found in translation: the human equivalent of mouse CD8+ dendritic cells.* J Exp Med, 2010. **207**(6): p. 1131-4.
120. Granot, T., et al., *Dendritic Cells Display Subset and Tissue-Specific Maturation Dynamics over Human Life.* Immunity, 2017. **46**(3): p. 504-515.
121. Villani, A.C., et al., *Single-cell RNA-seq reveals new types of human blood dendritic cells, monocytes, and progenitors.* Science, 2017. **356**(6335).
122. Yin, X., et al., *Human Blood CD1c+ Dendritic Cells Encompass CD5high and CD5low Subsets That Differ Significantly in Phenotype, Gene Expression, and Functions.* J Immunol, 2017. **198**(4): p. 1553-1564.
123. Leon, B., M. Lopez-Bravo, and C. Ardavin, *Monocyte-derived dendritic cells formed at the infection site control the induction of protective T helper 1 responses against Leishmania.* Immunity, 2007. **26**(4): p. 519-31.
124. Serbina, N.V., et al., *TNF/iNOS-producing dendritic cells mediate innate immune defense against bacterial infection.* Immunity, 2003. **19**(1): p. 59-70.

125. Boltjes, A. and F. van Wijk, *Human dendritic cell functional specialization in steady-state and inflammation.* Front Immunol, 2014. **5**: p. 131.
126. Segura, E. and S. Amigorena, *Identification of human inflammatory dendritic cells.* Oncoimmunology, 2013. **2**(5): p. e23851.
127. Segura, E., et al., *Human inflammatory dendritic cells induce Th17 cell differentiation.* Immunity, 2013. **38**(2): p. 336-48.
128. Beitnes, A.C., et al., *Rapid accumulation of CD14+CD11c+ dendritic cells in gut mucosa of celiac disease after in vivo gluten challenge.* PLoS One, 2012. **7**(3): p. e33556.
129. Sallusto, F. and A. Lanzavecchia, *Efficient presentation of soluble antigen by cultured human dendritic cells is maintained by granulocyte/macrophage colony-stimulating factor plus interleukin 4 and downregulated by tumor necrosis factor alpha.* J Exp Med, 1994. **179**(4): p. 1109-18.
130. Kawasaki, T. and T. Kawai, *Toll-like receptor signaling pathways.* Front Immunol, 2014. **5**: p. 461.
131. Honda, K., et al., *Spatiotemporal regulation of MyD88-IRF-7 signalling for robust type-I interferon induction.* Nature, 2005. **434**(7036): p. 1035-40.
132. Agrawal, S., et al., *Cutting edge: different Toll-like receptor agonists instruct dendritic cells to induce distinct Th responses via differential modulation of extracellular signal-regulated kinase-mitogen-activated protein kinase and c-Fos.* J Immunol, 2003. **171**(10): p. 4984-9.
133. d'Ostiani, C.F., et al., *Dendritic cells discriminate between yeasts and hyphae of the fungus Candida albicans. Implications for initiation of T helper cell immunity in vitro and in vivo.* J Exp Med, 2000. **191**(10): p. 1661-74.
134. Nakahara, T., et al., *Differential role of MAPK signaling in human dendritic cell maturation and Th1/Th2 engagement.* J Dermatol Sci, 2006. **42**(1): p. 1-11.
135. Puig-Kroger, A., et al., *Extracellular signal-regulated protein kinase signaling pathway negatively regulates the phenotypic and functional maturation of monocyte-derived human dendritic cells.* Blood, 2001. **98**(7): p. 2175-82.
136. Rescigno, M., et al., *Dendritic cell survival and maturation are regulated by different signaling pathways.* J Exp Med, 1998. **188**(11): p. 2175-80.
137. Hopkins, A.L. and C.R. Groom, *The druggable genome.* Nat Rev Drug Discov, 2002. **1**(9): p. 727-30.
138. Melnikova, I. and J. Golden, *Targeting protein kinases.* Nat Rev Drug Discov, 2004. **3**(12): p. 993-4.
139. Kubach, J., et al., *Human CD4+CD25+ regulatory T cells: proteome analysis identifies galectin-10 as a novel marker essential for their anergy and suppressive function.* Blood, 2007. **110**(5): p. 1550-8.
140. Tran, T.T., M. Strozynski, and B. Thiede, *Quantitative phosphoproteome analysis of cisplatin-induced apoptosis in Jurkat T cells.* Proteomics, 2017. **17**(11).
141. Hughes, C.S., et al., *Ultrasensitive proteome analysis using paramagnetic bead technology.* Mol Syst Biol, 2014. **10**: p. 757.
142. Sielaff, M., et al., *Evaluation of FASP, SP3, and iST Protocols for Proteomic Sample Preparation in the Low Microgram Range.* J Proteome Res, 2017. **16**(11): p. 4060-4072.
143. Distler, U., et al., *Drift time-specific collision energies enable deep-coverage data-independent acquisition proteomics.* Nat Methods, 2014. **11**(2): p. 167-70.
144. Thrower, J.S., et al., *Recognition of the polyubiquitin proteolytic signal.* EMBO J, 2000. **19**(1): p. 94-102.

145. Dong, C., R.J. Davis, and R.A. Flavell, *MAP kinases in the immune response.* Annu Rev Immunol, 2002. **20**: p. 55-72.
146. Kaiser, F., et al., *TPL-2 negatively regulates interferon-beta production in macrophages and myeloid dendritic cells.* J Exp Med, 2009. **206**(9): p. 1863-71.
147. Verhasselt, V., et al., *Bacterial lipopolysaccharide stimulates the production of cytokines and the expression of costimulatory molecules by human peripheral blood dendritic cells: evidence for a soluble CD14-dependent pathway.* J Immunol, 1997. **158**(6): p. 2919-25.
148. Burns, S., et al., *Maturation of DC is associated with changes in motile characteristics and adherence.* Cell Motil Cytoskeleton, 2004. **57**(2): p. 118-32.
149. Dogan, T., et al., *X-linked and cellular IAPs modulate the stability of C-RAF kinase and cell motility.* Nat Cell Biol, 2008. **10**(12): p. 1447-55.
150. Mooz, J., et al., *Dimerization of the kinase ARAF promotes MAPK pathway activation and cell migration.* Sci Signal, 2014. **7**(337): p. ra73.
151. Willimann, K., et al., *The chemokine SLC is expressed in T cell areas of lymph nodes and mucosal lymphoid tissues and attracts activated T cells via CCR7.* Eur J Immunol, 1998. **28**(6): p. 2025-34.
152. MartIn-Fontecha, A., et al., *Regulation of dendritic cell migration to the draining lymph node: impact on T lymphocyte traffic and priming.* J Exp Med, 2003. **198**(4): p. 615-21.
153. Gunn, M.D., et al., *A chemokine expressed in lymphoid high endothelial venules promotes the adhesion and chemotaxis of naive T lymphocytes.* Proc Natl Acad Sci U S A, 1998. **95**(1): p. 258-63.
154. Bruckner, M., et al., *Converse regulation of CCR7-driven human dendritic cell migration by prostaglandin E(2) and liver X receptor activation.* Eur J Immunol, 2012. **42**(11): p. 2949-58.
155. Hugues, S., et al., *The dynamics of dendritic cell-T cell interactions in priming and tolerance.* Curr Opin Immunol, 2006. **18**(4): p. 491-5.
156. Iezzi, G., K. Karjalainen, and A. Lanzavecchia, *The duration of antigenic stimulation determines the fate of naive and effector T cells.* Immunity, 1998. **8**(1): p. 89-95.
157. Kurtz, J.E. and I. Ray-Coquard, *PI3 kinase inhibitors in the clinic: an update.* Anticancer Res, 2012. **32**(7): p. 2463-70.
158. Yap, T.A. and P. Workman, *Exploiting the cancer genome: strategies for the discovery and clinical development of targeted molecular therapeutics.* Annu Rev Pharmacol Toxicol, 2012. **52**: p. 549-73.
159. Kim, G., et al., *FDA approval summary: vemurafenib for treatment of unresectable or metastatic melanoma with the BRAFV600E mutation.* Clin Cancer Res, 2014. **20**(19): p. 4994-5000.
160. *ClinicalTrials.gov*. Available from: https://clinicaltrials.gov/ct2/home.
161. Chen, D.S. and I. Mellman, *Oncology meets immunology: the cancer-immunity cycle.* Immunity, 2013. **39**(1): p. 1-10.
162. Vinay, D.S., et al., *Immune evasion in cancer: Mechanistic basis and therapeutic strategies.* Semin Cancer Biol, 2015. **35 Suppl**: p. S185-S198.
163. Pasche, B., *Role of transforming growth factor beta in cancer.* J Cell Physiol, 2001. **186**(2): p. 153-68.
164. Curiel, T.J., et al., *Specific recruitment of regulatory T cells in ovarian carcinoma fosters immune privilege and predicts reduced survival.* Nat Med, 2004. **10**(9): p. 942-9.

165. Baljuls, A., et al., *Positive regulation of A-RAF by phosphorylation of isoform-specific hinge segment and identification of novel phosphorylation sites.* J Biol Chem, 2008. **283**(40): p. 27239-54.
166. Hekman, M., et al., *Novel C-Raf phosphorylation sites: serine 296 and 301 participate in Raf regulation.* FEBS Lett, 2005. **579**(2): p. 464-8.
167. Kolbus, A., et al., *Raf-1 antagonizes erythroid differentiation by restraining caspase activation.* J Exp Med, 2002. **196**(10): p. 1347-53.
168. Rubiolo, C., et al., *A balance between Raf-1 and Fas expression sets the pace of erythroid differentiation.* Blood, 2006. **108**(1): p. 152-9.
169. Schulte, T.W., et al., *Disruption of the Raf-1-Hsp90 molecular complex results in destabilization of Raf-1 and loss of Raf-1-Ras association.* J Biol Chem, 1995. **270**(41): p. 24585-8.
170. Dou, F., L.D. Yuan, and J.J. Zhu, *Heat shock protein 90 indirectly regulates ERK activity by affecting Raf protein metabolism.* Acta Biochim Biophys Sin (Shanghai), 2005. **37**(7): p. 501-5.
171. da Rocha Dias, S., et al., *Activated B-RAF is an Hsp90 client protein that is targeted by the anticancer drug 17-allylamino-17-demethoxygeldanamycin.* Cancer Res, 2005. **65**(23): p. 10686-91.
172. Schulte, T.W., W.G. An, and L.M. Neckers, *Geldanamycin-induced destabilization of Raf-1 involves the proteasome.* Biochem Biophys Res Commun, 1997. **239**(3): p. 655-9.
173. Grbovic, O.M., et al., *V600E B-Raf requires the Hsp90 chaperone for stability and is degraded in response to Hsp90 inhibitors.* Proc Natl Acad Sci U S A, 2006. **103**(1): p. 57-62.
174. Glickman, M.H. and A. Ciechanover, *The ubiquitin-proteasome proteolytic pathway: destruction for the sake of construction.* Physiol Rev, 2002. **82**(2): p. 373-428.
175. Demand, J., et al., *Cooperation of a ubiquitin domain protein and an E3 ubiquitin ligase during chaperone/proteasome coupling.* Curr Biol, 2001. **11**(20): p. 1569-77.
176. Eskelinen, E.L., *New insights into the mechanisms of macroautophagy in mammalian cells.* Int Rev Cell Mol Biol, 2008. **266**: p. 207-47.
177. Mauthe, M., et al., *Chloroquine inhibits autophagic flux by decreasing autophagosome-lysosome fusion.* Autophagy, 2018. **14**(8): p. 1435-1455.
178. Wu, Y.T., et al., *Dual role of 3-methyladenine in modulation of autophagy via different temporal patterns of inhibition on class I and III phosphoinositide 3-kinase.* J Biol Chem, 2010. **285**(14): p. 10850-61.
179. Kholodenko, B.N., *Negative feedback and ultrasensitivity can bring about oscillations in the mitogen-activated protein kinase cascades.* Eur J Biochem, 2000. **267**(6): p. 1583-8.
180. Nakayama, K., et al., *FGF induces oscillations of Hes1 expression and Ras/ERK activation.* Curr Biol, 2008. **18**(8): p. R332-4.
181. Waters, K.M., et al., *ERK oscillation-dependent gene expression patterns and deregulation by stress response.* Chem Res Toxicol, 2014. **27**(9): p. 1496-503.
182. Kawai, T. and S. Akira, *Signaling to NF-kappaB by Toll-like receptors.* Trends Mol Med, 2007. **13**(11): p. 460-9.
183. Hacker, H., et al., *CpG-DNA-specific activation of antigen-presenting cells requires stress kinase activity and is preceded by non-specific endocytosis and endosomal maturation.* EMBO J, 1998. **17**(21): p. 6230-40.

184. Hacker, H., et al., *Cell type-specific activation of mitogen-activated protein kinases by CpG-DNA controls interleukin-12 release from antigen-presenting cells.* EMBO J, 1999. **18**(24): p. 6973-82.
185. Symons, A., S. Beinke, and S.C. Ley, *MAP kinase kinase kinases and innate immunity.* Trends Immunol, 2006. **27**(1): p. 40-8.
186. Reimann, T., et al., *Lipopolysaccharide induces activation of the Raf-1/MAP kinase pathway. A putative role for Raf-1 in the induction of the IL-1 beta and the TNF-alpha genes.* J Immunol, 1994. **153**(12): p. 5740-9.
187. Geppert, T.D., et al., *Lipopolysaccharide signals activation of tumor necrosis factor biosynthesis through the ras/raf-1/MEK/MAPK pathway.* Mol Med, 1994. **1**(1): p. 93-103.
188. Marais, R., et al., *Differential regulation of Raf-1, A-Raf, and B-Raf by oncogenic ras and tyrosine kinases.* J Biol Chem, 1997. **272**(7): p. 4378-83.
189. Rebocho, A.P. and R. Marais, *ARAF acts as a scaffold to stabilize BRAF:CRAF heterodimers.* Oncogene, 2013. **32**(26): p. 3207-12.
190. Shaw, A.S., et al., *Kinases and pseudokinases: lessons from RAF.* Mol Cell Biol, 2014. **34**(9): p. 1538-46.
191. Wen-Sheng, W., *Protein kinase C alpha trigger Ras and Raf-independent MEK/ERK activation for TPA-induced growth inhibition of human hepatoma cell HepG2.* Cancer Lett, 2006. **239**(1): p. 27-35.
192. Johannessen, C.M., et al., *COT drives resistance to RAF inhibition through MAP kinase pathway reactivation.* Nature, 2010. **468**(7326): p. 968-72.
193. Nyunoya, T., et al., *Macrophages survive hyperoxia via prolonged ERK activation due to phosphatase down-regulation.* J Biol Chem, 2005. **280**(28): p. 26295-302.
194. Xie, J., et al., *Critical roles of Raf/MEK/ERK and PI3K/AKT signaling and inactivation of p38 MAP kinase in the differentiation and survival of monocyte-derived immature dendritic cells.* Exp Hematol, 2005. **33**(5): p. 564-72.
195. Dillon, S., et al., *A Toll-like receptor 2 ligand stimulates Th2 responses in vivo, via induction of extracellular signal-regulated kinase mitogen-activated protein kinase and c-Fos in dendritic cells.* J Immunol, 2004. **172**(8): p. 4733-43.
196. Dumitru, C.D., et al., *TNF-alpha induction by LPS is regulated posttranscriptionally via a Tpl2/ERK-dependent pathway.* Cell, 2000. **103**(7): p. 1071-83.
197. Nakagawa, S., et al., *p38 Mitogen-Activated protein kinase mediates dual role of ultraviolet B radiation in induction of maturation and apoptosis of monocyte-derived dendritic cells.* J Invest Dermatol, 2004. **123**(2): p. 361-70.
198. Ott, P.A., et al., *Inhibition of both BRAF and MEK in BRAF(V600E) mutant melanoma restores compromised dendritic cell (DC) function while having differential direct effects on DC properties.* Cancer Immunol Immunother, 2013. **62**(4): p. 811-22.
199. Sallusto, F. and A. Lanzavecchia, *The instructive role of dendritic cells on T-cell responses.* Arthritis Res, 2002. **4 Suppl 3**: p. S127-32.
200. Viola, A., et al., *T lymphocyte costimulation mediated by reorganization of membrane microdomains.* Science, 1999. **283**(5402): p. 680-2.
201. Preynat-Seauve, O., et al., *Tumor-infiltrating dendritic cells are potent antigen-presenting cells able to activate T cells and mediate tumor rejection.* J Immunol, 2006. **176**(1): p. 61-7.
202. Cella, M., et al., *Ligation of CD40 on dendritic cells triggers production of high levels of interleukin-12 and enhances T cell stimulatory capacity: T-T help via APC activation.* J Exp Med, 1996. **184**(2): p. 747-52.

203. Pulendran, B., et al., *Lipopolysaccharides from distinct pathogens induce different classes of immune responses in vivo.* J Immunol, 2001. **167**(9): p. 5067-76.
204. Zhu, J. and W.E. Paul, *CD4 T cells: fates, functions, and faults.* Blood, 2008. **112**(5): p. 1557-69.
205. Ebert, P.J.R., et al., *MAP Kinase Inhibition Promotes T Cell and Anti-tumor Activity in Combination with PD-L1 Checkpoint Blockade.* Immunity, 2016. **44**(3): p. 609-621.
206. McArthur, G.A. and A. Ribas, *Targeting oncogenic drivers and the immune system in melanoma.* J Clin Oncol, 2013. **31**(4): p. 499-506.
207. Vella, L.J., et al., *MEK inhibition, alone or in combination with BRAF inhibition, affects multiple functions of isolated normal human lymphocytes and dendritic cells.* Cancer Immunol Res, 2014. **2**(4): p. 351-60.
208. Reddy, S.M., A. Reuben, and J.A. Wargo, *Influences of BRAF Inhibitors on the Immune Microenvironment and the Rationale for Combined Molecular and Immune Targeted Therapy.* Curr Oncol Rep, 2016. **18**(7): p. 42.
209. Cooper, Z.A., et al., *Response to BRAF inhibition in melanoma is enhanced when combined with immune checkpoint blockade.* Cancer Immunol Res, 2014. **2**(7): p. 643-54.